UNIVERSITY of MODENA and REGGIO EMILIA

PhD SCHOOL
MOLECULAR AND REGENERATIVE MEDICINE

CYCLE XXV

DEPARTMENT OF LIFE SCIENCES

Functional characterization of novel mutations in *APOB* and *ANGPTL3* genes in familial hypobetalipoproteinemia and familial combined hypolipidemia

Tutor:

Prof. PATRIZIA TARUGI

PhD School Coordinator:

Prof. ROSSELLA TUPLER

PhD thesis of:

ANTONIA LUCIA MAGNOLO

Academic Years 2010-2012

INDEX

1. INTRODUCTION

1.1 PRIMARY HYPOBETALIPOPROTEINEMIAS

Primary hypobetalipoproteinemias (pHBLs) represent a heterogeneous group of monogenic disorders characterized by low plasma levels of total cholesterol (TC), due to a reduction of plasma lipoproteins containing apolipoprotein B (apoB). The diagnostic criteria adopted for the biochemical diagnosis of these conditions include plasma levels of total cholesterol below the 5th percentile of the distribution in the population, LDL-C below 75 mg/dl and apoB below 50 mg/dl, after the exclusion of secondary causes of low plasma levels of LDL-C and apoB.

Primary HBLs may have dominant or recessive transmission. Dominant HBLs include Familial Hypobetalipoproteinemia Type 1 (FHBL-1), due to mutations in *APOB* gene, Familial Hypobetalipoproteinemia Type 2 (FHBL-2), due to mutations in *PCSK9* gene (1) and Familial Combined Hypolipidemia (FHBL-3), a novel form of primary hypobetalipoproteinemia due to mutations in *ANGPTL3* gene. Recessive HBLs include two rare conditions: Abetalipoproteinemia (ABL, OMIM 200100), due to mutations in *MTTP* gene, and Chylomicron Retention Disease (CMRD, OMIM 246700), due to mutations in *SAR1B* gene.

The diagnosis of dominant pHBLs derives from the observation of the multigenerational presence of related individuals carrying the biochemical HBL trait (low LDL-C and apoB plasma levels). (1)

The diagnosis of recessive pHBLs derives from the observation early in life of the presence of the biochemical pHBLs trait associated with a generally severe clinical phenotype in offspring of normolipidemic parents. (1)

PART I

1.2 *APOB* GENE AND APOLIPOPROTEIN B

APOB gene, located on chromosome 2, spans 43 kb and consists of 29 exons, one of which exon 26, contains more that 7,000 bp which encodes about one half of the full-length protein (2). The proximal promoter region within -150 and +124 controls the gene expression in hepatocytes and enterocytes, so the *APOB* gene expression is tissue-specific since it is expressed only in liver and intestine.

In the liver the transcription of *APOB* gene produces a mRNA of 14 Kb which encodes a protein of 4,536 amino acids, corresponding to apoB-100, the full-length translation product of apoB mRNA. (Figure 1). It is the major protein constituent of liver-derived VLDL, and of IDL and LDL, (the lipoproteins generated from the intravascular metabolism of VLDL) and it acts as a ligand for LDL receptor (LDLr).

The internalization and catabolism of LDL occur mainly via the interaction between apoB and LDLr. ApoB plays a central role in the transport and metabolism of plasma cholesterol and triglycerides. (1)

In the intestine apoB mRNA undergoes a post-transcriptional editing process that converts the glutamine codon CAA at position 2153 into a stop codon. The translation of this mRNA leads to the production of a shorter protein corresponding to the 48% of apoB-100 and designated apoB-48, which is the protein constituent of chylomicrons (Figure 1).

ApoB-100 is one of largest monomeric proteins known. A pentapartite model for apoB-100 on LDL has been proposed, in which the apoB polypeptide can be divided into five structurally distinct domains, namely NH_2-$\beta\alpha$1- β1- α2-

β2- α3-COOH. (3) The amino acid sequence of the βα1 domain is homologous to lamprey lipo-vitellin and microsomal triglyceride transfer protein (MTP) (4, 5). The βα1 domain of human apoB has thus been modelled on the basis of the solved lipovitellin structure, in which 13- β-strands (amino acids 21–263) form a β barrel, followed by a two-layered helical bundle consisting of 17 α-helices (amino acids 294–592). In vitro experiments suggest that the βα1 domain contains multiple MTP binding sites encompassing residues 430–570 (6), 512–721 (7), and probably 2–154 (4).

FIGURE 1

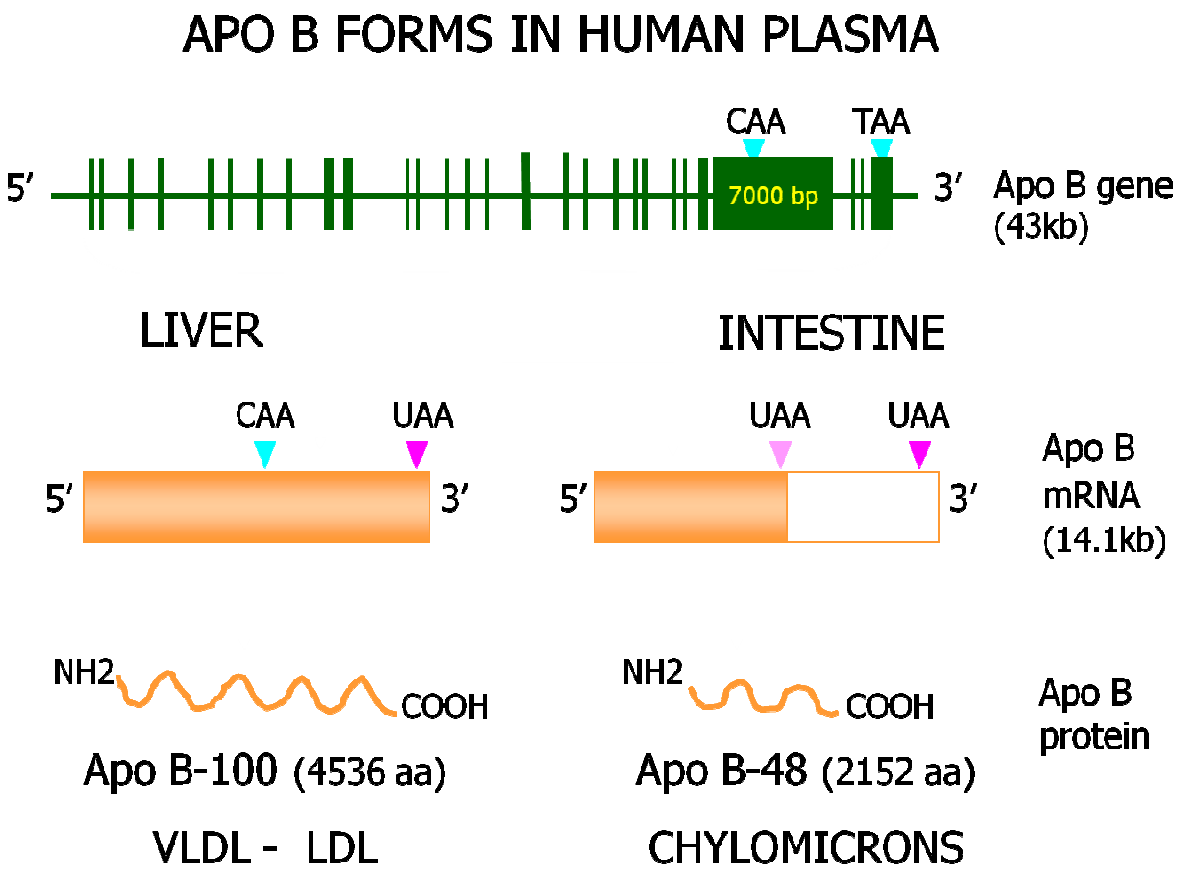

Figure 1. ApoB forms in human plasma.

ApoB-100 and apoB-48 are encoded by the same gene, APOB gene that is located on chromosome 2 and spans 43 kb.

APOB gene is expressed only in the liver and intestine. In the liver the transcription of APOB gene produces a mRNA of 14 kb encoding a protein of 4536 amino acids, corresponding to apoB-100, the protein of VLDL and LDL. In the intestine apoB mRNA undergoes a post-transcriptional editing process that converts the glutamine codon CAA at position 2153 into a stop codon. The translation product of this mRNA is a shorter protein corresponding to the 48% of apoB-100 and designated apoB-48 which is the protein of chylomicrons.

1.3 APOB-CONTAINING LIPOPROTEINS: ASSEMBLY AND SECRETION

ApoB-containing lipoproteins include Chylomicrons, VLDL and LDL.

The common feature of these lipoproteins is the presence of apoB as the main constituent protein. Chylomicrons contain apoB-48 , VLDL and LDL contain apoB-100. (Figure 2)

The assembly of VLDL in the liver and CM in the intestine occurs cotranslationally, during the synthesis of apoB; while the C-terminal end of apoB is still being synthesized, the N-terminal portion is translocated across the endoplasmic reticulum (ER) and is assembled with lipids to form nascent lipoprotein particles for correct targeting to the pathway of lipoprotein secretion. The apoB is targeted to the ER via the signal sequence spanning amino acids 1-27. (8, 9) The assembly of apoB-containing lipoproteins requires the activity of microsomal triglyceride transfer protein (MTP), which is located in the ER lumen as a component of a protein complex involved in the early stages of apoB lipidation in liver and intestine. (10) MTP is a protein of 894 amino acids which has been shown to bind the first 1000 amino acids of mature apoB. The interaction between the apoB $\beta\alpha 1$ domain and MTP appears to be ionic; chemical modification of Lys and Arg residues within LDL or recombinant apoB-18 abolished interactions between apoB and MTP (11). It has been postulated that interaction of MTP and the $\beta\alpha 1$ domain of apoB creates a lipid pocket that facilitates lipid recruitment during lipoprotein assembly (5). The apoB domain involved in the binding with MTP contains the regions spanning amino acid residues 1-264 and 512-721 or 270-570 (4,10).

The physical interaction between apoB and MTP is important for the initiation of translocation of the nascent apoB chain and for the co-translational addition of lipids to this chain (8,9,10). Via these mechanisms, MTP is believed to avoid

improper folding and premature degradation of apoB. So MTP has a crucial role in the assembly and secretion of apoB-containing lipoproteins.

The addition of lipids to apoB is believed to occur in two steps. At first, a small amount of lipids is added to apoB during its translation and translocation into the ER lumen. This initial lipidation prevents apoB degradation and leads to the formation of a partially lipidated small lipoprotein particle. In the second step, the bulk of neutral lipid is added to the primordial lipoprotein particle to form a mature particle for secretion (12, 13). (Figure 3)

The maturation of VLDL and CM, which starts in the ER, is completed in the Golgi apparatus (14). The transport through the secretory pathway is mediated by the coat protein (COP) machinery. The COPII complex, which involves Sar1 proteins, associates with apoB-containing lipoprotein particles and forms ER-derived vesicles that initiate their intracellular transport to the Golgi apparatus, followed by their release into the circulation (15).

In the capillary bed of muscle and adipose tissue, VLDL particles are subjected to the action of Lipoprotein Lipase which hydrolyzes triglycerides to fatty acids. The residual particles (intermediate density lipoproteins, IDL) are either taken up by the liver or further converted to LDL by the action of Hepatic Lipase. LDL contains less TG than VLDL or IDL, and more cholesterol.

FIGURE 2

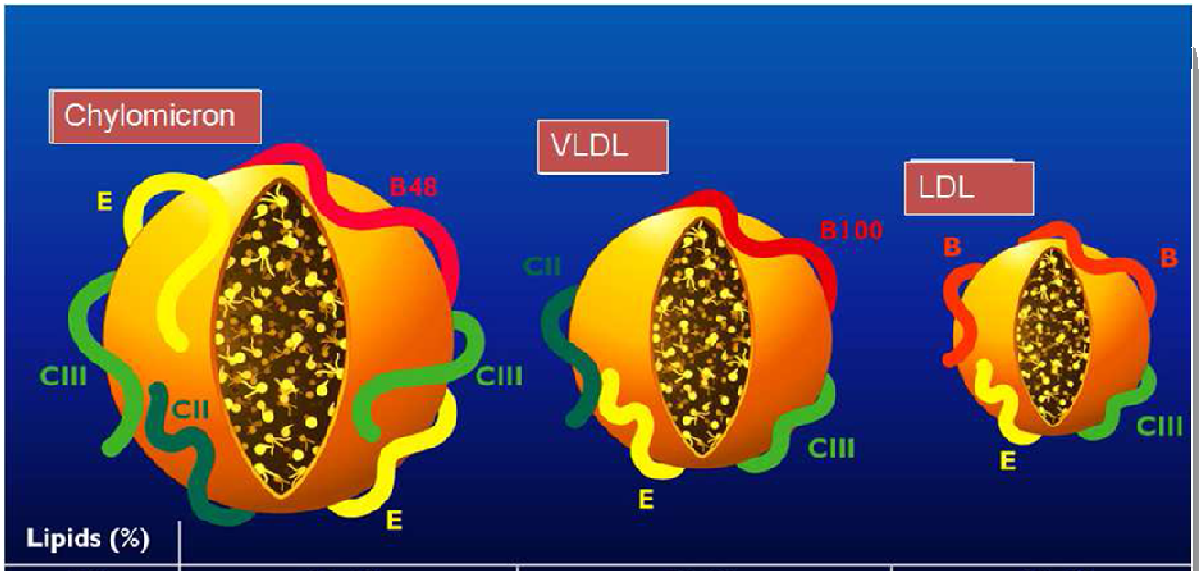

Lipids (%)			
TG	85–90	50–60	18–25
Cholesterol	2–6	14–22	30–38
Phospholipid	6–9	12–20	20–28
Size (Å)	800–5000	300–800	200–350

Figure 2. ApoB-containing lipoproteins.

ApoB-containing lipoproteins include Chylomicrons, VLDL and LDL.
The common feature of these lipoproteins is the presence of apoB, indicated in red, as the main constituent protein.
Chylomicrons contain apoB-48 , VLDL and LDL contain apoB-100

FIGURE 3

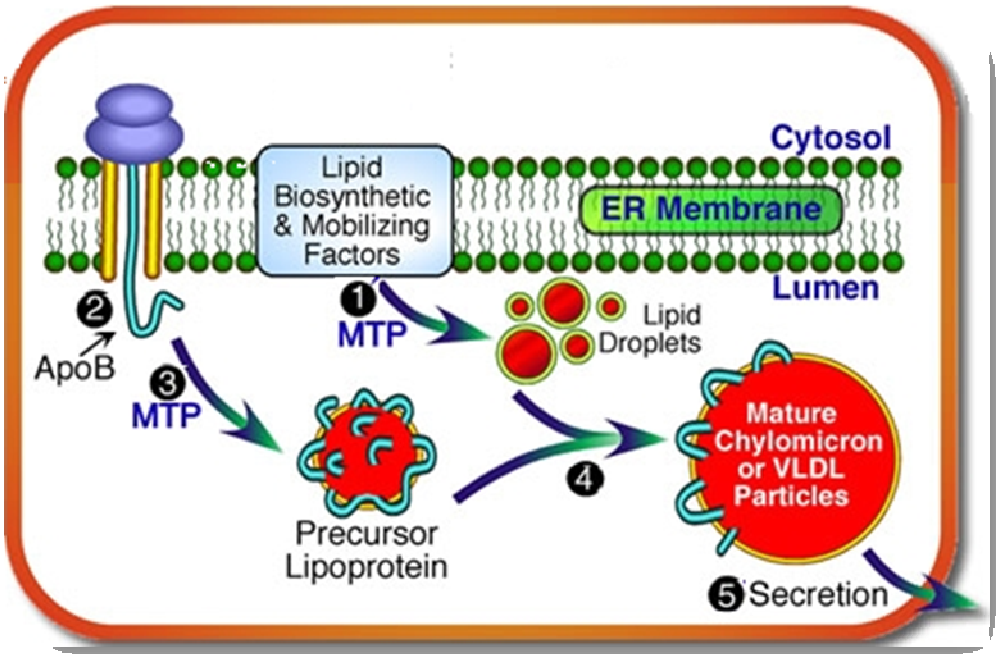

Figure 3. Assembly and secretion of apoB-containing lipoproteins.

In both liver and intestine, the assembly and secretion of apoB-containing lipoprotein requires not only APOB but also another protein designated microsomal triglyceride transfer protein (MTP), a protein complex present in the lumen of the ER.

MTP is involved in the lipidation of apoB during its translocation in the ER lumen to form lipid droplets (1); it promotes the transfer of lipids to nascent apoB (2) to form precursor lipoprotein particles (3); finally these lipoprotein particles fuse with lipid droplets (4) to form mature intestinal chylomicrons or VLDL particles (5), which are then secreted via the classical secretory pathway.

(http://www.wakehealth.edu/Research/Lipid-Science/Gregory-S--Shelness,-PhD.htm)

1.3.1 CONTROL OF APOB PRODUCTION AND SECRETION OF APOB-CONTAINING LIPOPROTEINS

In view of the essential role of apoB in the assembly and secretion of apoB-containing lipoproteins, the production of apoB protein is regulated at multiple levels. The transcriptional regulation of *APOB* gene expression in the liver and intestine is mediated by two sets of very different regulatory elements in separate spatial locations, sharing only the promoter. Regulatory elements extending upstream and downstream of the *APOB* promoter are adequate for hepatic expression of the *APOB* gene, whereas intestinal expression depends on the intestinal control region located upstream of the *APOB* gene (16, 17).

Under physiological conditions, the regulation of apoB secretion may occurs at the level of translation, translocation and degradation. Structural properties of the 5'- and 3'- untranslated regions of apoB mRNA, containing sequence elements with the potential to form stable secondary structure, are important regulators of the expression and translation of apoB mRNA (18).

The newly synthetized apoB chain must be translocated across the endoplasmic reticulum (ER) membrane for correct targeting to the pathways of lipoprotein assembly and secretion *(section 1.3).*

Successful transport and correct folding of apoB may lead to its final secretion as a lipoprotein constituent. Several factors influence the translocation process of newly synthesized apoB. Most relevant is the availability of lipids at the site of apoB synthesis in the ER, which appears to dictate the amount of apoB secreted. In addition, the process of translocation is affected by the characteristics of apoB itself, including length, signal peptide polymorphism and apoB folding to attain lipid-binding capability, which regulate its ability to

assemble into lipoproteins (16). In the case of lipid shortage, nascent apoB translocation into the ER lumen is inefficient and domains of apoB are exposed to the cytosol, where newly synthesized apoB undergoes rapid intracellular degradation (9).

1.3.2 INTRACELLULAR DEGRADATION OF APOB

The regulation of the secretion of apoB-containing lipoproteins is complex and is related to the intracellular apoB degradation. Availability of the lipid components of VLDL and hormonal factors play critical roles in determining the fate of apoB in hepatocytes (19). Early studies in both human HepG2 cells and rat primary hepatocytes indicated that a significant proportion of newly synthesized apoB was not secreted, but degraded intracellularly (19).

Hepatic secretion of apolipoprotein B is regulated primarily by post-translational degradation of the newly synthesized protein. There are three known pathways for post-translational degradation of apoB:

i) Endoplasmic reticulum association degradation (ERAD), which is stimulated by severe lipid deprivation and mediated by the ubiquitin-proteasome system (20);

ii) post-ER presecretory proteolysis (PERPP), achieved by autophagy, which is triggered by intracellular reactive oxygen species (ROS) and may explain the lipid-lowering effects of polyunsaturated fatty acids; (20)

iii) receptor-mediated degradation, also known as reuptake, which occurs via cell surface and intracellular interactions of nascent apoB-particles with LDL receptors (32-33) and heparan sulfate proteoglycans (21).

PERPP occurs when TG availability and incorporation into VLDL is normal while ERAD plays a major role in the degradation of apoB that occurs when lipids are limiting.

Autophagy is a degradation pathway that reduces ER stress, particularly from the threat of protein aggregation. If ERAD efficiency is compromised, substrates that accumulate over time might also aggregate, but in some cases this threat is reduced by autophagy-mediated destruction. During ER-stress-induced autophagy, portions of the ER, along with proteins and protein aggregates, are engulfed in double-membrane structures called autophagosomes and delivered to the lysosomes or vacuoles for degradation. (22)

ERAD and autophagy are part of an elaborate surveillance system of endoplasmic reticulum called the ER quality control (ERQC) system that facilitates folding and modification of secretory and membrane proteins and eliminates terminally misfolded polypeptides. (23)

1.3.2.1 ENDOPLASMIC RETICULUM ASSOCIATED DEGRADATION, ERAD

Endoplasmic reticulum (ER)-associated protein degradation (ERAD) eliminates misfolded or unassembled proteins that are unable to acquire their native structure to prevent fruitless folding attempts and the accumulation of misfolded polypeptides in the ER. (23) This degradation process occurs in three steps: **1)**recognition and targeting; **2)**retrotranslocation and **3)**degradation (24). (Figure 4)

1)Recognition and targeting (substrate recognition within the ER and targeting to the retrotranslocon). The mechanism by which ERAD substrates are recognized and distinguished from properly folded proteins or those that

are in the process of being correctly folded remains largely unknown. (24) The recognition of misfolded or mutated proteins depends on the detection of substructures within proteins such as exposed hydrophobic regions, unpaired cysteine residues and immature glycans. At this first step the molecular chaperones plays a crucial role; they include several families of highly conserved proteins. The main function of molecular chaperones is the maintenance of the protein structure and the prevention of incorrect folding and the aggregation of misfolded or unfolded proteins, both in physiological conditions and in stress conditions.

Most of these chaperones are also Heat shock proteins and are classified according to their molecular weight. The main Heat-shock protein involves in recognition phase is a heat-shock protein of 70 kDa (Hsp70), characterized by a carboxy-terminal domain (about 25 kDa) containing the binding site for the polypeptide and an amino-terminal domain (approximately 40 kDa) with ATPase activity containing the binding site for ADP/ATP. Its activation requires the hydrolysis of ATP stimulated by a co-chaperone family of Heat-shock protein 40 kDa (Hsp40). The interaction between a substrate and Hsp70 may be sufficient to allow the poly-ubiquitination and subsequent degradation of the same (22).

2) Retrotranslocation (substrate delivery from the ER to the cytosol): after recognition and targeting of the substrates, they must be dislocated/retrotranslocated from the ER into the cytosol for degradation.

3) Degradation (ubiquitin–proteasome dependent degradation): it occurs in cytosol by ubiquitin–proteasome system. The ubiquitin protein consists of 76 amino acids and it is highly conserved among eukaryotic species. Its main function is to ensure efficient delivery of the substrates to the proteasome. The

ubiquitin protein form a covalent bond with the proteins that are to be subsequently recognized and degraded by the proteasome. (Figure 4)

ERAD substrates are ubiquitinated at serine/threonine residues and less frequently at lysine residues (24). Ubiquitinated substrates are transferred to the proteasome by shuttle proteins, which contain ubiquitin-associated (UBA) and ubiquitin-like (UBL) domains that bind to polyubiquitin chains and the proteasome subunits, respectively (23-27)

The ubiquitination of terminally misfolded proteins is caused by a cascade of enzymatic reactions. The first of these reactions takes place when the ubiquitin-activating enzyme E1 hydrolyses ATP and forms a high-energy thioester linkage between a cysteine residue in its active site and the C-terminus of ubiquitin. The resulting activated ubiquitin is then passed to E2, which is a ubiquitin-conjugating enzyme. Another group of enzymes, more specifically ubiquitin protein ligases called E3, bind to the misfolded protein. Next they align the protein and E2, thus facilitating the attachment of ubiquitin to lysine residues of the misfolded protein. Following successive addition of ubiquitin molecules (at least four) to lysine residues of the previously attached ubiquitin, a polyubiquitin chain is formed. (Figure 5). A polyubiquitinated protein is produced and this is recognized by specific subunits in the 19S capping complexes of the 26S proteasome. The proteasome is a cylindrical complex containing a "core" of four stacked rings forming a central pore. Each ring is composed of seven individual proteins. The inner two rings are made of seven β subunits that contain three to seven protease active sites. These sites are located on the interior surface of the rings, so that the target protein must enter the central pore before it is degraded. The outer two rings each contain seven α subunits whose function is to maintain a "gate" through which proteins enter the barrel. These α subunits are controlled by

binding to "cap" structures or regulatory particles that recognize polyubiquitin tags attached to protein substrates and initiate the degradation process.

Although the identities of the components that comprise the retrotranslocation channel remain unclear, Sec61 complex and Derlin-1 are possible candidates. (23, 24) Specifically, Sec61 complex has been reported to interact with several ERAD substrates and ERAD machineries including proteasome. (23, 24)

The polypeptide chain is fed into the central chamber of the 20S core region of the 26S proteasome that contains the proteolytically active sites. Ubiquitin is cleaved before terminal digestion by deubiquitinating enzymes.

The ERAD pathway is not only an ER quality control process but is also used to regulate metabolic processes. For example, in the lipid-ligand deficient state, which occurs if MTP activity is low (9, 28), or when lipid availability or synthesis is reduced (9,29,30), apoB is cotranslationally targeted for ubiquitinylation and degradation by the proteasome. As observed for some ERAD substrates (9,31), the cytosolic Hsp70 and Hsp90 molecular chaperones are critical for this process; by contrast, the Hsp110 chaperone protects apoB from degradation (9,30,32). The ER lumenal chaperone, BiP, also facilitates apoB degradation (33), as does a BiP-interacting co-chaperone, known as p58 (9,34,35). Although apoB has hydrophobic interactions with the ER membrane, its removal to the cytosol is most likely via retrotranslocation based on its persistent association with Sec61 (9,34,36).

Because the ERAD machinery cannot access protein aggregates in the Golgi, it was not clear how these apoB-containing particles were destroyed. However, it was discovered that the turnover of the apoB aggregates is related to the correct efficiency of the autophagic pathway. (Figure 6) (9)

FIGURE 4

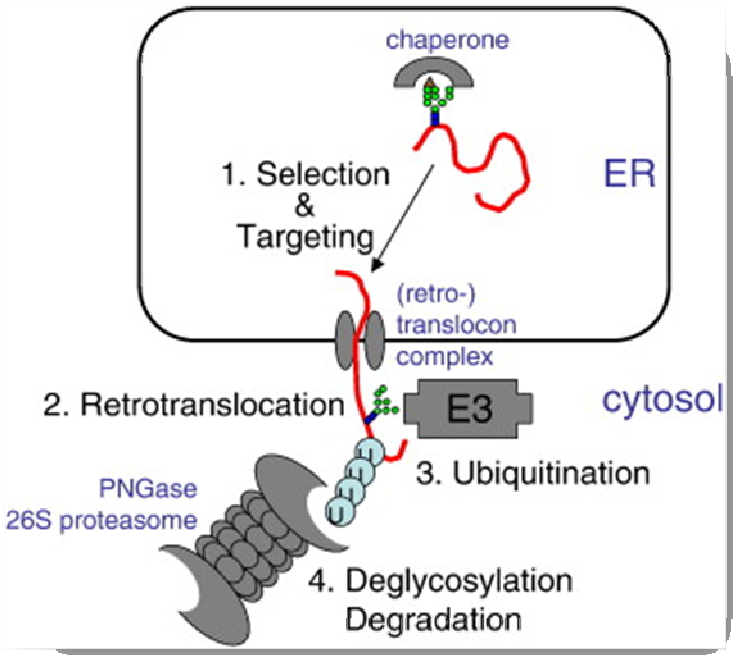

Figure 4. The ERAD pathway.

In step 1, misfolded glycoproteins are recognized by chaperone molecules or enzymes and targeted to the (retro-)translocon complex. In step 2, polypeptides are retrotranslocated from the ER into cytosol through the channel. In step 3, polyubiquitination occurs when the polypeptide chain becomes accessible in the cytosol. In step 4, polypeptides modified by the polyubiquitin chain are degraded by the proteasome.

(Yukiko Yoshida, Lectin-like ERAD players in ER and cytosol, BBA 2010; 1800:172-180)

FIGURE 5

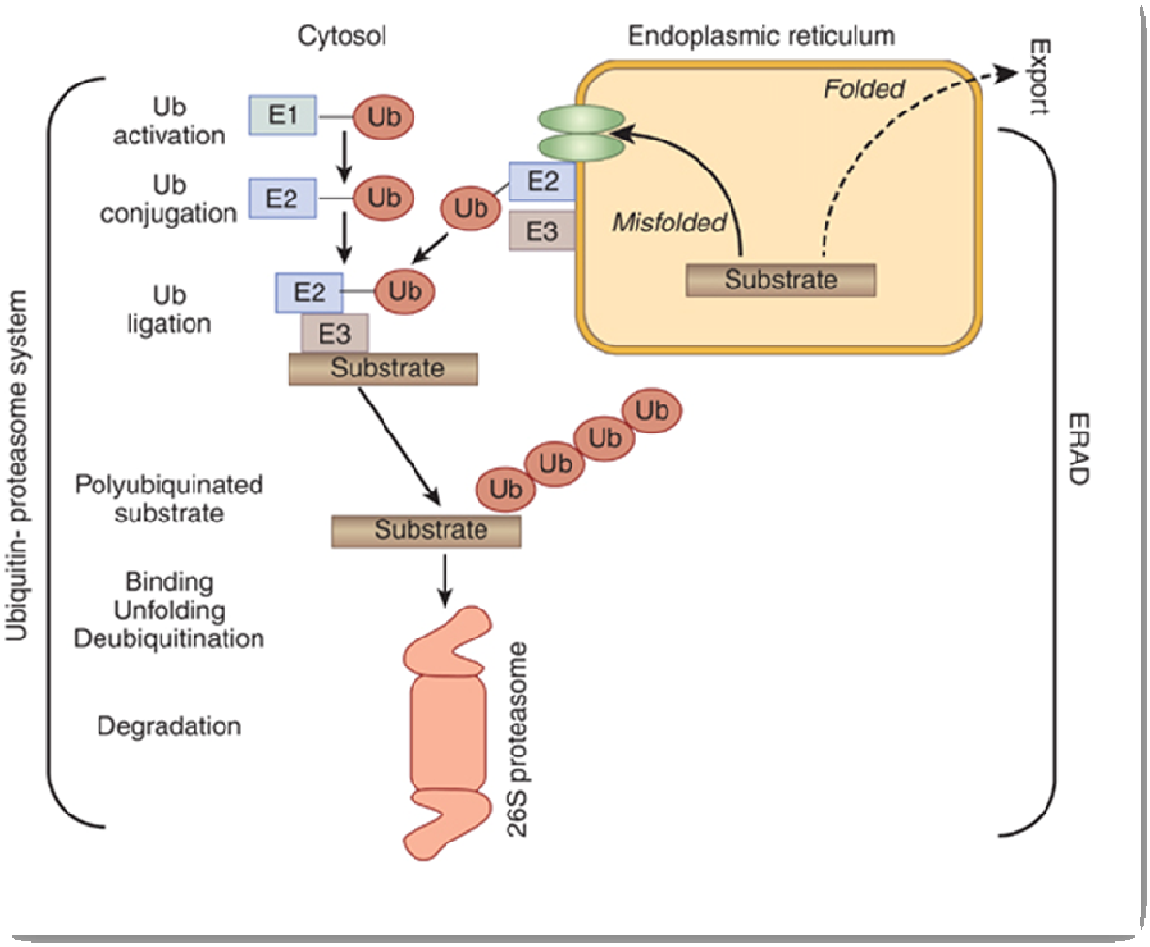

Figure 5. The ubiquitin–proteasome system (UPS) and endoplasmic reticulum–associated degradation (ERAD).

In the cytosol, or at the cytosolic face of the endoplasmic reticulum (ER), ubiquitin (Ub) is attached to a misfolded protein or a protein with a degradation signal through an enzymatic cascade involving E1, E2, and E3 enzymes. After attachment of at least four ubiquitin molecules, the substrate is targeted to the 26S proteasome. Unfolding and deubiquitination of the substrate take place before degradation in the interior chamber.

(Cybulsky AV, The intersecting roles of endoplasmic reticulum stress, ubiquitin-proteasome system, and autophagy in the pathogenesis of proteinuric kidney disease, Kidney International 201

FIGURE 6

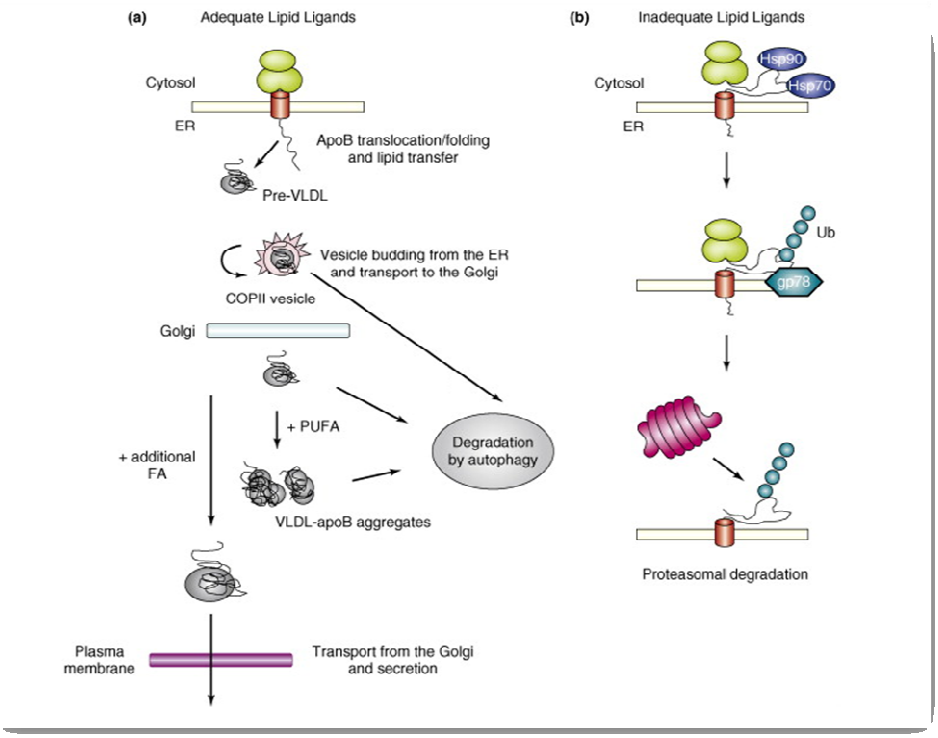

Figure 6. Schematic summary of apoB secretory regulation.

a*) With adequate lipid ligands, apoB is translocated into the ER where it is folded and stabilized in the proper conformation. Primordial VLDL particles are formed (pre-VLDL) and transported to the Golgi apparatus in COPII vesicles. When polyunsaturated fatty acids (PUFA) comprise a critical complement of lipid species associated with apoB lipoproteins, lipid peroxides are produced that damage and cross-link apoB, most likely in the Golgi as part of the VLDL maturation process. Eventually, aggregates are formed that are degraded by autophagy. At subcritical PUFA levels, VLDL matures normally and is secreted.*

b) *With insufficient lipid ligands nascent apoB translocation into the ER lumen is inefficient and domains of apoB are exposed to the cytosol where the particle is selected by chaperones (Hsp70 and Hsp90) for ERAD. The substrate is polyubiquitined and degraded by the proteasome.*

(Brodsky JL, Fischer EA, The many intersecting pathways underlyng apolipoprotein B secretion and degradation, Trends Endocrinol Metab, 2008; 7: 254-9)

1.3.2.2 AUTOPHAGIC DEGRADATION OR AUTOPHAGY

Originally, autophagy was thought to operate only during nutrient starvation to reclaim essential amino acids from cytosolic proteins. It is now recognized that autophagy mediates the degradation of damaged organelle fragments, cytosolic proteins, and protein aggregates, each of which can be engulfed by double-membrane vesicles (autophagosomes) that deliver these cargo for degradation in the lysosome (37,38).

Autophagy acts as a survival mechanism under conditions of stress, maintaining cellular integrity by regenerating metabolic precursors and clearing subcellular debris components through the lysosomal machinery (38-40). This process contribuites to basal cellular and tissue homeostasis, as well as development regulation in higher organism and can affect pathogenesis. Autophagy participates in the turnover of mitochondria and other organelles; it is involved in the clearance of polyubiquitinated protein aggregates which accumulated during stress, aging and disease owing to perturbation in protein structure or folding. Autophagy has also been implicated as a regulator of lipid metabolism (40, 41); it acts as a protective mechanism that prevents cell death and it can ensure cellular survival during starvation by maintaining cellular energy levels. (42)

Autophagy assists in the immune response by degrading intracellular bacteria and viruses (40); it contributes to the suppression of inflammation, and play a crucial roles in adaptive immune responses.

During autophagy process, targeted cytoplasmic constituents are isolated from the rest of the cell within the autophagosomes, which are then fused with lysosomes and degraded or recycled. There are three different forms of

autophagy that are commonly described, which include chaperone-mediated autophagy, microautophagy and macroautophagy.

In chaperone-mediated autophagy, the cytosolic proteins containing the recognition site, are recognised and bound from a chaperonine. The complex then moves to the lysosome membrane where the proteins were degraded.

The microautophagy involves the direct engulfment of cytoplasmic material into the lysosome, through invagination, meaning the inward folding of the lysosomal membrane, or cellular protrusion.

Macroautophagy is the main pathway, often defined simply as autophagy, involves the sequestration of cytoplasmic components in double-membraned autophagosome (Figure 7). These structures subsequently fuse with lysosomes (40) forming the autolysosome. The autophagosomal contents are degraded by lisosomal acid hydrolases and the contents of the autolysosome are released for metabolic recycling (40).

Many genes and regulatory complex are known to be required for autophagy induction and autophagosome formation. When the signal induces the formation of double membrane structure which sequester portion of cytoplasm along with proteins or damaged cell organelles to be degraded, the Atg12-Atg5-Atg16L complex and LC3 (microtuble-associated protein light chain 3) localize to the phagophore throughout its elongation process. The precursor form of LC3 is cleaved to generate the LC3-I form; the conjugation of LC3-I (free form) with the cellular lipid phosphatidylethanolamine (PE) generates the LC3-II (PE-conjugated form). Upon completion of autophagosome formation, the Atg12-Atg5-Atg16L complex dissociates from the membrane while LC3-II remain on it. LC3 has been used as a specific marker to monitor autophagy; when autophagosome formation is activated,

LC3-II is increased. The conversion of LC-I to LC-II is a key regulatory step in autophagosome formation (40)

FIGURE 7

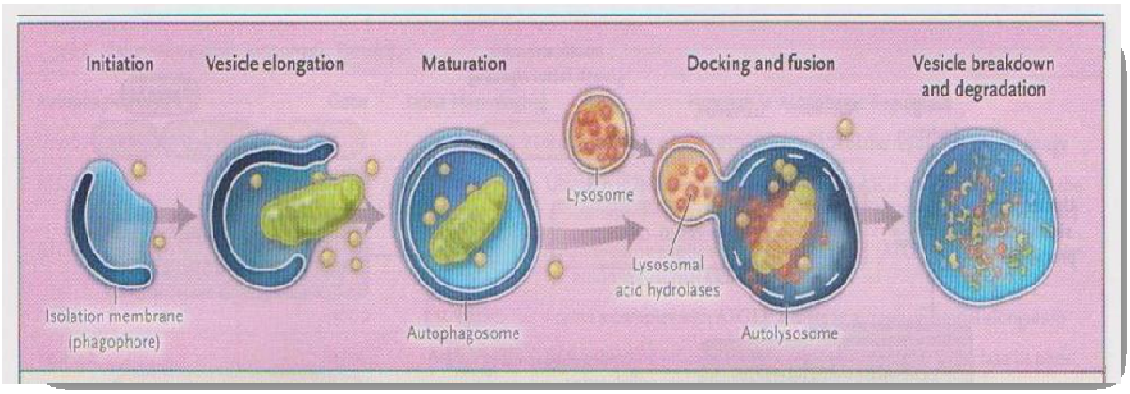

Figure 7. Phases of the Autophagic Pathway.

The autophagic pathway proceeds through several phases, including initiation (formation of a preautophagosomal structure leading to an isolation membrane or phagophore), vesicle elongation, autophagosome maturation and cargo sequestration, and autophagosome-lysosome fusion. In the final stage, autophagosomal contents are degraded by lysosomal acid hydrolases and the contents of the autolysosome are released for metabolic recycling.

(Choi AM, Ryter SW, Levine B., Autophagy in human health and disease, The New England Journal of Medicine, 2013; 368:651-62)

1.4 FAMILIAL HYPOBETALIPOPROTEINEMIA TYPE 1 (FHBL-1)

Familial Hypobetalipoproteinemia Type 1 (FHBL-1) is a dominant primary HBL due to mutations in *APOB* gene *(section 1.5)* whose frequency in the heterozygous form (as estimated by clinical criteria) is 1:500/1:1000. FHBL heterozygotes are often asymptomatic or have fatty liver disease associated with mild elevation of serum liver enzymes; occasionally they present intestinal manifestations related to mild fat malabsorption. They might be identified either during population screening for low plasma cholesterol levels or in clinical settings when low plasma LDL-C concentrations are associated with unexplained "non alcoholic fatty liver disease " (NAFLD). (2, 43)

FHBL homozygotes are extremely rare. They are identified in clinical settings for extremely low or undetectable plasma levels of LDL-C and apoB, usually associated with variable clinical manifestations (severe intestinal fat malabsorption and fatty liver, neurological disorders). (8, 43-45)

In a substantial number of FHBL-1 (varying from 36% to 56% in the literature) the genetic defect underlying the disorder remains elusive.

1.5 *APOB* MUTATIONS CAUSING FHBL-1

1.5.1 *APOB* MUTATIONS CAUSING THE FORMATION OF TRUNCATED APOBs

Most of the *APOB* gene mutations causing FHBL-1 are nonsense or frameshift mutations (insertions, deletions, splicing mutations) that introduce a premature stop codon in the apoB mRNA leading to the formation of truncated apoBs of various lengths. The truncated apoBs are in the range from

apoB-2 to apoB-89 (i.e. from 2% to 89% of the apoB-100, according to a centile nomenclature) (1,43,45).

Truncated apoBs may be or may be not detectable in plasma. The term "detectable truncation" is used to indicate truncated apoBs which are secreted into the plasma as constituents of plasma lipoproteins and are detected by immunoblot with an anti-apoB antibody. Only truncated apoBs with a size above that of apoB-29/30 are detectable in plasma (43-45). They result from mutations located in the *APOB* gene region spanning from exon 26 to exon 29 (mostly in the 7571 bp long exon 26). Truncated apoBs, whose size is below that of apoB-29/30, are not detectable in plasma, as they are not secreted. They are mostly due to mutations located in the first 25 exons of the *APOB* gene (44).

Plasma apoB and LDL-C levels in heterozygous FHBL subjects carrying apoB truncations are <30% of the normal; these lower than expected levels for the activity of one normal allele are due to a reduction in the production rate of both normal and truncated forms of apoB (44,46,47). Truncated apoB forms represent only 3–9% of the total apoB concentration found in normal subjects; this is due to a combination of low production rate and rapid clearance rate of the truncated forms (48). The relative importance of production and clearance rates in setting plasma levels depends on the size of the truncation: the shorter the truncation, the lower the production rate (49,50). Truncated apoBs shorter than apoB-70.5 are cleared very rapidly from plasma, mostly by the kidney (44,51,52).

An essentially linear relationship between the length of truncated apoB and the secretion rate was observed. *Parhofer KG et al.* demonstrated that apoB secretion is reduced by approximately 1.4% for each 1% of apoB truncated and

that truncated forms of apoB smaller than apoB-28 will not be secreted into plasma. (49) (Figure 8)

Yao et al. (53) speculated that the association with lipid is a prerequisite for secretion and thus the inefficient secretion of short truncated apoBs (apoB-18 to apoB-23) may be due to their inability to acquire a sufficient amount of lipid. This speculation is supported by the finding that in all studied cell systems some apoB is degraded intracellularly (53).

Truncated apoBs lower than apoB-48 are associated with apoB-containing lipoproteins secretion defect in the liver and intestine; the formation of apoB longer than apoB-48 only affect the hepatic secretion of VLDL.

FIGURE 8

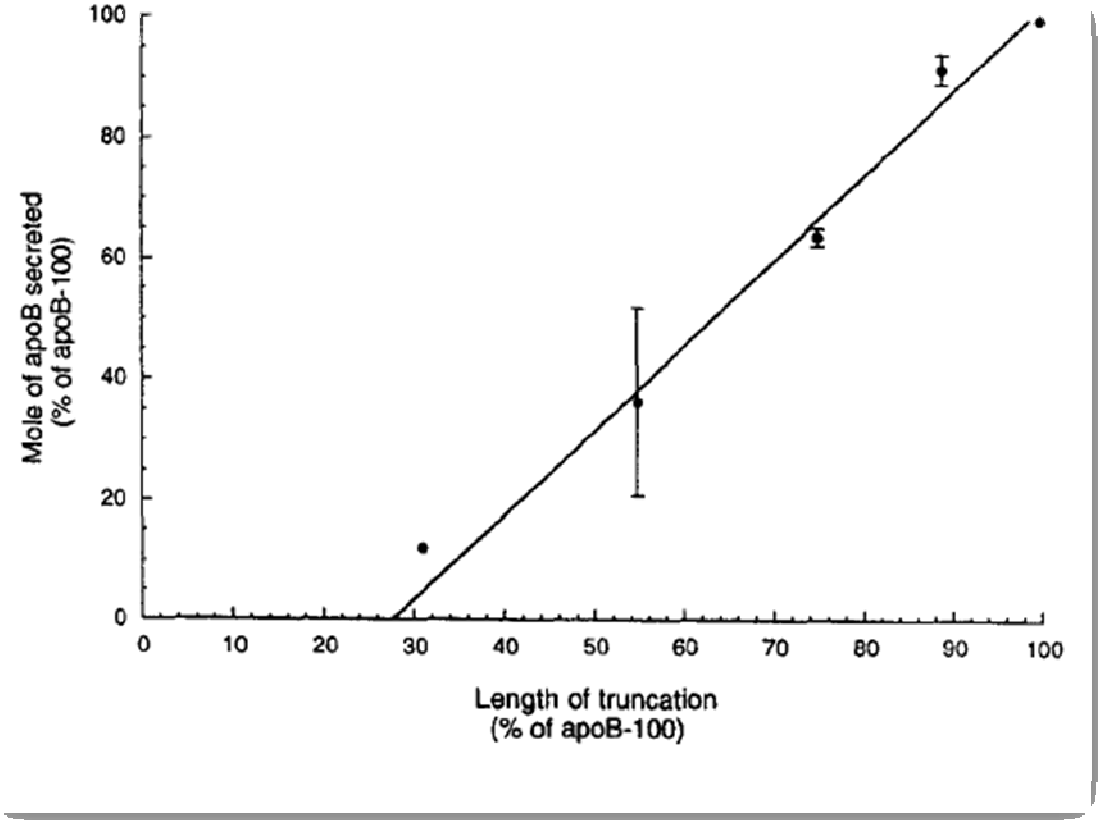

Figure 8. Linear relationship between the length of truncated apoB and the secretion rate.

Secretion of truncated apoB as a function of the size of the apoB truncation. ApoB secretion is expressed on a molar basis as a percentage of apoB-100 secretion determined under identical conditions in the same subject.

Truncated forms of apoB smaller than apoB-28 will not be secreted into plasma.

Brackets indicate standard deviations.

(K.G. Parhofer et al., Positive linear correlation between the length of truncated Apolipoprotein B and its secretion rate: in vivo studies in human apoB-89, apoB-75, apoB-54.8 and apoB-31 heterozygotes. J. Lipid Res 1996; 37:844-852)

1.5.2 NON-CONSERVATIVE APOB AMINO ACID SUBSTITUTIONS AS CAUSE OF FHBL

Few non-conservative apoB amino acid substitutions have been reported to be the cause of FHBL. The amino acid substitutions, R463W and L343V, were the first missense mutations associated to FHBL-1. They were found to co-segregate with FHBL-1 phenotype in two large Libanese kindred (54,55). The effect of these mutations on apoB secretion was assessed by transfection studies using McA-RH7777 cells expressing wild type or mutant forms of human apolipoprotein B. In both cases the mutant proteins were poorly secreted and retained within endoplasmic reticulum. These mutations involve the N-terminal $\beta\alpha$1domain of apoB which contains sequence elements shown to be important for the proper folding of apoB (4,56), for the physical interactions between apoB and MTP (5,58) and for lipid recruitment during lipoprotein assembly and effective secretion (59). This study demonstrated that the missense mutations, R463W and L343V, are cause FHBL because they are associated with a decreased secretion of the mutant apoBs due to a retention in the ER associated with an increased binding to MTP (55, 56).

Other carriers of R463W have been recently identified in Italian, Dutch and Spanish FHBL subjects, suggesting that R463W may be a recurrent mutation in the population (45,60). Recently, five novel amino acid substitutions (A31P, G275S, L324M, G912D, and G945S) have been identified in our laboratory in heterozygous state in Italian FHBL-1 subjects. They are located within the N-terminal 1000 amino acids of apoB (Figure 9). The functional effect of these variants was defined during my pre-PhD experience in Yao's laboratory at University of Ottawa. All of the mutations occur within the $\beta\alpha$1 domain and exhibited varied inhibition on apoB-48 secretion. Although mutations within

the α-helical domain (e.g. G275S, L324M, L343V and R463W) or β-sheets (e.g. G912D and G945S) only moderated impaired apoB secretion (the extent of inhibition varied from 30 to 80% of normal), the A31P mutation that occurred within the β-barrel entirely blocked apoB secretion. (61). In contrast to the two missense mutations L343V and R463W, the A31P mutant did not lead to ER retention as the aberrantly folded protein is degraded intracellularly by proteasomes and autophagosome/lysosome pathway (61).

Plasma levels of LDL-C and apoB in heterozygous carriers of the *APOB* missense mutations are comparable with those present in FHBL due to apoB truncations. The two homozygotes for the missense mutation R463W described so far have barely detectable apoB-containing lipoproteins in plasma (55) as observed in patients homozygotes/compound heterozygotes for short truncated apoBs (62,63).

FIGURE 9

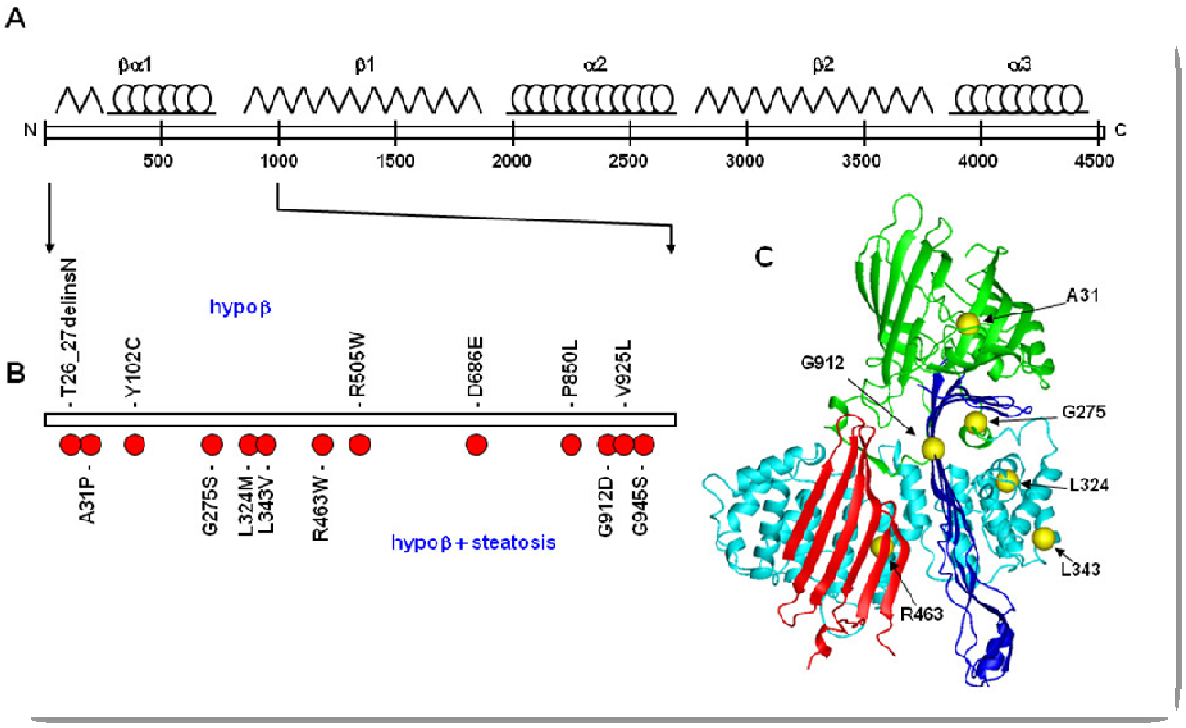

Figure 9. Model of the N-terminal of apoB and positions of FHBL mutations.
A, schematic diagram of apoB-100, with predicted locations of βα1, β1, α2, β2, and α3 domains are shown on the top. B, positions of non-truncating FHBL mutations within the N-terminal 1,000 amino acids of apoB-100. Mutations associated with phenotype of hypobetalipoproteinemia (hypoβ) are shown on the top, whereas mutations associated with phenotype of both hypoβ and hepatic steatosis are shown below. C, proposed homologous model of the N-terminal ~930 amino acids of apoB. The β-barrel, α-helical, and β sheet (C-sheet and A-sheet) are highlighted in green, cyan, red, and blue, respectively. Locations of Ala31, Gly275, Leu324, Leu343, Arg463, and Gly912 within the modeled βα1 domain are shown as yellow spheres.
(Sundaram and Yao, Recent progress in understanding protein and lipid factors affecting hepatic VLDL assembly and secretion, Nutrition & Metabolism; 2010, 7:35)

PART II

1.6 FAMILIAL COMBINED HYPOLIPIDEMIA (FHBL-3)

Recently a novel form of primary hypobetalipoproteinemia has emerged: the condition defined as Familial Combined Hypolipidemia (FHBL-3) is characterized by reduced plasma levels of total cholesterol, LDL-C and apoB, (similar to those found in classic FHBL-1), associated with a reduction of plasma TG and HDL-C.

This combined hypolipidemia phenotype has been associated with mutations in *ANGPTL3* gene about two years ago, when, by using the strategy of exome sequencing, *Musunuru et al*. identified *ANGPTL3* gene mutations in four individuals belonging to a kindred originally diagnosed as affected by FHBL, in whom mutations in *APOB* and *PCSK9* genes had been excluded. (64) The four individuals with a combined hypolipidemia phenotype were found to be compound heterozygotes for loss-of-function (LOF) mutations (p.E129*/p.S17*), in *ANGPTL3* gene which are expected to cause a complete deficiency of ANGPTL3.

Martin-Campos et al. resequenced the *ANGPTL3* gene in three hypocholesterolemic individuals belonging to two Spanish families with FHBL not linked to the *APOB* gene (65, 66). These individuals were found to be homozygotes for a 5-bp deletion resulting in a truncated ANGPTL3 protein (p.N121K*3). More recently, *Minicocci et al.* resequenced the *ANGPTL3* gene in a cluster of FHBL families identified in a small town in Central Italy and apparently not linked to *APOB* gene (67). Overall, the *ANGPTL3* gene was resequenced in nine index cases (plasma LDL-C <fifth percentile), 28 first-degree relatives, 11 second-degree relatives and four spouses. This survey led

to the identification of six homoygotes and 24 heterozygotes for a 2-bp change at nucleotides 50–51 of exon 1 (c.50 CC>GA), introducing a premature termination (p.S17*) (67). The plasma lipid profile found in the homoyzgotes was consistent with a familial combined hypolipidemia phenotype, even though, on average, the values of TC, LDL-C and HDL-C were higher than those found in carriers of two LOF alleles belonging to the other kindreds investigated so far (64, 66).

Thus, ANGPTL3 gene has recently emerged as novel gene in lipoprotein arena, as a promising candidate gene involved in FHBL cases not linked to other candidate genes.

Recently, *Noto et al.* reported the impact of *ANGPTL3* mutations as the cause of a combined hypolipidemia phenotype in subjects with the clinical diagnosis of putative FHBL (68). From a large cohort of putative FHBL subjects (390 Italians and 523 Americans) they selected 78 individuals negative for mutations in APOB gene who presented with a combined hypolipidemia phenotype, defined by stringent criteria (i.e., TC <second percentile and HDL-C <second decile of the populations) (64). The analysis of A*NGPTL3* gene revealed that eight of them were carriers of rare *ANGPTL3* mutation (four carriers of two mutant alleles and four carriers of one mutant allele). The mutations resulted in either truncated proteins or single rare non conservative amino acid substitutions expected to be deleterious for ANGPTL3 function. In this study, the plasma lipid profile of carriers of two mutant *ANGPTL3* alleles was fairly similar to that found in other subjects with familial combined hypolipidemia (64, 66).

FHBL-3 does not seem to be associated with specific clinical manifestations, such as premature atherosclerosis or fatty liver disease

1.6.1 *ANGPTL3* GENE AND ANGPTL3 PROTEIN

Human *ANGPTL3* (*Angiopoietin-like 3)* gene is located on chromosome 1 (1p31), contains seven exons and extends for about 7 Kb. (69) (Figure 10A)
ANGPTL3 mRNA consists of 2,805 nucleotides and is exclusively expressed in the liver. It encodes for a secreted protein indicated as ANGPTL3, a 460-amino acid polypeptide which belongs to the angiopoietin-like family. As the other members of the angiopoietin-like family, it shows the characteristic structure of the angiopoietins, members of the vascular endothelial growth factor family; in contrast with other members of the angiopoietin family, ANGPTL3 cannot bind the angiopoietin receptors (TIE1 and TIE2) specifically expressed on endothelial cells (1, 70).
ANGPTL3 consists of a signal peptide, an N-terminal segment containing coiled-coil domains and a C-terminal fibrinogen-related domain, which are connected by a linker region. ANGPTL3 is susceptible to proteolytic cleavage at specific sites (position 221 and 224) in the interlinker region by the action of several hepatic pro-protein convertases (PCs): Furin, PCSK2,PCSK4, PACE4, PCSK5 and PCSK7 (65, 71). (Figure 10B). It has been observed that the substitutions of five different amino acid residues located in and near the linker region alters ANGPTL3 susceptibility to the cleavage in *vivo* (72). ANGPTL3 is involved in lipid metabolism as it acts as dual inhibitor of Lipoprotein Lipase (LPL) and Endothelial Lipase (EL) activity. Recently, a specific amino acid sequence of the N-terminal of ANGPTL3 has been identified as the domain responsible of interaction of ANGPTL3 with LPL and EL *(section 1.6.2.1 and 1.6.2.2).*

FIGURE 10

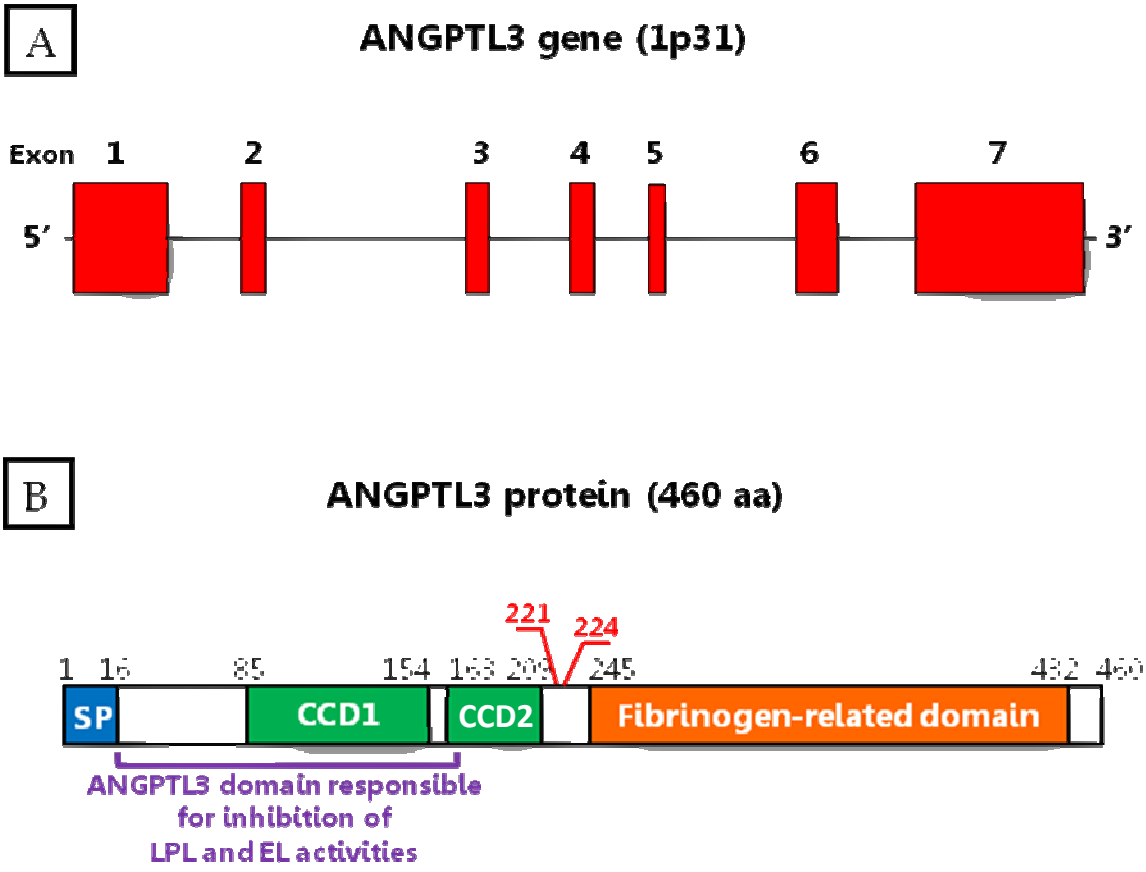

Figure 10. ANGPTL3 gene and functional domains of ANGPTL3 protein.

A. Schematic representation of human ANGPTL3 gene, encoding for 460 amino acids angiopoietin-like 3 protein (ANGPTL3).

B. A linear representation of the ANGPTL3 protein showing the main functional domains: a signal peptide (amino acids 1-16), followed by the coiled-coils domain (CCD, amino acids 17-209) and the Fibrinogen-related domain (FBG-like domain, amino acids 245-460). The position of the two major cleavage sites in the linker region is indicated in red; the domain responsible for ANGPTL3 inhibition of LPL and EL activities is indicated in violet (amino acids 17-165).

1.6.2 FUNCTIONS OF ANGPTL3 PROTEIN

ANGPTL3 protein is involved both in angiogenesis and in the regulation of lipid metabolism. The study of ANGPTL3 structure-activity relation has pointed out that two different domains of the protein are responsible for the two different functions. It is reported that, even if it lacks of the cystein-based motif important for Tie2 binding, ANGPTL3 can elicit angiogenesis: the FBN-like domain allows ANGPTL3 protein to bind α-5 and β-3 integrins, inducing endothelial cell adhesion and migration. (73)

On the other side, the N-terminus coiled-coils domain is responsible for ANGPTL3 regulation of lipid metabolism, as it contains the functional domains involved in Lipoprotein Lipase (LPL) and Endothelial Lipase (EL) inhibition *(section 1.6.2.1 and 1.6.2.2).* LPL, located on the luminal surface of capillaries, catalyzes the hydrolysis of tryglicerides (TG), such as those found in chylomicrons and very low-density lipoproteins, releasing free fatty acids. EL, secreted by endothelial cells, catalyzes the hydrolysis of HDL phopsholipids, facilitating HDL clearance from circulation. ANGPTL3 markedly inhibits both LPL and EL activity in a dose-dependent manner, thus increasing the plasma levels of circulating TG and HDL, respectively. (74, 75) The amino acid sequence of EL and LPL is 44% identical; the clusters of positively charged residues involved in heparin binding domain are conserved between EL and LPL. (75)

The first observation which demonstrated a link between ANGPTL3 and lipoprotein metabolism was made by *Koishi et al.* who investigated a mouse strain (KK/San or KK/Snk) derived from the colony of KK mice characterized by obesity, diabetes and hypertriglyceridemia (65, 76). The KK/San mice, despite maintaining the phenotype of obesity and diabetes, had a marked

decrease (>90%) of plasma triglyceride (TG) as compared with the original hyperlipidemic KK mice (65). This hypotriglyceridemia was associated not only with a reduction in pre-β lipoproteins (VLDL), but also in the β- and α-lipoproteins (LDL and HDL, respectively). The hypotriglyceridemia of KK/San mice was found to be inherited as a recessive trait.

Koishi et al. also showed that treatment with recombinant ANGPTL3 or adenovirus-mediated overproduction of ANGPTL3-elevated plasma TG and total cholesterol (TC) (65, 76). Subsequent studies showed that ANGPTL3 increased VLDL-TG levels by inhibiting lipoprotein lipase (LPL) activity (69, 72) and that the plasma TG level was markedly reduced in *Angptl 3* null mice (*Angptl3-/-*) (65, 77). An extensive investigation of *Angptl3-/-* mice fed a normal diet or a high-fat diet revealed a great reduction of plasma lipid levels (78). This confirmed that the complete ANGPTl3 deficiency had a profound effect not only on TG-containing lipoproteins (VLDL), but also on cholesterol-carrying lipoproteins such as LDL and HDL (65).

1.6.2.1 ANGPTL3 AND LPL INTERACTION

ANGPTL3 is a potent inhibitor of LPL and it enhances LPL turnover by increasing its cleavage. The region involved in interaction between ANGPTL3 and LPL, corresponds to amino acids E32–H55; a mouse antibody against this region inhibited the binding of ANGPTL3 to LPL and neutralized ANGPTL3-mediated inhibition of LPL (65, 79). The mechanism underlying the inhibition of LPL by ANGPTL3 appears to be manifold. By using enzyme kinetic analysis with purified recombinant proteins, *Shan et al.* found that ANGPTL3 reduced LPL catalytic activity (i.e., the activity of the dimeric form of LPL), but did not

significantly alter the LPL self inactivation rate (i.e., the process leading to the irreversible disruption of the dimeric form of the enzyme) (65).

An alternative or complementary mechanism of inhibition of LPL has emerged from *in vitro* cell-based studies that investigated the interactions among ANGPTL3, hepatic pro-protein convertases (PCs) and LPL. These studies demonstrated that LPL is inactivated by cleavage by PCs and that ANGPTL3 is a potent inhibitor of LPL in physiological concentrations and in the presence of cells by enhancing the cleavage of LPL by PCs such as furin and PACE-4. By enhancing LPL cleavage, ANGPTL3 dissociates LPL from the cell surface, thus inhibiting both the catalytic and non catalytic functions of this enzyme (65, 80). So ANGPTL3-mediated LPL suppression is an indirect process; ANGPTL3 is not able to directly cleave LPL but it indirectly inhibits LPL activity by enhancing LPL cleavage.

One interesting question is whether ANGPTL3 exerts its inhibitory effect on the LPL that is bound to TG-rich lipoproteins (chylomicrons and VLDL) or to GPIHBP1, the platform for LPL-processing of TG-rich lipoproteins (65, 81). Recently, *Nilsson et al.* have investigated the effects of some lipoproteins (chylomicrons, VLDL and LDL) on the inactivation of LPL *in vitro* by the human N-terminal fragment of ANGPTL3 (65, 82). They found that the presence of chylomicrons and VLDL protected LPL against inactivation by ANGPTL3. On the other hand, it has been shown that ANGPTL3 inhibits heparin-bound LPL but not LPL bound to GPIHBP1 (65, 83). So it appears that ANGPTL3 exerts its inhibitory effect predominantly on nonstablized LPL (65).

1.6.2.2 ANGPTL3 AND EL INTERACTION

Several study have revealed that EL regulates HDL metabolism. An over-expression of EL in mice resulted in reduced plasma HDL levels, while EL knockout mice showed significant increase of plasma HDL. (84, 85)

ANGPTL3 is capable of inhibiting endothelial lipase (EL). *Shimamura et al.* found that *Angptl3*-/- had low plasma HDL cholesterol (HDL-C) levels accompanied by increased phospholipase activity (75), indicating that the activity of EL (which acts as a phospholipase) is elevated in these mice and that ANGPTL3 acts as an endogenous inhibitor of EL (65). The inhibition of hepatic pro-protein convertases, which are responsible for the activation of ANGPTL3 attenuated the inhibitor effect of ANGPTL3 on EL (65, 86).

By producing truncated and/or mutated ANGPTL3 proteins, *Shimamura et al.* demonstrated that both full-length ANGPTL3 and the N-terminal coiled-coils region of the protein suppressed EL activity in a similar manner. Then they observed that this inhibitory effect was completely abolished when the region of the heparin-binding site was mutated: the putative heparin-binding site in the N-terminal region is essential for ANGPTL3-induced suppression of EL activity.

FIGURE 11

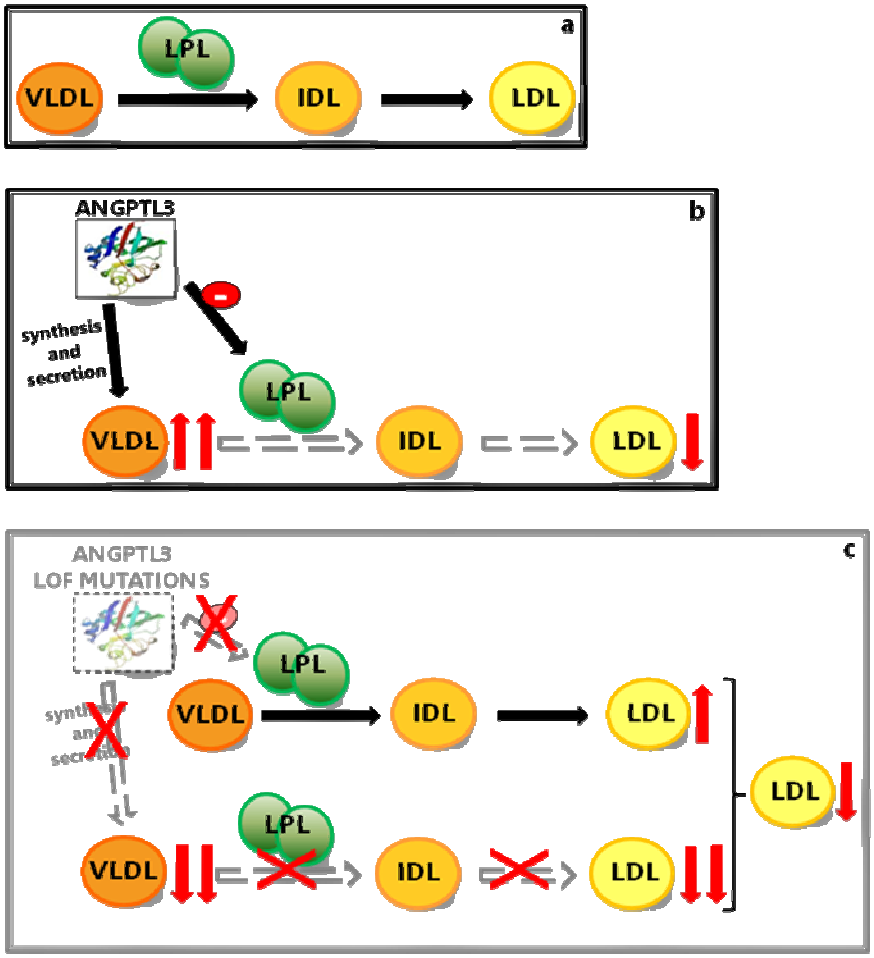

Figure 11. A proposed working model: ANGPTL3 loss-of-function mutations. *a)Lipoprotein lipase (LPL) is involved in the intravascular conversion of VLDL into LDL.*

b)ANGPTL3 protein is a potent inhibitor of LPL and, as a consequence, it inhibits the process of conversion of VLDL into LDL; it is also possible that ANGPTL3 increase hepatic synthesis and secretion of VLDL, thus increasing VLDL plasma levels.

c) In the presence of ANGPTL3 loss-of-function (LOF) mutations, which result in ANGPTL3 deficiency, LPL-mediated lipolysis of plasma VLDL may increase, resulting in an increase of plasma LDL levels. In addition, ANGPTL3 deficiency may also reduce the hepatic synthesis and secretion of VLDL; in this case ANGPTL3 LOF mutations down-regulate the VLDL conversion into LDL, causing low plasma levels of both VLDL and LDL.

2. AIM OF THE STUDY

PART I

Aim of this study was the *in vitro* functional characterization of novel amino acid variants of *APOB* gene identified in hypocholesterolemic blood donors recruited for low plasma TC (below the 2th percentile) during population screening.

PART II

Aim of study was the resequencing of *ANGPTL3* gene in a subject with a lipid phenotype consistent with the diagnosis of Familial Combined Hypolipidemia and the functional assessment of the intronic mutation identified.

3. PATIENTS, MATERIALS AND METHODS

I PART

3.1. FHBL SUBJECTS

We investigated 169 unrelated subjects suspected to have familial hypobetalipoproteimenia (FHBL), who had been admitted to divisions of gastroenterology/hepatology for the presence of fatty liver and/or intestinal fat malabsorption associated with primary hypobetalipoproteinemia. For all of them, the criteria for the diagnosis of FHBL were TC, LDL-C and apoB plasma levels below the 5th percentile of the distribution in the population and the exclusion of secondary forms of hypolipidemia.

The systematic sequence of *APOB* gene had revealed that 60 of them were carriers of pathogenic mutations (mutations that lead to the formation of truncated apoBs of various size); 4 subjects were carriers of pathogenic missense mutations (45). In 105 subjects no pathogenic mutations in *APOB* gene were found among which 7 subjects were found to carry rare non-conservative amino acid substitutions with unknown functional effect on apoB protein.

Informed and written consent was obtained from the probands and their family members. The study was approved by the ethics committees of the participating institutions

3.1.2 HYPOCHOLESTEROLEMIC BLOOD DONORS

A group of 7000 white blood donors (recruited in the Blood Banks of Hospitals in the city of Palermo, Sicily, Italy) were screened for low-plasma cholesterol during routine laboratory tests (45). This screening led to the identification of 548 subjects with plasma cholesterol level below the 5th percentile (128 mg/dl) of the general population. From this group, 100 individuals with the lowest plasma cholesterol values (below the 2nd percentile of the population) were selected for genetic analysis.

None of those subjects was found to be carriers of mutations in *APOB* gene resulting in truncated apoBs. Some of them were found to be heterozygous carriers of rare amino acids variants in *APOB* gene whose functional effect was unknown.

3.2 GENE ANALYSIS

3.2.1 ISOLATION OF DNA FROM PERIPHERAL BLOOD

Blood was collected in presence of Na_2EDTA after overnight fasting, unless otherwise specified. Genomic DNA was extracted from peripheral blood leukocytes using *NucleoSpin® Blood L extraction kit* (*Macherey-Nagel*), according to the following procedure:

1. Lysis of blood sample: 150 µl of proteinase K and 2ml of BQ1 lysis buffer (both provided by the kit) were added to 2 ml of blood sample; then the mixture was vigorously mixed by vortex for 10 seconds and incubated at 56°C for 15 minutes.

2. Adjustment of DNA binding conditions: after the lysate has cooled down to room temperature, 2 ml of ethanol (96 – 100 %) were added and the sample was mixed by inverting the tube 10 times.

3. DNA binding: 3 ml of lysate was loaded on NucleoSpin® Blood column placed in a collection tube (15 ml) and centrifuged for 3 minutes at 4,500 xg; then, the remaining lysate was loaded on the same column and centrifuged at 4,500 xg for 5 minutes. The flow-through was discarded and the column placed back into the collection tube.

4. Silica membrane washing: 2 ml of BQ2 washing buffer (provided by the kit) was added to the sample. After centrifugation for 2 min at 4,500 x*g*, other 2 ml of BQ2 washing buffer was added and the sample centrifuged for 10 min at 4,500 x*g* to dry the silica membrane of the column.

5. Highly pure DNA elution: the column was placed in a new collection tube (15 ml); then 200 µl of elution buffer BE (provided by the kit and preheated at 70°C) were added directly onto the silica membrane. After incubation at room temperature for 2 minutes, the column was centrifuged at 4,500 xg for 2 minutes.

6. Quantification of DNA: the DNA concentration was measured in a spectrophotometer by measuring the absorbance at 260 nm. At this wavelength, 1U of Optical Density (O.D.) corresponds to a concentration of 50 µg of DNA.

The quality of the extracted DNA was evaluated by calculating the ratio of the O.D. at 260 nm and 280 nm. A 260/280 ratio of 1.7-2.2 is considered optimal, while lower ratios indicate protein contamination.

3.2.2 AMPLIFICATION OF *APOB* GENE

The entire *APOB* gene coding region (exons 1-29), including the 5′-flanking region and at least 50 base-pairs of intronic sequence at each intron–exon boundary, were amplified by PCR. The strategy for the amplification of *APOB* gene consists of 28 PCR reactions:

Exons	1 – 25	no. 19 amplicons
Exon	26 (Fragments *a – f*)	no. 6 amplicons
Exons	27-28	no. 1 amplicons
Exon	29 (Fragments *a – b*)	no. 2 amplicons

In view of their size, exons 26 (7571 bp) and 29 (1981 bp) were separated into overlapping fragments indicated by lowercase letters *(see legend of table 1)*. The PCR reactions of the 28 amplicons were set up by using an automated liquid handling system (ROBOT MULTIPROBE WINPREP II - PACKARD BIOSCIENCE) in 96 well plates.

The standard protocol for DNA amplification reaction is the following:

- Genomic DNA (~ 100 ng/μl)	1 μl
- Buffer (10X with 15 mM $MgCl_2$)	5 μl
- $dNTP_s$ Mix (10 mM of each dNTP)	1 μl
- primers (25 pmol/μL)	1 μl
- Taq Expand ™	1.75U
- ddH_2O	added up to 50 μl

In our laboratory we employ a *DNA polymerase Expand™ High Fidelity PCR System* (*Roche*) that is optimized to amplify DNA fragments up to 5kb.

The primer pairs used for PCR amplification are listed in table 1.

Table 1. Oligonucleotide primers for PCR amplification of *APOB* gene.

Exon	5′ Forward Primer (5'→3')	3′ Reverse Primer (5'→3')	Size of PCR product (nucleotides)
1	TGTAGAAAAGCAAACAGGTCAGGC	CCGCCAGCTGGTCCAATGCC	453
2	GGAAGCTCACAGAATTTCTTTCTC	GTAGAAGAGAGTTGGCATCCCTT	~572
3	CCAGAATTGGCTGTCCTTGGGAG	TACACAACTCCGGGAAGGTCGCG	280
4	TTGGTGCTCTGATTAGAGATTAAGC	CACAAGTTCATACCTCAGCGGAC	301
5-6	AGTGCCACCCAGCTTACTTCCA	TCAAAGGTGCCCACTAGCTCAA	1200
7-8	TCTGAGTTTATCTAGTGGTACAG	TGGCTAAGCCATGATAGGCACAT	1083
9	AGCAGATCTAGCAGGCATTGAA	TTGAAAGTTCAGTCAGTTACCAT	~724
10	TTCTGAGCTCCAAGTTGGGTT	AAGAATTCAATTTGTGTTTGCTGA	~065
11-12	ATCTTTCCCAGCACCACTTATTGA	GATGAAATCTAGAGTCTCATTCC	703
13	AGAAGATTCAATACCAGCCATTT	GGTCTAGATCTGCTACACATTT	486
14	AGATCTAGACCCAAAGACTTAGG	CTTAGTTTTCCTCTGGGTAGCT	472
15	ACATCAAGAGTGGGACTACTAGG	GAATTGTTTTTGCATTGAGACCC	315
16	TGGGAACTGAAAGGTGTTTGACA	CAGTGAATTCAAGGCAAACCTCC	400
17	ATAAAGAGTAATTACTCTCCAATG	CATTCTGGTGGAAGCTTGAAGTT	432
18	AACTCTAGAGAACTGAGAACTCG	TGATCTAGATCAACTGTTTAGCC	~054
19-20	CCCTGAGAATTTGTGATGTCCATT	GAATTCTGAACCTGAGACTGCG	816
21	AAACATAGCTTCTTACCACACATC	AGAACATGGCTTGGTCAGGTATGA	358
22	CTCTGAACCATCCTTGTATCT	CACCTGCATTACTTTGGAAGT	339
23	CTGTGGTTACAGGCTGAACTA	TGCACCTAGCTCAGAGTTGAG	318
24	GTCCAGCTTAATAATTAACTTGTC	ACAGGTTGTACTGAATAAAATATC	508
25	TTTGAATGACTGATGTCTGACTG	AAGACTTCCAAGTAGCAAGGAAG	554
26a	CAGATGGAGGAGTCTATTGCACA	TGAACCTTAGCAACAGTGTCTGCTT	1492
26b	ACATCTATGCCATCTCTTCTG	ATCAATAGCCTCAATGTGTTG	1367
26c	AAGAGACACATACAGAATATAG	ACAAAGTCAATTGTAAAGGAAG	1190
26d	GGTTTTCCACACCAGAATTTACCAT	TACTTATACTGATTGAACCTAGCAC	1363
26e	TAACTATGCACTGTTTCTGAG	GAGTACAGCATTGAAGAATTG	1197
26f	AGTCAAAACCTACTGTCTCTTCCTC	ACGTGTAGGGTATACATGTATCTCTTTTCT	1595
27-28	CGTCCTACTGTTATGAATCTAATAAAATAC	CTCGCTCTTGGGGGCGTGTCACTCATTAGG	494
29a	ACACATGAACTGACATATGAAAGAT	TGAAGATTACGTAGCACCTCTG	963
29b	ATAGATGTAATCTCGATGTATAGG	TGCAAGGCTGGCTCACTGTATG	1018

For some exons, the indicative size (~) of the PCR products is given. In view of their size, exons 26 and 29 were separated into fragments (indicated by lowercase letters). The nucleotide positions of the 5′ and 3′ end of each fragment (fr.) in cDNA are as follows: fr. 26a, from nt 2129 (in intron 25 with respect to the first nucleotide of exon 26) to nt 5707; fr. 26b, nt 5641–7007; fr. 26c, nt 6936–8125; fr. 26d, nt 8059–9421; fr. 26e, nt 9344–10540; fr. 26f, from nt 10474 to nt 152 of intron 26; fr. 29a, from nt 2151 (in intron 28 with respect to the first nucleotide of exon 29) to nt 13027; fr. 29b, nt 12915–13932. Nucleotide numbering according to *Knott et al* (Nucleic Acids Res. 1986; 14: 7501-3)

PCR reactions were carried out in the 96-Well GeneAmp® PCR System 9700 thermalcycler (AppliedBiosystem).

Three different amplification programs were used for the 28 amplicons of *APOB* gene, due to the different annealing temperature required by the primers pairs. The amplification conditions were:

Program A: used for exons 2, 4, 5-6, 7-8, 11-12, 15, 16, 19-20, 21, 22, 23, 24-25, 26-fragment d, 27-28, 29 fragment a, 29 fragment b.

Initial denaturation	5 minutes at 95°C	1 cycle
Denaturation	1 minute at 95°C	30 cycles
Annealing	1 minute at 60°C	
Elongation	3 minutes at 72°C	

Program B: used for exons: 3, 26 fragment f

Initial denaturation	5 minutes at 95°C	1 cycle
Denaturation	1 minute at 95°C	30 cycles
Annealing	1 minute at 67°C	
Elongation	3 minutes at 72°C	

Program C: used for exons: 9, 10, 13, 14, 17, 18, 26 fragment a, 26 fragment b, 26 fragment c, 26 fragment e

Initial denaturation	5 minutes at 95°C	
Denaturation	1 minute at 95°C	30 cycles
Annealing	1 minute at 55°C	
Elongation	3 minutes at 72°C	

3.2.3 AGAROSE GEL ELECTROPHORESIS

The amplification products were analysed by 2% agarose gel electrophoresis in TAE buffer (25 mM Tris, 20 mM acetic acid, 1 mM EDTA pH 7.2) stained with Ethidium Bromide; 5 µl of each amplification product are mixed with 1 µl of Loading Buffer III 6X (0.25% Bromophenol Blue, 0.25% Xilene cyanol, 30% Glycerol) and loaded on the gel together with a molecular weight marker, in order to verify the correct size of the PCR product of the DNA fragment of interest.

3.2.4 PURIFICATION OF PCR PRODUCT

In order to eliminate unincorporated nucleotides, residual primers, salts and the thermostable DNA polymerase which may inhibit subsequent enzymatic reactions, the amplification products were purified by using two methods.

3.2.4.1 EXOSAP-IT™METHOD (AMERSHAM)

The ExoSAP-IT is a commercially available enzymatic method used to purify PCR products of length from 100 bp to more than 20 kb. This system consists of two hydrolytic enzymes, exonuclease (EXO) and Shrimp Alkaline Phosphatase (SAP): EXO degrades residual primers, SAP hydrolyzes the unincorporated dNTPs that could interfere with the sequence reaction. By a liquid handling system (ROBOT MULTIPROBE WINPREP II - PACKARD BIOSCIENCE) 1 µl of ExoSAP-IT was added to 5 µl of each PCR product in a 96 well plate. The mixture was incubated, in the 96-Well GeneAmp® PCR

System 9700 thermalcycler (Applied Biosystem), at 37ºC for 15 minutes to allow enzymatic digestion and then at 80ºC to inactivate enzymes.

3.2.4.2 HIGH PURE PCR PRODUCT PURIFICATION KIT (ROCHE)

In some experiments the purification of PCR products was performed using another commercially available purification kit. The principle of this method is based on the ability of PCR products (DNA fragments 100 bp-50kb) to bind selectively to glass fiber fleece in the presence of choatropic salts. The DNA fragments remain bound while a series of rapid "wash and spin" steps remove contaminating small molecules including short DNA (<100bp) and proteins (thermostable enzymes). The DNA fragments are eluted from the matrix with low salt solution.

3.2.5 DIRECT SEQUENCING OF PURIFIED PCR PRODUCTS

Sequencing of *APOB* gene was performed using the method of "cycle sequencing"; it is based on the Sanger sequencing method with fluorescently labeled dideoxynucleotide triphosphates (ddNTPs). We used the *Big Dye Cycle Sequencing Ready Reaction Kit (Applied Biosystem, Warrington, UK),* which contains a thermostable DNA polymerase and the ddNTPs. The DNA polymerase, specific to sequence, has a better stability than the native enzyme (half-life 2.5 hours at 96-98ºC) and it is devoid of 5'→3' exonuclease activity normally associated with Taq.

The ddNTPs are labeled in the terminal position with four different fluorochromes (Big Dye terminators); ddATP is linked to a green fluorochrome, ddTTP is linked to a red fluorochrome, ddCTP is linked to a

blue fluorochrome and ddGTP is linked to a black fluorochrome. Each amplicon was sequenced in both directions (with a forward primer and a reverse primer) in order to compare the two complementary sequences and have a more reliable result. The primers used for sequencing reaction are the same primers used for PCR amplification. For sequencing of the exons 26 and 29 amplicons of *APOB* gene whose size was 1000-2000 bp, we used additional exonic primers (table 2).

Table 2. Oligonucleotide primers for sequencing of exons 26 and 29 of *APOB* gene.

Exon	5′ Forward Primer (5′→ 3′)	3′ Reverse Primer (5′→ 3′)
26a	CAGATGGAGGAGTCTATTGCACA	TCCATCTTCATATCTTCCTGTTATCT
	CACATATGGCCTGTCTTGTCAGA	ATCCTTAGTGTCGCCTTGTGAG
	GCTATCACTGGGAAGTGCTTATCA	TGAACCTTAGCAACAGTGTCTGCTT
26b	ACATCTATGCCATCTCTTCTG	GGGAGTCTAGTAGTAGAGTTAGGTC
	ACAGGCACCTGGAAACTCAAGAC	TGTGAGAGCAGTCAGTTTCTCCT
	CACAGCAAGCTAATGATTATCTGA	ATCAATAGCCTCAATGTGTTG
26c	AAGAGACACATACAGAATATAG	GTCTCTGAGTCACCTCACGGATTT
	CGAGAGGTATGAAGTAGACCAAC	TCATGTGAGCCAAAGATGATGAAC
	AAATCCGTGAGGTGACTCAGAGA	ACAAAGTCAATTGTAAAGGAAG
26d	GGTTTTCCACACCAGAATTTACCA	TGGCAGTGATGGAAGCTGCGATC
	TTGAAGTACCTACTTTTGGCAAGC	CCAAGTTTTGGTTTACTCTTAGGTG
	TCTCAGATGAGGGAACACATGAA	TACTTATACTGATTGAACCTAGCAC
26e	TAACTATGCACTGTTTCTGAG	GTTTCATTATAGGATTTGGTGACA
	AACAAACACAGGCATTCCATC	CTTGAAATCTGGAAGAGAAAGCT
	TTCTCCATCCTAGGTTCTGAC	GAGTACAGCATTGAAGAATTG
26f	AGTCAAAACCTACTGTCTCTTCCT	GGACCTGAACAAGAGCTGACATT
	GATGATATCTGGAACCTTGAAG	CTGAGATTCAGGCACGGTTATCTCA
	TTGTCATGCCTACGTTCCATGTCCC	ACGTGTAGGGTATACATGTATCTCTT
29a	ACACATGAACTGACATATGAAAG	GCCTTCCTGAGTCAACAGTTCCTG
	TGATGATACGACGTGAGGTTC	TGAAGATTACGTAGCACCTCTG
29b	ATAGATGTAATCTCGATGTATAGG	GGATCGGTAAGGATGCTAAGATA
	CTGTTAGTTGCTCTTAAGGACTTC	TGCAAGGCTGGCTCACTGTATG

A) AUTOMATED SYSTEM SEQUENCE REACTION

The sequencing reaction was performed in a 96 well plate as follows:

- Big Dye Terminator Ready Reaction Mix	2 µl
- Purified PCR product	5 -7 µl
- Forward or Reverse primer (5 pmol/µl)	1 µl
- dd_2HO	added up to 10 µl

The reaction was carried out in the 96-Well GeneAmp® PCR System 9700 thermalcycler (AppliedBiosystem) at the following conditions:

96 °C for 10 seconds
50 °C for 15 seconds } 25 cycles
60 °C for 4 minutes

At the end, the sequence reaction can be stored at 4 ºC.

B) MANUAL SEQUENCE REACTION

The sequencing reaction was performed as follows:

- Big Dye Terminator Ready Reaction Mix	2 µl
- Purified PCR product	5 -7 µl
- Forward or Reverse primer (3,2 pmol/µl)	1 µl
- dd_2HO	added up to 10 µl

The reaction was carried out in the GeneAmp® PCR System 9700 thermalcycler (*AppliedBiosystem*) at the following conditions:

96°C for 10 seconds
50°C for 5 seconds } 30 cycles
60°C for 4 minutes

3.2.6 PURIFICATION OF SEQUENCE REACTIONS

To eliminate unincorporated fluorochromes, that could interfere with the detection system of the instrument, a purification step was accomplished as follows:

- Addition of 2 μl of 3M sodium acetate (pH 4.6) and 50 μl of Ethanol 100% to each sequence reaction.
- Incubation for 15 minutes at room temperature to facilitate precipitation of the pellet.
- Centrifugation at 2000 xg for 30 minutes at 4°C.
- Elimination of the supernatant.
- Washing with 75 μl of Ethanol 75%.
- Centrifugation at 1650 xg for 10 minutes at 4°C.
- Elimination of the supernatant.
- Drying of the pellet for at least 30 minutes/1 hour at room temperature.
- Rehydration of the pellet with 6 μl dd_2H_2O. Samples may be maintained at -20°C before analysis.

At the time of analysis 2 μl of each sample are run in the sequencer after addition of 10 μl of formamide.

The instrument used in our laboratory is ABI PRISM ® 3100 GENETIC ANALYZER a 16 capillaries automated DNA sequencer.

3.2.7 ANALYSIS AND DATA PROCESSING

After running, a DATA COLLECTION software automatically collect and analyze data, displaying electropherograms with the text sequence of the data. The results are analyzed by: a) DNA SEQUENCING ANALYSIS SOFTWARE™ (*Applied Biosystems*) which allows basecalling, that is the identification of mixed bases with IUB codes; b) SEQSCAPE™ SOFTWARE (*Applied Biosystems*), a specifically designed software for sequence assembly and alignment, which compares the sample sequences with the reference sequence, allowing the identification of nucleotide variants.
Sequence variants found by sequence analysis were always checked by performing a second independent amplification of the affected DNA region and re-sequencing the PCR product in both directions.

3.3 *IN VITRO* SITE-DIRECTED MUTAGENESIS

To investigate the effect of the rare amino acids variants found in *APOB* gene, we performed in vitro mutagenesis experiments and functional studies in cells transfected with an expression plasmid containing mutant *APOB-48* cDNAs. The pCMV5-vector containing human *APOB-48* cDNA was a gift of Prof. Yao laboratory (University of Ottawa, Canada).
The pCMV-5 expression vector contains the *Cytomegalovirus* promoter, which allows constitutive expression of the cloned DNA in a wide variety of

mammalian cell lines. Furthermore, pCMV-5 contains β-lactamase coding region, which confers ampicillin resistance for selection in bacterial culture.

The expression plasmid encoding human apoB-48 was used as templates to prepare mutants by using the *QuikChange® II XL site-directed mutagenesis kit* (*Stratagene, La Jolla, CA).*

In vitro site-directed mutagenesis is a molecular technique which introduces a specific mutation into a fragment of wild type cDNA. With this strategy, it is possible to introduce substitutions of single nucleotides or to introduce small nucleotide deletions or insertions.

The vector harbouring the cDNA of interest is treated, chemically or enzimatically, to introduce the desired mutation.

The *Quick Change II XL Site-Directed Mutagenesis Kit* is specifically optimized for large, difficult constructs and does not require specialized vectors, unique restriction sites, multiple transformations or *in vitro* methylation treatment steps, as other kits do.

The *Quick Change II XL Kit* involves a three-step procedure which generates mutants with greater than 80% efficiency. The basic procedure utilizes a supercoiled double-stranded DNA (dsDNA) vector with the insert of interest and two synthetic oligonucleotide primers, both containing the desired mutation *(section 3.3.1 and 3.3.2)*.

The oligonucleotide primers, each complementary to opposite strands of the vector, are extended during temperature cycling by a *PfuUltra high-fidelity (HF) DNA polymerase*. *PfuUltra HF DNA polymerase* is responsible of mutagenic primer-directed replication of both plasmid strands and generates a mutated plasmid containing staggered nicks. Next, obtained product is treated with *Dpn I endonuclease* (target sequence: 5′-Gm^{6}ATC-3′). *Dpn I,* specific for methylated and hemimethylated DNA, is used to digest the parental DNA

template (because DNA isolated from almost all *E. coli* strains is dam methylated) and to select mutation-containing synthesized DNA. The nicked vector DNA incorporating the desired mutation can be transformed into *E. coli* ultracompetent bacterial cells.

3.3.1 SPECIFIC MUTAGENIC OLIGONUCLEOTIDE PRIMERS

Specific mutagenic oligonucleotide primer pairs must be designed according to the desired mutation. Both mutagenic primers must contain the desired mutation, ideally in the middle of each primer, and anneal to the same sequence on opposite strands of the plasmid. They should be between 25 and 45 bases in length and have a melting temperature (T_m) of ≥78 °C, calculated by the following formula:

$$T_m = 81.5 + 0.41(\%GC) - 675/N - \%\ mismatch$$

where values for *%GC* and *%mismatch* are whole numbers and *N* is the primer length in bases. The primers optimally should have a minimum GC content of 40% and should terminate in one or more C or G bases.

Mutant primer pairs generated for each mutation are indicated below:

◊ Tyr102Cys (Y102C) APOB missense mutation:

It is due to a A/G transition at nucleotide c. 386, in exon 5.

Codon TAT, codifying for Tyrosine, is substituted by codon TGT, codifying for Cysteine (mutated base is underlined).

Forward primer:

CAGCCATGTCCAGGT**G**TGAGCTCAAGCTGGCC

Reverse primer:

GGCCAGCTTGAGCTCA**C**ACCTGGACATGGCTG

◊ Thr26_27del (T26-27del) APOB mutation:

It is due to a deletion of 6 nucleotides c. 158_163 in exon 3; consequently codon ACA, codifying for Threonine and codon TAC codifying for Tyrosine at position 26 and 27 respectively are deleted. The mutant sequence presents a new codon AAC corresponding to Asparagine. This is the same aminoacid present in the normal sequence but specified by a new codon which is the result of the deletion junction.

Forward primer:

CAAGCACCTCCGGAAGTACAACTATGAGGCTGAGAGTTC

Reverse primer:

GAACTCTCAGCCTCATAGTTGTACTTCCGGAGGTGCTTG

3.3.2 MUTANT STRAND SYNTHESIS REACTION

The synthesis of the mutant strands was performed by *Quick Change II XL Site-Directed Mutagenesis Kit (Stratagene)* according to the manufacturer's instructions:

- Buffer 10x	5 µl
- pCMV-5APOB-48-WT [100ng/µl]	2.5 µl
- dNTPs mix (2.5mM of each dNTP)	1 µl
- Forward primer (100 ng/µl)	1.2 µl
- Reverse primer (100 ng/µl)	1.2 µl
- Quick Solution	5 µl

- ddH_2O added up to 50 µl

  Then add 1µl of *PfuUltra* HF DNA polymerase (2.5 U/µl)

The reaction was carried out in the GeneAmp® PCR System 9700 thermalcycler (*AppliedBiosystem*) at the following conditions:

Initial Denaturation	3 minutes	at 95°C	
Denaturation	50 seconds	at 95°C	18 cycles
Annealing	50 seconds	at 60°C	
Elongation	20 minutes	at 68°C	
Final elongation	7 minutes	at 68°C	

3.3.3 DIGESTION OF THE AMPLIFICATION PRODUCT

The amplification product was digested with 1µl of *Dpn I* restriction enzyme (10 U/µl). Reaction mixture was gently and thoroughly mixed by pipetting the solution up and down several times and spinned down in a microcentrifuge for 1 minute. Next the mixture was immediately incubated at 37°C for 1 hour to let the *Dpn I* restriction enzyme digest the parental supercoiled dsDNA.

3.4 TRANSFORMATION

Mutant cDNA is introduced in *E.Coli* ultracompetent bacterial cells (cells made capable of being transformed). Colonies containing mutant vectors are selected through a specific antibiotic resistance and grown up to isolate mutant plasmid DNA.

For transformation we used *XL10-Gold® Ultracompetent Cells (Stratagene)*.

The following protocol was used for each transformation reaction:

- thaw out on ice for 5 minutes an aliquot of *XL10-Gold® Ultracompetent Cells* (*E. Coli*) for each transformation reaction;
- transfer 100µl of *XL10-Gold® Ultracompetent Cells* in a pre-chilled 17x100mm polypropylene tube;
- add 4µl of *XL10-Gold® β-Mercaptoethanol (β-ME) mix* on ice, to increase bacterial membrane permeability;
- flick the tube and place on ice for 10 minutes, flicking every two minutes;
- add 5 µl of digestion product and place on ice for 30 minutes;
- heat shock the cells for exactly 30 seconds at 42°C in a water bath without shaking;
- immediately return the tube to ice for 2 minutes;
- add 895µl of room temperature SOC medium to each sample tube;
- incubate for 1 hour at 37°C with shaking (250 rpm);
- plate variable volumes (from 50 to 150 µl) of each transformation reaction onto LB-agar plates with ampicillin for selection of colonies harbouring mutant vectors;
- incubate the plates overnight at 37°C to allow colonies growth.

After over-night incubation at 37°C, only colonies harbouring pCMV-5 vector, and having ampicillin resistance as a consequence, were grown on LB-Agar-ampicillin plates.

The media were prepared as follows:

LB-agar plates:

- Agar 20g/L
- NaCl 10g/L

- Bacto Tryptone 10g/L
- Yeast Extract 5g/L
- Ampicillin [50mg/ml] 1mL

  pH 7.0 adjusted with NaOH 5N

SOB medium:

- Bacto Tryptone 20 g/L
- Yeas Extract 5 g/L
- NaCl 0,5 g/L
- KCl 250mM 10 mL/L

pH 7.0 con NaOH 5N

SOC medium:

- SOB medium 10mL
- $MgCl_2$ 2M (5µl/mL)
- Glucose 1mM (20µl/mL)

3.5 ISOLATION OF RECOMBINANT PLASMID DNA

After over-night incubation at 37°C, only colonies harbouring pCMV-5 vector (and so ampicillin-resistant) were grown on LB-Agar-ampicillin plates. Numerous colonies were picked up and single colonies were further grown (as specified below) in order to identify the clones containing the mutated insert of interest by plasmid DNA isolation and sequencing.

3.5.1 SMALL SCALE DNA ISOLATION (MINIPREP)

Plasmid Miniprep procedure provides a simple and rapid method for the isolation of plasmid DNA from transformed competent cells.

First of all it was necessary to prepare a number of 15 ml-tubes corresponding to the number of colonies to test. In each tube containing 3 ml of LB medium, supplemented with 3 μl of ampicillin [50 mg/ml], was added a single colony picked up from the plate. Bacterial cells were grown at 37°C overnight in a shaking incubator at 160 rpm. The following day 1.5 ml of each bacterial culture were processed to isolate high copy plasmid DNA by using the *JETquick Plasmid Miniprep Spin Kit (Genomed)* (while the remaining 1.5 ml of each bacterial culture were stored as "glycerol stock", by adding 318μl of 80% glycerol solution).

The procedure consists in a modified alkaline/SDS method to obtain a cleared lysate of bacterial cells. After neutralization, the cleared lysate is applied directly onto a *JETquick Micro-Spin Column* and the plasmid DNA is bound to the adsorption matrix. RNA, proteins and all other impurities are removed by a medium-salt wash. The purified plasmid DNA is eluted from the spin column with TE buffer pH 8.0 (10 mM Tris-HCl, 1 mM EDTA) . Eluted DNA is stored at -20°C.

LB medium:

- NaCl 10g/L
- Bacto Tryptone 10g/L
- Yeast Extract 5g/L
- Ampicillin [50mg/ml] 1mL

  pH 7.0 adjusted with NaOH 5N

3.5.2 LARGE SCALE DNA ISOLATION (MAXIPREP)

Plasmid Maxiprep procedure provides a simple and rapid method for the isolation of large amounts of recombinant plasmid DNA, by using the *QIAGEN Plasmid Maxi Kit (Qiagen)*.

First of all, 5 ml of LB medium, supplemented with 5µl of ampicillin [50 mg/ml], were inoculated with 200 µl of a single transformed bacterial cell culture, stored as "glycerol stock", and incubated for about 7 h at 37°C in a shaking incubator at 250 rpm.

This starter culture was then diluted 1/1000 into the same selective LB medium and grown at 37°C in a shaking incubator at 250 rpm overnight. The following day the bacterial culture was processed to isolate high copy plasmid DNA by using the *QIAGEN Plasmid Maxi Kit*.

QIAGEN Plasmid Maxi Kit protocol is based on a modified alkaline lysis procedure, which is followed by binding of plasmid DNA to the Qiagen Anion-Exchange Resin under appropriate low-salt and pH conditions. RNA, proteins, dyes and low-molecular-weight impurities are removed by a medium-salt wash. Plasmid DNA is eluted in a high-salt buffer, then it is concentrated and desalted by isopropanol precipitation. Finally, recombinant plasmid DNA is dissolved in 150µl of sterile buffer pH 8.0 and the concentration measured as described above. All steps were performed following the manufacturer's instructions.

3.5.3 SEQUENCING OF PLASMID DNA

Plasmid DNA, isolated by the selected transformed bacterial cells by Miniprep and Maxiprep, was sequenced to verify: I) the normal sequence of the insert in

pCMV-5 vector harbouring wild-type APOB-48 cDNA; II) the presence of the desired mutation in APOB sequence in each mutant vectors; III) the absence of other sequence variations, introduced by chance during mutagenesis and amplification.

The sequencing of plasmid DNA was performed according to the *ABI PRISM Big Dye Cycle Sequencing Ready Reaction Kit (Applied Byosistem*) as previously described *(sections 3.2.5, 3.2.6 and 3.2.7*).

The primers used to sequence the plasmid DNA are listed in table 3.

Sequence reactions of plasmid DNA obtained by Miniprep/Maxiprep were performed as follows:

- Big Dye Terminator Ready Reaction Mix	8 µl
-Plasmid DNA from Miniprep/Maxiprep	10/5 µl
- Forward or Reverse primer (5 pmol/µl)	2/1 µl
- dd_2HO	added up to 20 µl

The sequence reactions were carried out in the GeneAmp® PCR System 9700 thermalcycler (*AppliedBiosystem*) at the following conditions:

96°C for 10 seconds
50°C for 5 seconds } 30 cycles
60°C for 4 minutes

Table 3. Oligonucleotide primers for APOB-48 cDNA sequencing, designed to sequence overlapping regions.

	APOB cDNA	*APOB cDNA*
	5′ Forward Primer (5'→3')	**3' Forward Primer (3'→5')**
1F	GTGCCCTTCTCGGTTGC	
1R		CCTGGTGGCACTTCTTGAA
2F	GGCTGAGAGTTCCAGTGGAG	
2R		GCTTGGCTTCTTCTGTCTCTG
3F	CTGAACATCAAGAGGGGCAT	
3R		TGTGTCACTTGTGCTACCATCC
4F	GAAGCCATCTGCAAGGAGC	
4R		GTCCACACTGAACCAAGGCT
5F	CTCTTGCCACAGCTGATTGAG	
5R		GACCCGCAGAATCAAATAGG
6F	CAGGAGCTGCTGGACATTG	
6R		GCCTGTGAAGGACTCCTCATC
7F	GCGACTGGCTGCCTATCTTA	
7R		CAAGCCAATCTCGATGAGGT
8F	TGACCTCATCGAGATTGGCT	
8R		CCTTCCTGATGACCTCTCCA
9F	CAGTCTCCATGACCTCCAGC	
9R		GACTCGTGGAAGAAGTTGGTG
10F	CATTCCGGACTTCGCTAGG	
10R		GGCCTCAGTTCCAGCTCTAA
11F	AGACTCCGCCTCCTACTATCC	
11R		CAACTTAGGTGGCCCATGAG
12F	CACCCTGGACATTCAGAACA	
12R		GGACTCTGTGATCCAGGAGTCT
13F	GGAACACAGGCACCAATGTAG	
13R		TGGAATCCCACAGACTTGAAG
26.1R		ACGAAGAGACTCTGAACTGC
26.2F	GCAGTTCAGAGTCTCTTCGT	
26.3F	TCACCTCCACCTCTGATCT	
26.4F	GAAGTGTAGTCTCCTGGTGC	
26.5F	GCAGGCTTATCACTGGACT	
26.6F	CATCGGCTCAACACAGAC	
26.7F	TACTCCAGCTGAGCAGACA	
26.8F	AATACAGAGCAGCCCTGG	

3.6 TRANSFECTION OF MUTANT PLASMID IN MAMALIAN CELLS

3.6.1 McA-RH7777 CELL CULTURE

McA-RH7777 are rat hepatoma cell line derived from the Morris hepatoma 7777 (obtained from a male Buffalo strain rat). They were epithelial-like cells, growing as monolayer.

McA-RH7777 cells were grown in the Dulbecco's Modified Eagle Medium (DMEM) containing 20% Fetal Bovine Serum (FBS) and 1% Penicillin/Streptomicin (*Life Technologies*^{TM}) at 37°C in a humidified 5% CO_2 incubator.

Every 2-3 days the cell monolayer was trypsinized with a solution of trypsin-EDTA (0.25% trypsin, 1mM EDTA) in PBS (KCl 2.7mM, KH_2PO_4 1.8mM, NaCl 137mM, $Na_2HPO_4 \cdot 12\ H_2O$ 10.1mM).

3.6.2 TRANSIENT TRANSFECTION OF McA-RH7777 CELLS

To transfect transiently McA-RH7777 we used the calcium phosphate precipitation technique in order to allow in vitro expression of APOB-48 mutant cDNAs cloned into pCMV5 vector.

This transfection method is based on the formation of a calcium phosphate-DNA co-precipitate to increase the uptake of DNA by cells in culture.

The transfected DNA enters the cytoplasm of the cell by endocytosis and is transferred to the nucleus.

For transfection experiments, 1.5 x 10^6 cells were counted and plated in 100x15 mm dishe (*Falcon*) with 10 ml of complete culture medium (DMEM+20%FBS).

Cells were incubated at 37°C in a humidified 5% CO_2 incubator for 24 hours.

About two hours before transfection, 10 ml of fresh medium (DMEM+20%FBS) was added to each plate.

The transfection reaction was performed in sterile tube as follows:

- 8 μg of DNA in 100 μl of sterile ddH_2O (gently mix by flicking);
- 500 μl of 2xBES (50 mM BES N,N-bis [2-hydroxyethyl]-2aminoethanesulfonic acid, 280 mM NaCl, 1.5 mM $Na_2HPO_4x2H_20$);
- 400 μl of 2M $CaCl_2$ freshly prepared and added very gently dropwise to the solution.

The calcium-phosphate-DNA complexes were incubated for 30 minutes at room temperature and added to the cells gently and dropwise. The media were swirled to ensure complexes distribution and then the cells were incubated at 37°C in a humidified 5% CO_2 for 4 hours.

After incubation the media were removed and 3 ml of 15% glycerol was added to the cells. After incubation at room temperature for 2 minutes, the glycerol was removed by aspiration and the cells were washed two times with 8 ml/times of sterile PBS.

The cells were incubated in 5 ml of complete growth medium at 37°C in a humidified 5% CO_2 for 48 hours.

For the analysis of protein expression the cells were incubated in DMEM containing 20%FBS and 0.4 mM oleic acid (*Sigma*) for 4 hours.

3.6.3 STABLE TRANSFECTION OF McA-RH7777 CELLS

The cells were co-transfected with plasmid DNA and pSV-neo that confers them the G418 Geneticin resistence. In this way only the transfected cells were able to grow in media containing G418.

7 x 10^5 cells were plated in 100x15 mm dishes (*Falcon*) in 10 ml of complete

culture medium (DMEM+20%FBS) and incubated at 37°C in a humidified 5% CO_2 incubator for 24 hours. Two hours before transfection, culture media were replaced by fresh medium (DMEM+20%FBS). At the end of incubation the cells were co-tranfected with 5 μg or 10 μg of plasmid DNA and 300 ηg or 500 ηg of pSV-neo. The trasfection protocol was the same as for transient transfection *(section 3.6.2).*

The cells were incubated in 10 ml of complete medium at 37°C in a humidified 5% CO_2 for two days. Subsequently the media were change every 2-3 days for 3 weeks with complete media containing 400 μg/ml of G418 (*Promega*) to remove cell debris and to allow colonies of resistant cells to grow.

Then individual colonies were trypsinized, picked up, transferred in 6-well plates and incubated in 2 ml of complete medium containing 400 μg/ml of G418 until confluence, changing the media every 2-3 days. The colonies are let to grow to expand the number of cells to be screened. Cells from each colony were lysed and tested for the presence of human apoB-48 as specified below.

Positive clones were maintained in G418 200 μg/ml for further experiments.

3.7 PREPARATION OF CELL EXTRACTS

In all experiments the stable transfected cells were incubated in DMEM containing 20%FBS and 0.4 mM oleic acid for different times. At the end of the incubation time, culture media were collected, centrifuged for 10 minutes at 1200 rpm and supplemented with 1 μl/ml phenylmethanesulfonylfluoride (PMSF, *Sigma*, 15% in dimethyl sulfoxide), 40μl/ml Complete Protease Inhibitor Cocktail (*Roche*) dissolved in water.

The cells were washed two times with sterile PBS and treated with a preheated lysis buffer (0.1% SDS-Ripa Buffer).

Cells were scraped, transferred in *Eppendorf* tubes and heated for 15 minutes at 75°C for two times. The cell lysates were stored at -20°C.

Lysis buffer SDS-Ripa

- EDTA 0.5 mM pH 8.0 — 0.2 ml
- Triton X-100 — 1 ml
- Sodium deoxycholate — 1 g
- 2.5M NaCl — 6 ml
- Tris-HCl 1M pH8 — 5 ml
- ddH_2O — added up to 100 ml

Just before use an appropriate aliquot of SDS-Ripa was supplemented with 0.1ml/ml SDS 10%, 1 μl/ml PMSF 15%, 0.5 μl/ml DTT (dithiothreitol) 2 M, a tablet of Complete Protease Inhibitor Cocktail (*Roche*).

The protein content in cell lysates was measured by Lowry method.

3.8 WESTERN BLOT ANALYSIS

Aliquots of cells lysates (200 μg of total proteins) or incubation media (100 μg of proteins) were dissolved in Sample buffer 4X (Tris 400 mM pH 7.3, β-mercaptoethanol 20%, SDS 40%, Glycerol 0.28% and Bromophenol blue 0.2%), heated to 95°C for 5 minutes and separated by gradient 5%-10% SDS-polyacrylamide gel electrophoresis (SDS-PAGE) in a running buffer (0.38M glycine, 50mM Tris, 3mM SDS) at 40mA and then (after the samples entered the running gel) at 60mA for approximately three hours in a PROTEAN cell

(*BioRad Laboratories, Richmond, CA, USA*). As a molecular weight standard, *Precision Plus Protein™ All Blue Standards* (*BioRad*) was used.

Cell lysate and media proteins were electro-transferred from the gel to a PVDF (polyvinylidene fluoride) membrane *HybondP* (*GE Healthcare*) according to the manufacturer's instructions. The transfer was performed at 80V (constant voltage) for two hours at 4 C°.

After the transfer, the membrane was incubated with 5% non-fat dry milk in PBS containing 0.1% Tween-20 (*Blocking solution*) at room temperature with gentle agitation to block non-specific binding of the antibodies.

After one hour incubation, the membrane was cut to be incubated with different antibodies.

To detect human apoB-48 the upper section of the membrane (spanning from 150kDa to 250kDa) was incubated with mouse monoclonal antibody 1D1 (that has an epitope at amino acids 401-582 of human apoB, gift from Prof. Yao, Ottawa) at a 1:10,000 dilution in PBS Buffer containing 5% non-fat dry milk and 0.1% Tween20.

To detect β-Actin protein the lower part of the membrane (spanning from 20kDa to 50kDa) was incubated with anti-human β-Actin mouse monoclonal antibody (*Sigma*) at a 1:20,000 dilution in PBS Buffer containing 5% non-fat dry milk and 0.1% Tween20. To detect apoE protein the membrane region spanning from 50kDa to 100kDa was incubated with rabbit anti apoE polyclonal antibody (Gift from Prof. Yao, Ottawa) at a 1:8,000 dilution in PBS Buffer containing 5% non-fat dry milk and 0.1% Tween20.

After overnight incubation with primary antibodies at 4°C with gentle agitation, the membranes were washed twice with 0.1% Tween20 in PBS Buffer to remove unbound primary antibody.

Then the membranes were incubated with horseradish peroxidase-linked (HRP-linked) secondary antibodies. HRP-linked antibodies are able to cleave a chemiluminescent agent: the reaction produce luminescence in proportion to the amount of protein detected. This type of detection is called Electrochemiluminescence (ECL).

The secondary antibody used to detect human apoB-48 and β-Actin proteins was *Amersham ECL Anti-Mouse IgG, Horseradish Peroxidase-Linked Species-Specific Whole Antibody* from sheep (*GE Healthcare*), diluted in PBS Buffer containing 5% non-fat dry milk and 0.1% Tween20, with a 1:10,000 and 1:20,000 ratio, respectively.

The secondary antibody used to detect apoE protein was *Amersham ECL Anti-Rabbit IgG, Horseradish Peroxidase-Linked Species-Specific Whole Antibody* from donkey (*GE Healthcare*), diluted in PBS Buffer contining 5% non-fat dry milk and 0.1% Tween20, with a 1:8,000 ratio.

After 1 hour incubation at room temperature under gentle agitation, the membranes were washed three times with 0.1% Tween20 in PBS Buffer.

The proteins were detected by ECL method (*GE Healthcare*): the chemiluminescent signal was detected by exposure of the membrane to autoradiographyc films (*CL-Xposure™Film, Thermo Scientific*) and analyzed by densitometry using a Molecular Imager Gel Doc System (*Bio-Rad*), which evaluates the relative amount of protein signal and quantifies the results in terms of optical density.

3.9 SEPARATION OF LIPOPROTIENS FROM THE INCUBATION MEDIA

Lipoproteins secreted in the culture medium were fractionated into very low density lipoproteins (VLDL, density < 1.006 g/ml), low density lipoprotein

(LDL 1.006-1.063 g/ml) and high density lipoproteins (HDL, density 1.063-1.21 g/ml).

Cells expressing wild type or mutant apoB-48 were plated in 100x15 mm dishes (6.000.000cells/dish) and incubated at 37°C for 24 hours in a humidified 5% CO_2.

After the incubation the media were removed and the cells were incubated in 5 ml of fresh DMEM supplemented with 20% FBS and 0.4 mM oleate (to provide a suitable substrate for lipid synthesis) at 37°C in a humidified 5% CO_2 for 24 hours. At the end of incubation the media were collected in *Falcon* tubes and centrifuged for 10 minutes at 1200 rpm. Then media were transferred in new *Falcon* tubes and supplemented with 40µl/ml Complete Protease Inhibitor Cocktail (*Roche*) diluted in water.

Lipoproteins were separated by continuous density gradient ultracentrifugation from 3 ml of medium which was brought to a density of 1.210 g/ml by adding solid KBr.

Each density gradient was prepared stratifying from the bottom the following solutions:

- 2 ml of NaCl/KBr solution (density 1.240 g/ml);
- 3.3 ml of sample (density 1.210 g/ml);
- 2 ml of NaCl/KBr solution (density 1.063 g/ml);
- 2.5 ml of NaCl/KBr solution (density 1.019 g/ml);
- 2 ml of NaCl solution (density 1.006 g/ml).

The samples were centrifuged for 38 hours at 38,000 rpm in a SW 41 *Beckman* rotor at 15°C.

After centrifugation, aliquots of 500 µl (fraction 1) or 400 µl (fractions 2-24) were collected. Aliquot of equal volume of each fraction were used for apoB

immunoprecipitation. For each fraction the final volume was adjust to 700 µl with 0.5% NET/NP-40 and 30 µl of rabbit polyclonal anti-apoB antibody (Gift from Prof. Yao, Ottawa) was added to each fraction. After an overnight incubation with gently shaking at 4°C, 100 µl of protein A-Sheparose™CL-4B (*GE Healthcare*), previously prepared, were added to each fraction and then the samples were incubated for 3 hours at room temperature with shaking.

The protein A-antigen-antibody complexes were collected by centrifugation at 7,600 rpm for 10 minutes in an *Eppendorf* microfuge. The supernatant was removed by gentle aspiration and the immunoprecipitates were washed three times, the first two with NET/NP40 1% and the last one with NET. The pellet was collect by centrifugation at 7,600 rpm for 20 minutes at room temperature and resuspended in 40 µl of Sample Buffer 1X (SDS 10%, Glycerol 20%, Tris 100 mM pH 7.3, β-Mercaptoethanol 5%, Bromophenol blue 0.05%).

The samples were heated at 95°C for 5 minutes and centrifugated at 13,600 rpm for 1 minutes at room temperature. The supernatants were analyzed by SDS-PAGE and western blot *(section 3.8*).

NET:

- NaCl 0.1M
- EDTA 1mM
- Tris-Cl 10mM pH 7.5
- ddH_2O added up to 100 ml

NET-NP/40 0.5 %

- NET 100 ml
- Nonidet P40 0.500 ml

NET-NP/40 1 %

- NET 100 ml
- Nonidet P40 1 ml

3.10 CONFOCAL ANALYSIS

To evaluate the intracellular localization of wild type and mutant apoB we performed confocal microscopy analysis.

McA-RH7777 cells expressing apoB-48 wild type or mutant were plated in 60x15 mm dishes (800,000 cells/dish) and incubated for 48 hours at 37°C in a humidified 5% CO_2. The cells were washed two times using PBS, fixed with 400µl of 4% paraformaldehyde (in PBS) and incubated for 10 minutes at 4°C.

After washing with 1 ml of PBS for two times the cells were permeabilized with 500µl of 0.05% Triton-X 100 in water and incubated at room temperature for 5 minutes. To block the permeabilization the cells were washed two times using PBS and subsequently incubated in 1ml of 1% BSA (Bovine Serum Albumine) in PBS for 15 minutes at room temperature and washed to remove BSA.

Then the cells were incubated with primary antibodies at 4°C overnight. The primary antibodies used were:

- mouse monoclonal antibody 1D1 against human apoB;
- rabbit anti-Calnexin antibody (*Sigma*) diluted 1:200 in 1% BSA.

The day after the cells were washed twice with 1 ml of PBS for 5 minutes and with 1% BSA for 15 minutes. Then the secondary antibodies (*Alexa Fluor® 555 Goat Anti-Mouse IgG* and *Alexa Fluor® 488 Goat Anti-Rabbit IgG, Life Technologies™*) were added at 1:100 dilution in 1% BSA and incubated at room temperature for 1 hour.

After incubation cells were washed with PBS for 5 minutes for three times.
The dishes were dried at room temperature for about 4 hours.
A drop of 90% Glycerol in Tris 20 mM pH 8.0 was added to each dish and covered with a glass coverslip.
The images were acquired using Leica TCS-SP2 Confocal Microscope with an immersion 40X objective.

3.11 PULSE CHASE ANALYSIS OF APOB

Stably transfected McA-RH7777 cells expressing wild type or mutant apoB-48 were plated in 6 mm dishes (2.000.000 cells/dish) and incubated in complete medium at 37°C in a humidified 5% CO_2. for 24 hours.
For the experiments the cells were cultured in complete medium supplemented with 0.4 mM acid oleate and incubated for 1, 2, 4 hours at 37°C in a humidified 5% CO_2. Cycloheximide (*Sigma*) 10 μM was added at time 0.
The cell and medium samples were collected at the indicated time points, and the recombinant apoB-48 proteins were analysed by SDS-PAGE and western blot as described previously *(sections 3.7and 3.8*). The intensity of apoB-48 bands was quantified by scanning densitometry.

3.12 INHIBITION OF THE INTRACELLULAR DEGRADATION PATHWAYS

The cells were cultured as reported above *(sections 3.6.3 and 3.11*).
In some experiments 25 μM MG132 (*Cayman Chemical*) was added at time 0.
MG132 is a potent, reversible and cell permeable proteasome inhibitor that blocks the proteolytic activity of the 26S proteasome complex.

To inhibit the autophagosome/lysosome pathway we used 3-Methyladenine (3-MA, *Sigma*) and ammonium chloride (NH_4Cl) (*Sigma*).

The cells were plated and after 24 hours they were pretreated with DMEM containing 20% FBS, 0.4 mM acid oleate, 10 μM cycloheximide supplemented with/without 25 μM 3-MA (*Sigma*) for 25 minutes. After washing with 3 ml PBS, the cells were incubated with complete DMEM containing 0.4 mM oleic acid and 10 μM cycloheximide for 0, 1, 2, 4 hours at 37°C in a humidified 5% CO_2.

In the experiments with ammonium chloride the cells were incubated with complete DMEM containing 0.4 mM oleic acid, 10 μM cycloheximide supplemented with or without 0,02M NH_4Cl for 0, 1, 2, 4 hours at 37°C in a humidified 5% CO_2.

At the indicated time cells were processed as reported above *(sections 3.7 and 3.8).*

In the experiments with ammonium chloride was evaluated the expression of LC3.

Aliquots (60 μg of total protein) of cells lysates were dissolved in Laemmli buffer 4X (1M pH 6.8, Tris-HCl, β-mercaptoethanol, 20% SDS, 20% glycerol and 0.2% bromophenol blue), heated to 95°C for 5 minutes and separated by linear 12,5% SDS-PAGE and Western blot as described previously. The membrane was incubated with rabbit anti-LC3 antibody (*Sigma*) at 1:700 dilution. As secondary antibody *Amersham ECL Anti-Rabbit IgG, Horseradish Peroxidase-Linked Species-Specific Whole Antibody* from donkey (*GE Healthcare*) diluted at 1:5000 in PBS buffer was used.

PART II

3.13 FUNCTIONAL STUDY OF SPLICE SITE MUTATION IN *ANGPTL3* GENE

3.13.1 CONSTRUCTION OF *ANGPTL3* MINIGENE

To investigate the effect of intronic mutation involving the splice site of *ANGPTL3* we adopted an in vitro strategy to overcome the problem of availability of liver biopsy. This procedure is based on the construction of two minigenes: a wild-type and a mutant minigene through the amplification of the appropriate gene regions (i.e. those encompassing the splice sites harbouring the mutations). The minigene constructs were generated from genomic DNA of the proband and of a control subject respectively by using a single PCR fragment.

The primers and the conditions used for minigenes constructions are indicated below.

For genomic DNA amplification we used the following primers:

5′-AGA TAT ACT CCA TAG TGA AGC-3′ (forward primer complementary to exon 6)

5′-TCT GTT GGA TGG ATC AAC ATT-3′ (reverse primer complementary to exon 7).

The amplification conditions were: 1 cycle at 96°C for 5 minutes, 30 cycles at 96°C for 1 minute/53°C for 1 minute /68°C for 1 minutes followed by 1 cycle at 72°C for 5 min

Wild-type and mutant minigenes (806 bp in size) contained 3' end of of exon 6 (243 bp), intron 6 (397 bp) and 5' end of exon 7 (166 bp).

3.13.2 CLONING AND EXPRESSION OF PCR PRODUCTS

For cloning the Wild-type and mutant minigenes, the pTargeT™ Mammalian Expression Vector System (Promega, Madison, WI, USA) was used which contains the Neomycin resistance gene (NeoR gene) under the control of the SV40 early promoter.

pTARGET vector

pTarget vector is a mammalian expression T-vector. T-vectors are a specific type of cloning vectors which are linearized vectors containing a single thymidine at the 3'-ends. These single 3′-thymidine overhangs at the insertion site greatly improve the efficiency of ligation of a PCR product into the plasmid in two ways: i) the overhangs prevent recircularization of the vector; ii) they provide a compatible overhang for a PCR product containing single adenosine at the 3'-ends generated by certain thermostable polymerases which add a single deoxyadenosine, in a template-independent fashion, to the 3′-ends of amplified fragments. These vectors take advantage of the adenosine overhangs on PCR products by providing compatible ends for ligation.
The pTARGET vector (5670 bp) contains:
- Human Cytomegalovirus immediate early enhancer and promoter region to promote constitutive expression of cloned DNA inserts in mammalian cells;
- SV40 enhancer and early promoter region; the SV40 early promoter contains the SV40 origin of replication which will induce transient, episomal replication of the vector in cells expressing the SV40 large T antigen such as COS-1 or COS-7 cells;

- Chimeric intron (5'-donor site from the first intron of the human beta-globin gene and the branch and 3'-acceptor site from the intron of an immunoglobulin gene heavy chain variable region) located upstream of the cDNA insert in order to prevent utilization of possible cryptic 5'-donor splice sites within the cDNA sequence and increase the level of gene expression;
- T7 RNA Polymerase Promoter located downstream of the intron. This promoter can be used to synthesize RNA transcripts in vitro using T7 RNA polymerase;
- Multiple Cloning Region within within a *lacZα* region, allowing identification of recombinant clones by color screening on indicator plates;
- Neomycin phosphotransferase gene, a selectable marker for mammalian cells;
-Beta-lactamase coding region which conferes ampicillin resistance for blue/white recombinant screening.

3.13.3 LIGATION

The ligation reaction was performed according to manufacturer's instructions (*Promega*) as described below:

- T4 DNA ligase 10X Buffer	3 µl
- pTarget-Vector (60 ng/ µl)	1 µl
- PCR product (minigene)	20 µl
- T4 DNA ligase (3U/ µl)	3 µl
- dd_2HO	added up to 30 µl

The mixture was incubated at 4°C overnight.

3.13.4 TRANSFORMATION

High-efficiency JM109 competent cells supplied with the pTARGET™ System were used for transformation.

For each transformation reaction the following protocol was used:

- Thaw on ice for 5 minutes an aliquot of JM109 competent cells for each transformation reaction;
- Transfer 100 µl of JM109 competent cells in a prechill 17x100mm polypropylene tube;
- Add 30 µl of ligation reaction on ice;
- Flick the tube and place on ice for 20 minutes;
- Heat shock the cells for 45–50 seconds at exactly 42°C in a water bath without shaking;
- Immediately return the tubes to ice for 2 minutes;
- Add 870 µl of room temperature SOC medium to each sample tube;
- Incubate for 1.5 hours at 37°C with shaking (~150 rpm);
- Plate 200 µl of each transformation reaction onto LB-agar plates with ampicillin/IPTG/X-Gal for selection;
- Incubate the plates overnight at 37°C to allow colonies growth.

The media were prepared as previously described *(section 3.4).*

<u>LB-plates with Ampicillin/IPTG/X-Gal</u>:

To 1 liter of LB medium add:

15 g Agar

100 µg/ml Ampicillin

0.5 mM IPTG (*Promega*)

80 µg/ml X-Gal (*Promega*)

3.13.5 COLONY SCREENING

Recombinant clones can usually be identified by color screening on plates as the pTARGET™ Vector contains a modified version of the coding sequence of the α-peptide of β-galactosidase, which allows the easy identification of recombinant clones using blue/white screening.

White colonies generally contain inserts that interrupts the coding sequence of the α-peptide of β-galactosidase.

A lot of single white colonies were picked up and grown in order to identify clones containing the insert of interest by plasmid DNA isolation and sequencing *(sections 3.5.1, 3.5.2, 3.5.3).*

3.14 EXPRESSION OF MINIGENES IN TRANSEFECTED CELLS

3.14.1 COS-1 CELLS CULTURE

COS is a cell line often used for transfection studies to produce recombinant proteins. The word COS is an acronym, derived from the cells being **C**V-1 (simian) in **O**rigin, and carrying the **S**V40 genetic material. The COS cell line was obtained by immortalizing a CV-1 cell line derived from kidney cells of the African green monkey with a version of the SV40 genome that can produce large T antigen but has a defect in genomic replication. When an expression construct with an SV40 promoter is introduced into COS cells, the vector can be replicated substantially by the large T antigen. Two forms of COS cell lines commonly used are COS-1 and COS-7. COS-1 cells were maintained in DMEM containing 5% FBS at 37°C in a humidified 5% CO_2 incubator. Every 3-4 days the cell monolayer was trypsinized with a solution of 0.05% trypsin- EDTA

(0.25% trypsin, 1 mM EDTA in PBS). For transfection experiments, cells were counted and 1 x 10^6 cells were plated in 60 mm dishes (*Falcon*) with 5 ml of complete culture medium (DMEM + 10% FBS).

3.14.2 TRANSFECTION OF COS-1 CELLS

COS-1 cells, at a confluence of 90%, were transfected using Lipofectamine ™ 2000 (*Invitrogen*). It is a cationic liposome based reagent able to assemble absorption-complexes with the negatively charged plasmid DNA. An electrostatic reaction is thus created and complexes are able to enter plasma membrane. Plasmid DNA containing wild-type or mutant minigenes were transfected according to manufacturer's instructions.

3.14.3 RNA EXTRACTION FROM TRANSFECTED COS-1 CELLS

Forty-eight hours after transfection total RNA was extracted from transfected cells using the EUROZol ™ reagent (*Euroclone*) and treated with RNase-free DNase (*Promega*).

EUROZol extracts total RNA from tissues or isolated cells through the action of concentrated caothropic agents. Simultaneously to RNA extraction, DNA and proteins are precipitated by acid phenol. The RNA extraction must be followed by its purification. The RNA obtained is undegraded, free of proteins and DNA and contains all the different species of RNA.

The transfected cells were washed with 3 ml of sterile PBS and were lysed with 500 μl of *EUROZol*™ per plate kept in ice.

The cell lysates were collected into 15 ml COREX glass sterile tube. To each lysate chloroform was added in the proportion 1:10. After mixing the sample

was incubated on ice for 5 minutes and centrifuged at 12,000 x g for 15 minutes at room temperature. The upper aqueous phase containing RNA was collected in a new 15 ml COREX glass sterile tube and an equal volume of cold isopropanol was added. The sample was incubated at -80 ° C for 30 minutes and then centrifuged at 12,000 xg at 4°C for 15 minutes to facilitate the precipitation of the RNA pellet. The pellet was washed with 1 ml of 75% ethanol, centrifuged at 8,000 xg for 15 minutes at 4°C and dried on ice for approximately 30 minutes.

The pellet was dissolved in 30 μl of sterile ddH_2O and treated with RNase-free DNase to degrade single-strand or double-strand DNA and to remove contaminant DNA from RNA samples.

The reaction was performed according to the following protocol:

- 10X Reaction Buffer (provided by kit) 3 μl
- RQ1 RNase-free DNase (Promega) 3 μl
- RNA 20 μl
- ddH_2O added up to 30 μl

and carried out at 37°C for 30 minutes. The reaction was stopped by the addition of 3 μl of Stop Solution (provided by kit) and incubation for 10 minutes at 65°C.

3.14.4 REVERSE TRANSCRIPTION AMPLIFICATION (RT-PCR) OF MINIGENE mRNAs

Single-strand cDNA synthesis from purified total RNA was perform by using *SuperScript™ II Reverse Transcriptase kit* (*Invitrogen*) according to the manufacturer's instructions.

The RT-PCR reaction was performed in a 0.2 ml thin-walled PCR tube according to the following protocol:

a) First-Strand cDNA Synthesis

- total RNA pretreated with DNase (up to 5 μg)	15 μl
- primer oligo(dT)$_{12-18}$ (500μg/ml)	1 μl
- dNTP Mix (10 mM each)	1 μl
- RNase/DNase-free sterile ddH_2O	added up to 20 μl

The mixture was heated at 70°C for 10 minutes and then rapidly chilled on ice before the addition of:

- First-strand Buffer 5X	
(250 mM Tris-HCl, pH 8.3, 375 mM KCl, 15 mM $MgCl_2$)	4 μl
- DTT (0.1 M)	2 μl

After mixing the sample was incubated for 2 minutes at 42°C and 200U of *SuperScript II Reverse Transcriptase (RT)* were added. The mixture was incubated at 42°C for 50 minutes followed by heating at 70°C for 15 minutes to inactivate the reaction and then stored at 4°C.

b) PCR

The first-strand cDNA is used as template for amplification in PCR with *Taq* DNA polymerase.

To amplify the cDNA corresponding to the minigenes (minigene cDNAs) we used the primers and conditions described above (see section 3.8.1). The RT-PCR products were purified, separated on 2% agarose gel and sequenced.

Amplification of NeoR gene

To provide an internal control for transfection efficiency, the mRNA of Neomycin-resistance gene (NeoR gene) present in the vector under the control of the SV40 early promoter, was reverse transcribed and PCR amplified using the following primers:

forward primer: 5'-AAG CGG GAA GGG ACT GGC-3'

reverse primer: 5'-AGG CGA TAG AAG GCG ATG C-3'.

The amplification conditions were: 30 cycles at 95°C for 1.50 minutes, 55°C for 1.50 minutes and 68°C for 1.5 minutes, and 1 final cycle at 68°C for 10 minutes.

4. RESULTS

PART I

4.1 *APOB* AMINO ACID CHANGES IN HYPOCHOLESTEROLEMIC BLOOD DONORS.

The sequencing analysis of *APOB* gene performed in 100 hypocholesterolemic blood donors recruited for low plasma TC (below the 2th percentile) led to identification of heterozygous carriers of rare amino acid variants reported in Table 4. (45). The table shows all variants found in those subjects. They are eight single nucleotide substitution and one in frame 6 nucleotide deletion which eliminates two amino acids. Only four of them are accompanied by the reference to *db SNP Short Genetic Variations* and by the MAF value (=*Minor Allele Frequency*), which has been calculated on at least 1000 genomes in different populations. Two of them are accompanied only by the reference to *db SNP Short Genetic Variations* (Pro850Leu and Val1199Met) and three are new variants, not reported in the available data bases (Thr26_27del, Asp686Glu and Lys1160Thr).

In silico analysis (PolyPhen) revealed that most of them were probably damaging. No carriers of these variants were found in a large group of normolipidemic healthy control subjects.

The majority of these variants are located in the first N-terminal 1000 amino acids of mature protein, a crucial domain for proper folding of apoB, assembly of lipids with nascent apoB and secretion of lipoprotein particles.

Table 4. ApoB amino acid changes in hypocholesterolemic blood donors

Exon	cDNA variation	Variation effect on ApoB	No of probands	Clinical significance	Description
Ex 3	c.158_163del6	Thr26_27del	1	NA	New variant
Ex 5	c.386A>G	Tyr102Cys	1	PolyPhen: probably damaging	MAF 0,001 rs=201368319
Ex 12	c.1594C>T	Arg505Trp	1	PolyPhen: probably damaging	MAF 0,037 rs=13306194
Ex 15	c.2139C>A	Asp686Glu	1	PolyPhen: benign	New variant
Ex 18	c.2630C>T	Pro850Leu	1	PolyPhen: probably damaging	MAF n.a. rs=12714097
Ex 21	c.3220G>A	Gly1047Arg	1	PolyPhen: probably damaging	MAF 0,001 rs=72653074
Ex 22	c.3337G>C	Asp1086His	1	PolyPhen: possibly damaging	MAF 0,0034 rs=12713844
Ex 23	c.3560A>C	Lys1160Thr	6	PolyPhen: possibly damaging	New variant
Ex 23	c.3676G>A	Val1199Met	1	PolyPhen: benign	MAF n.a. rs=138681343

Rs # db SNP Short Genetic Variations- NCBI database (http://www.ncbi.nlm.nih.gov/SNP/snp_ref.cgi?locusId=338

4.2 FUNCTIONAL ANALYSIS OF *APOB* MUTATIONS IDENTIFIED IN HYPOCHOLESTEROLEMIC BLOOD DONORS

We specifically focused on two variants, Thr26_27del (c.158_163del6, T26_27del) and Tyr102Cys (c.386A>G, Y102C), both located within the βα1 domain of apoB.

The first variant is a two amino acid deletion (Threonine and Tyrosine at position 26 and 27 respectively of mature protein); the second variant replaces a tyrosine at position 102 with a cysteine, a residue potentially involved in the formation of a new sulfide bridge.

During my thesis work, I performed *in vitro* studies to evaluate role of these variants in causing hypocholesterolemia (hypobetalipoproteinemia)

4.2.1 TRANSIENT EXPRESSION OF WILD TYPE AND apoB-48 MUTANTS

To investigate the effect of amino acid changes found in *APOB* gene, I performed in vitro mutagenesis experiments and functional studies in cells transfected with plasmids containing mutant *APOB* cDNAs.

The procedure was based on human *APOB-48 cDNA* cloning into an expression vector (pCMV-5), which was performed by Professor Yao's laboratory (University of Ottawa).

By *in vitro* site-directed mutagenesis technique, the mutations producing T26_27del and Y102C amino acid variants were introduced in human *APOB-48* cDNA wild-type (WT) cloned in pCMV-5 expression vector *(see methods)*.

Plasmids obtained by mutagenesis were transformed in bacterial cultures and selected for ampicillin resistance.

Each positive plasmid was sequenced to ascertain the presence of the newly inserted mutation and to exclude that other mutations might be introduced by chance during the procedure.

The biological effect of mutants T26_27del and Y102C was assessed by functional studies based on the transfection of corresponding plasmids into a heterologous cell system.

We used McA-RH7777 cell lines as they are not able to produce endogenous apoB-48 protein but only apoB-100, therefore the apoB-48 detected by western blotting was only the transfected human apoB-48.

The plasmids containing apoB-48 wild type (apoB-48 WT), apoB-48-T26_27del and apoB-48-Y102C were transiently transfected into McA-RH7777 cells.

After 24 hours the cells were incubated with acid oleic for 4 hours. Cells and media were collected and analyzed by SDS-PAGE, followed by Western blot assay with a monoclonal antibody to detect human apoB-48.

Figure 12 shows the Western blot of apoB-48 in transiently transfected cells expressing wild type and mutant apoB-48. ApoB-48 was estimated in cells and media.

The western blot analysis shows that apoB-48 WT was secreted efficiently while the mutant T26_27del was not detectable in the media. The mutant Y102C was secreted as the wild type protein.

This result suggested that the mutation T26_27del impaired apoB-48 secretion. The other mutant had no effect on apoB-48 secretion.

In the subsequent experiments we focused only on the T26_27del mutant.

FIGURE 12

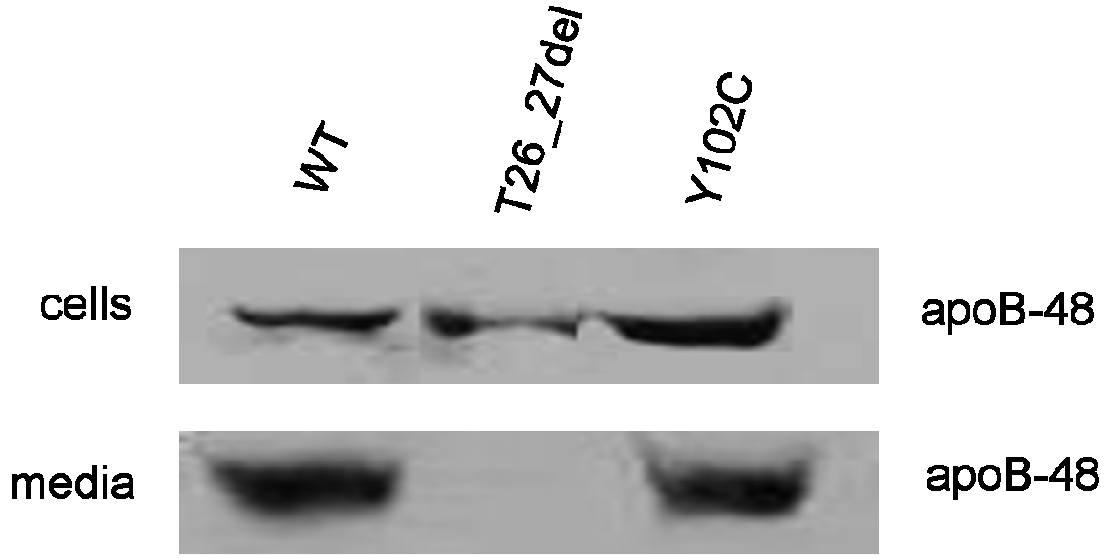

Figure 12. Transient expression of wild type and apoB-48 mutants.

The figure shows the western blot analysis of apoB-48 expressed McA-RH7777 cells The cells were transfected with human apoB-48-expressing plasmids harboring the two rare amino acid variants (T26_27del and Y102C) and wild type (WT) apoB-48. Two days post-transfection the cells were incubated with fresh DMEM containing 20% FBS and 0.4mM acid oleic for 4 hours. Cells and media were collected and subjected to SDS-PAGE. Human apoB-48 was detected by western blot analysis by using the monoclonal antibody 1D1 anti-human apoB-48.

4.2.2 STABLE EXPRESSION OF WILD TYPE AND apoB-48-T26_27del MUTANT

We generated stable clones using the calcium phosphate precipitation technique. The colonies were screened to select the colonies expressing human apoB-48. We obtained several stable clones expressing wild type and mutant apoB-48 at variable level. We chose one clone expressing wild type apoB-48 (WT clone) and two mutant stable clones (c.4 and c.14.1) which showed an intracellular level of apoB-48 expression comparable to that wild type clone.

Figure 13A shows the immunoblots of wild type and mutant apoB-48 in cells and media (the first two panels) after 4 hours incubation with acid oleic.

Compared to WT clone, in the clone c.4 the mutant apoB-48 is present in minute amounts in the medium; in the clone c.14.1 the mutant apoB-48 is present only in trace amounts.

The three clones are comparable in terms of content of control proteins (β-actin and apolipoprotein E) as shown in the last two panel of Figure 13A.

The densitometric analysis of apoB-48 in the cell lysates and media (Figure 13B) revealed that the wild type protein is more abundant in the medium than in the cell indicating an efficient secretion, as expected.

In the two mutant clones, apoB-48 is more abundant in the cells than in the medium suggesting a defective secretion.

The Figure 14 shows the secretion efficiency of apoB-48 calculated as the ratio between apoB-48 in media and total apoB-48 (cells plus media).

As shown in the histogram in the clone c.4 the secretion efficiency was reduced by 50%; in the clone 14.1 the reduction was about 70% compared to WT clone.

FIGURE 13

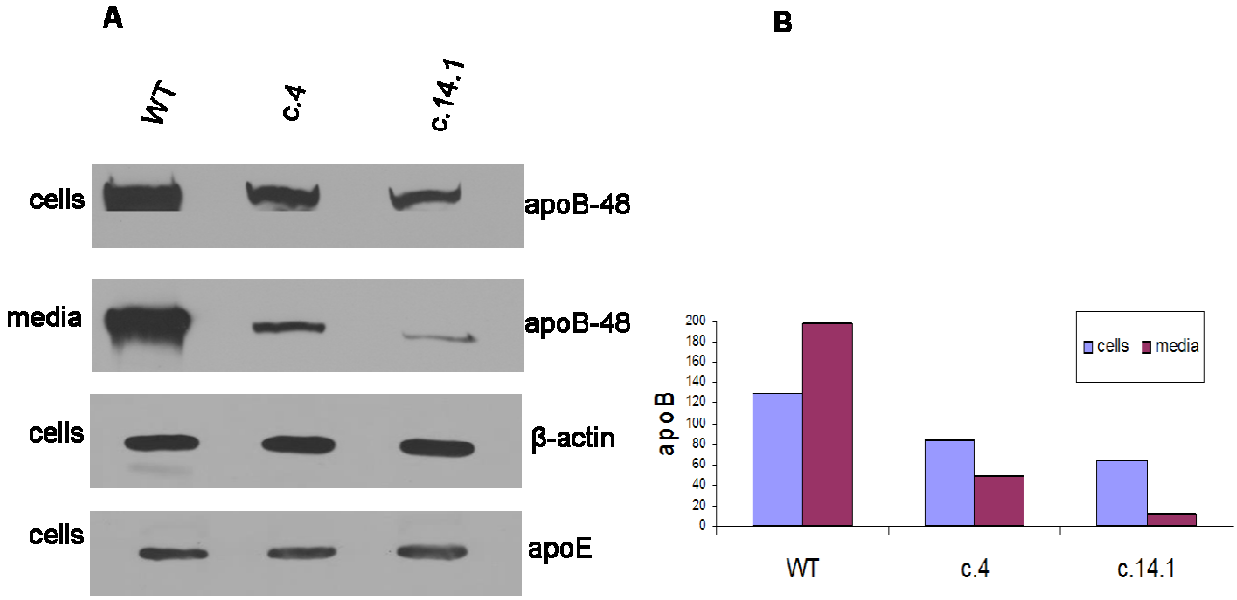

Figure 13. Stable expression of wild type and apoB-48-T26_27del mutant.

A. *Western blot analysis of stable cell lines expressing apoB-48 WT or apoB-48-T26_27del (clones 4 and 14.1). The cells were incubated with DMEM containing 20% FBS and 0.4mM acid oleic for 4 hours. Human apoB-48 was detected in cell lysates and media. The intracellular content of β-actin and apoE was used as control of protein synthesis.*

B. *Densitometric analysis of apoB-48 in the cell lysates and media shown in panel A.*

FIGURE 14

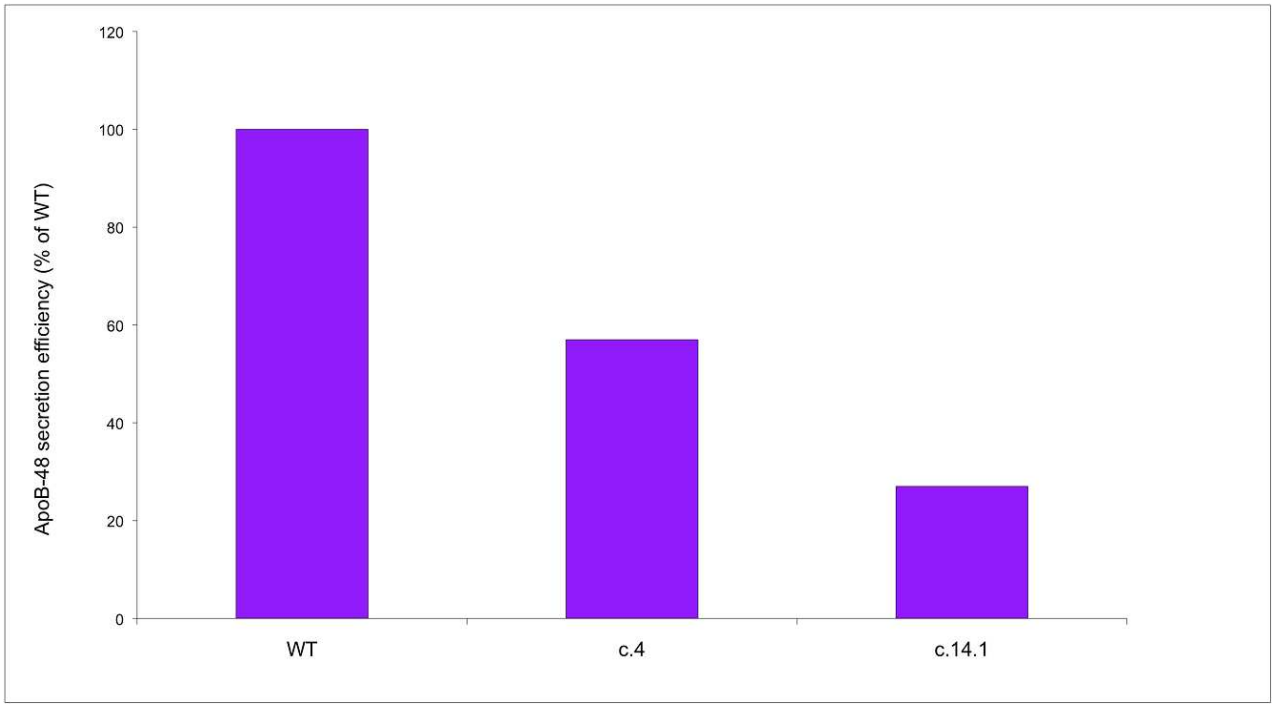

Figure 14. Secretion efficiency of apoB-48 in cell expressing wild type and mutant apoB-48.

The histogram shows the secretion efficiency of apoB-48 calculated as the ratio between apoB-48 in media and total apoB-48 (cell plus media). The data are expressed as percentage of apoB-48 WT.

So we decided to continue the experiments using only the clone c.14.1 which showed a more severe secretion defect.

We next performed time-course study to monitor the secretion of apoB-48 over a period of 4 hours.

Figure 15 shows that the wild type protein was secreted very efficiently; the secretion reached a plateau at 4 hours. By contrast only a trace amount of the mutant apoB-48 was detectable at 4 hours. These results confirm that the mutation induce a severe defect of secretion.

FIGURE 15

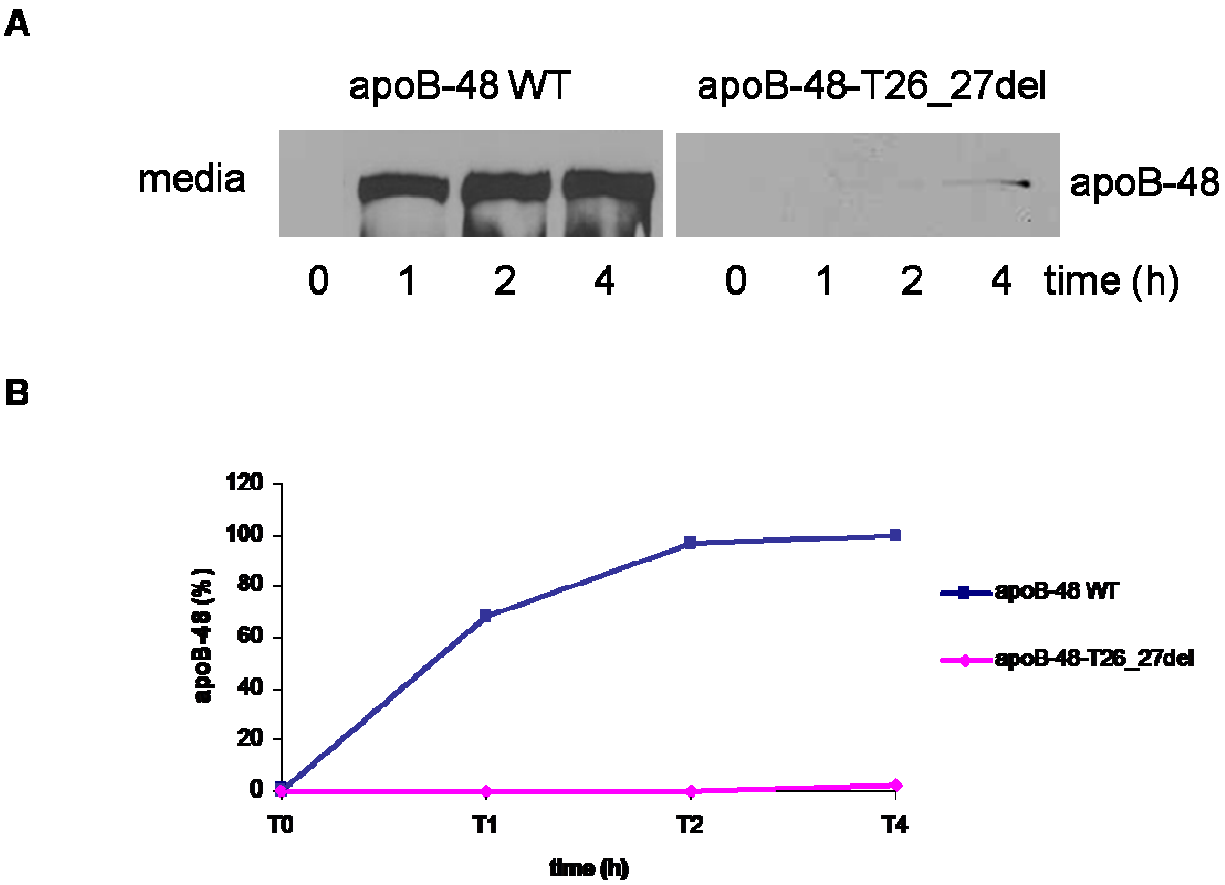

Figure 15. Secretion apoB-48 from WT and T26_27del expressing cells.

A. *Western blot analysis of apoB-48 in media. Cells expressing human apoB-48 WT and apoB-48-T26_27del were incubated with DMEM containing 20% FBS and 0.4mM acid oleic for 0, 1, 2, 4 hours. Cycloheximide was added to media at time 0. At the indicated time points the media were collected, the cells were lysed, and human apoB-48 was analyzed by SDS-PAGE and western blot.*

B. *The intensity of apoB-48 bands was quantified by densitometric scanning. Data are presented as percentage of initial level (time 0).*

4.2.3 DISTRIBUTION OF apoB-48-T26_27del MUTANT IN MEDIUM LIPOPROTEINS

To evaluate if the mutant clone was able to produce lipoprotein containing apoB, we incubated stable cells expressing wild type and mutant apoB-48, for 4 hours with acid oleic; then we collected the medium and separated the different classes of lipoproteins by density gradient ultracentrifugation (*see methods*).

In the wild type clone apoB is present in High Density Lipoprotein fractions as expected in rat hepatoma cells (Figure 16).

In the case of mutant clone no apoB containing lipoproteins were detected in the medium even after a prolonged exposure of the membrane.

This finding supports the previous results that apoB-48-T26_27del exhibits a severe defect on secretion and indicates that the mutant apoB is not suitable to form lipoprotein particles.

FIGURE 16

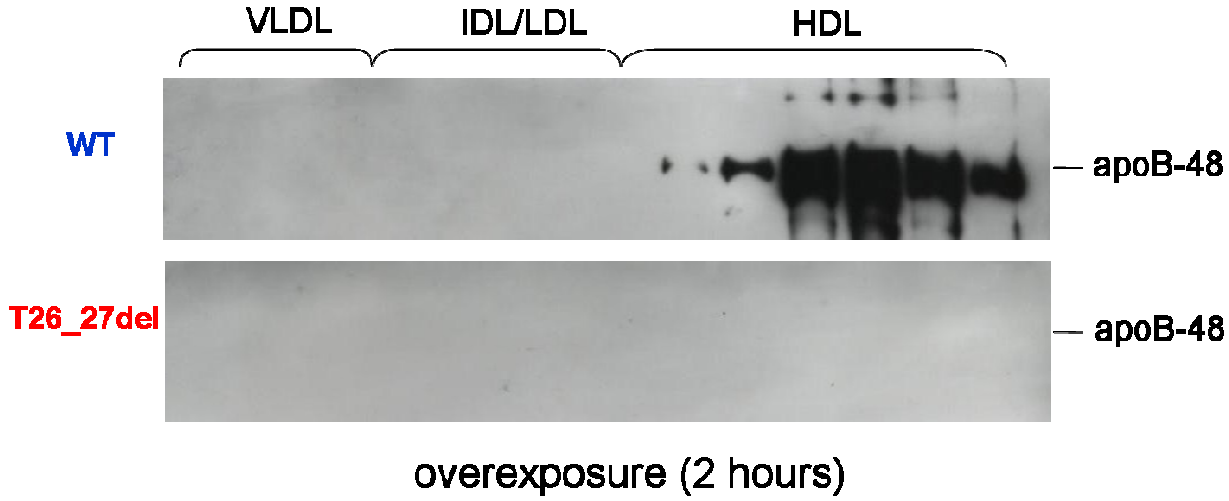

Figure 16. Distribution of apoB-48-T26_27del in medium lipoproteins.

The figure shows the western blot of apoB-48 containing lipoproteins secreted into the medium in cells expressing wild type protein (the first panel) and mutant protein (second panel).

Stably transfected cells (c.14.1 and wild type clone) were incubated with DMEM containing 20% FBS and 0.4mM acid oleic for 24 hours. At the end of incubation the media were collected and subjected to gradient ultracentrifugation to separate medium lipoproteins (VLDL, IDL/LDL and HDL). ApoB-48 was immunoprecipitated using anti-human apoB-48 polyclonal antibody. ApoB-48 was detected by western blotting analysis by using the monoclonal antibody (1D1) anti human apoB-48.

4.2.4 INTRACELLULAR LOCALIZATION OF apoB-48-T6_27del MUTANT

To establish if the lack of apoB-48-T26_27del secretion was accompanied by its intracellular retention we looked at the intracellular localization of the wild type and mutant apoB-48.

Stably transfected cells were co-stained with an anti-calnexin antibody, a marker of endoplasmic reticulum, and anti human apoB-48 followed by confocal imaging.

Figure 17 shows the intracellular localization of wild type and mutant apoB-48. The green color indicates the localization of calnexin, while the red color shows the localization of human apoB-48.

As indicated in the merge the apoB-48-T26_27del co-localized with calnexin indicating that it is retained in endoplasmic reticulum.

FIGURE 17

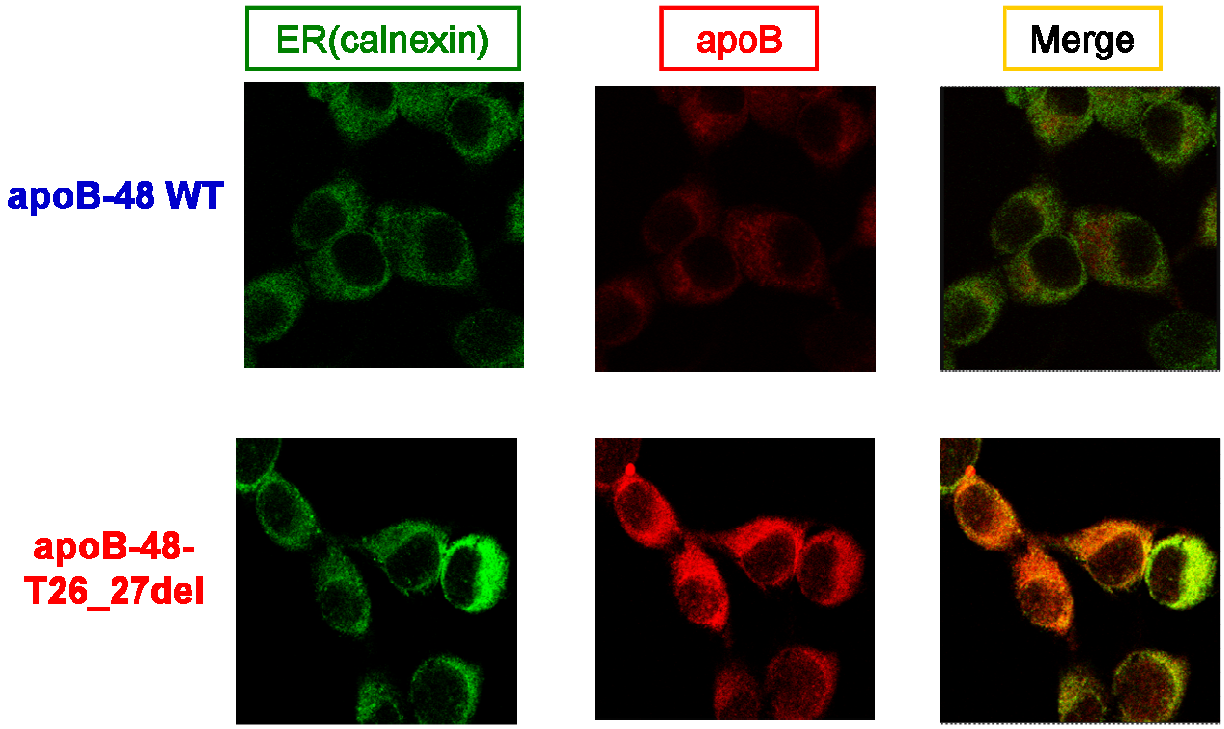

Figure 17. Intracellular localization of apoB-48-T26_27del.

The figure shows the immunolocalization of apoB-48-T26_27del.

In green is visualized the localization of endoplasmic reticulum marker (calnexin), in red the human apoB-48 protein and in merge the co-localization of apoB-48-T26_27del with calnexin.

4.2.5 INTRACELLULAR CONTENT OF THE apoB-48-T26_27del MUTANT

To better define the intracellular accumulation of mutant apoB-48, we performed a time-course study by incubating cells expressing wild type and mutant apoB-48 for 4 hours in the presence of cycloheximide to block protein synthesis.

As shown in Figure 18 the intracellular content of the wild type apoB-48 showed a progressive decrease as a consequence of an efficient secretion; after 1 hour of incubation the decrease was 10%, and at 4 hours was about 30%.

In the case of the apoB-48-T26_27del the intracellular apoB-48 content decreased very rapidly; at 1 hours it was 50% of the amount present at time 0 and after 4 hours it was only 10% even though it was not secreted.

This result suggested that a relevant proportion of mutant apoB-48 is degraded intracellularly and is not available for binding lipid and forming lipoprotein.

FIGURE 18

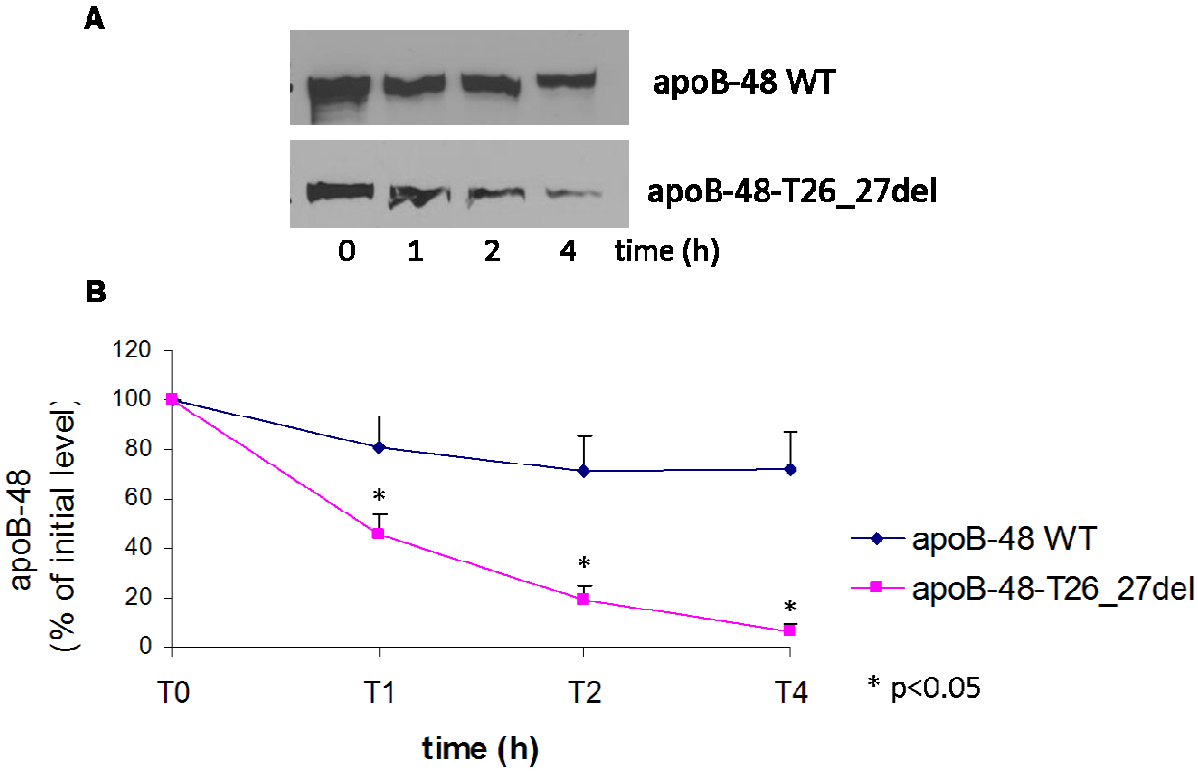

Figure 18. Intracellular content of apoB-48 in wild type or mutant expressing cells.

A. *Western blot analysis of apoB-48 in cells expressing human apoB-48 WT and apoB-48-T26_27del. Cells were incubated with DMEM containing 20% FBS and 0.4mM acid oleic for 0, 1, 2, 4 hours. Cycloheximide was added to media at time 0. At the indicated time points the cells were lysed and human apoB-48 was analyzed by SDS-PAGE and western blotting.*

B. *The intensity of apoB-48 bands was quantified by densitometric scanning. Data are given as percentage of initial level (time 0). Each point represents the media ± standards deviation of 3 experiments. Statistical significance was evaluated by Student T-test.*

4.2.6 EFFECT OF MG132 ON POST-TRANSLATIONAL STABILITY OF apoB-48-T26-27 del MUTANT.

To evaluate which pathways was involved in the degradation of apoB-48-T26_27del we looked at proteasomal degradation by using a specific inhibitor, MG132.

The cells expressing wild type and mutant apoB-48 were incubated in presence or in absence of MG132 for 0, 1, 2 and 4 hours. Cycloheximide was included at the beginning of incubation to block protein synthesis. The experiment was repeated three times at the same conditions.

As indicated in Figure 19 in cells expressing apoB-48 WT there was no difference in the amount of intracellular apoB-48. In contrast, in cells expressing apoB-48-T26_27del the amount of intracellular apoB-48 decreased by 40% in presence of the inhibitor of proteasomal degradation (similarly to the WT) as compared with 80% reduction observed in its absence. Thus in the presence of MG132 the expected intracellular decay of the mutant apoB-48 is partly prevented. These results suggested that a significant proportion of mutant apoB-48 is degraded by the proteasome.

FIGURE 19

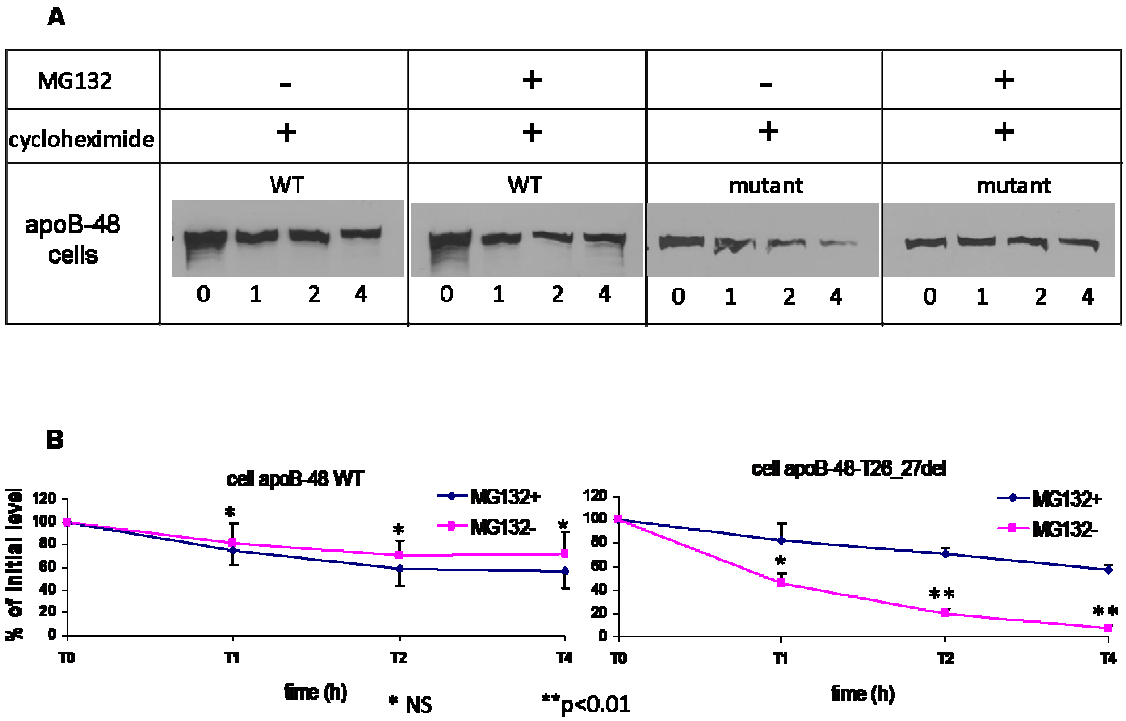

Figure 19. Effect of MG132 on post-translation stability of wild type and mutant apoB-48.

A. *Western blot analysis of apoB-48 in cells expressing human apoB-48 WT and apoB-48-T26_27del. The cells were incubated with DMEM containing 20%FBS and 0,4mM acid oleic for 0, 1, 2 and 4 hours in the presence of cycloheximide and in presence or absence of MG132. At the indicated time points the cells were lysed and apoB-48 was analyzed by SDS-PAGE and western blotting.*

B. *The intensity of apoB-48 bands was quantified by densitometric scanning. Data are given as percentage of initial level (time 0). Each point represents the media ± standard deviation of 3 experiments. Statistical significance was evaluated by Student T-test.*

4.2.7 EFFECT OF THE AUTOPHAGOSOME/LYSOSOME SYSTEM INHIBITION

We next tested the role of autophagy on the intracellular degradation of mutant apoB-48. We used two lysosomal inhibitors: 3-methyl adenine (3-MA) and ammonium chloride (NH_4Cl). 3-MA inhibits autophagy by blocking autophagosome formation via the inhibition of type III Phosphatidynositol 3-kinase (PI-3K); NH_4Cl blocks the phagosome-lysosome fusion.

ApoB-48 wild type and mutant expressing cells were pretreated with or without 3-methyl adenine for 25 minute and then incubated for 0, 1, 2 and 4 hours in presence of cycloheximide. At each time point the cells were processed (*see methods*) and the apoB-48 protein was analyzed by SDS-PAGE and Western blot. The experiment was repeated two times at the same conditions.

As shown in Figure 20 the intracellular content of mutant apoB-48 is the same in the presence or in the absence of the inhibitor, as the wild type protein.

The treatment with 3-methyl adenine did not induce a decrease of mutant protein stability suggesting that the autophagy does not play a role in the protein degradation.

FIGURE 20

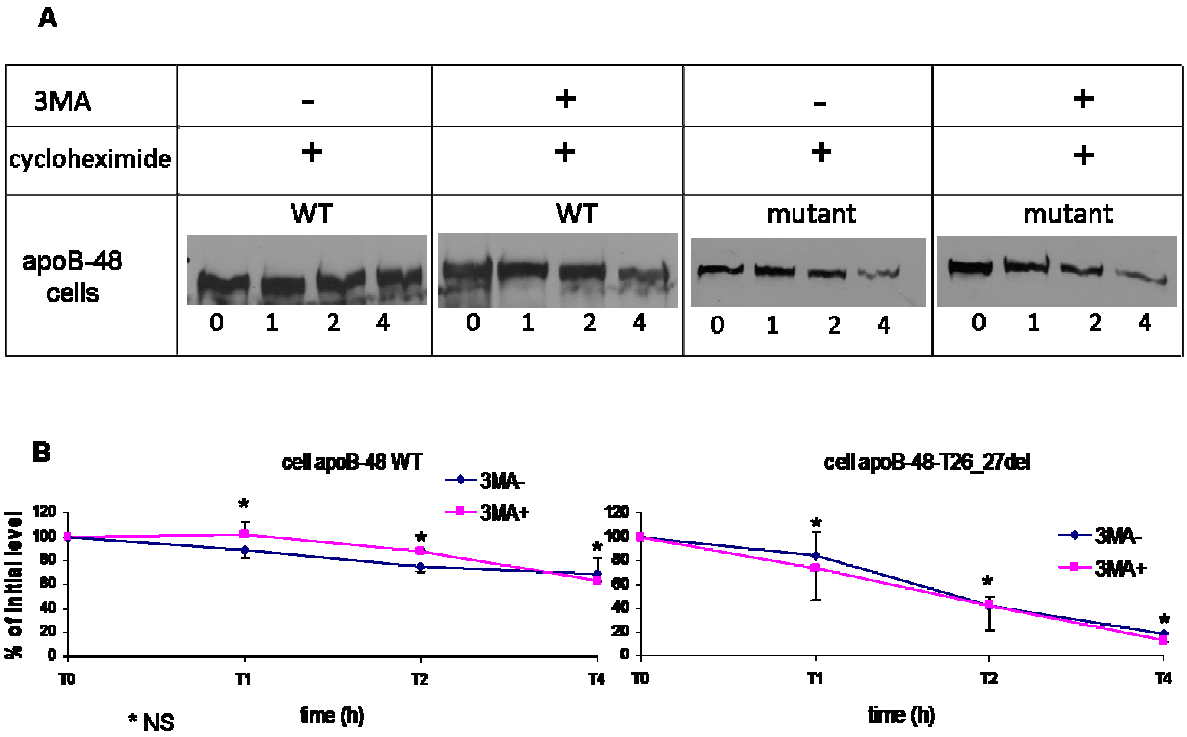

Figure 20. Effect of the autophagosome/lysosome system inhibition by using 3MA.

A. *Western blot analysis of human apoB-48 in cells expressing apoB-48 WT and apoB-48-T26_27del. Cells were incubated in DMEM containing 20% FBS and 0,4 mM acid oleic with or without 3-methyladenine (3-MA) for 25 minutes. Cycloheximide was added at time 0. After 3-MA pre-treatment, the cells were incubated for 1, 2 and 4 hours. At the indicated time points the cells were lysed and human apoB-48 was analyzed by SDS-PAGE and western blotting.*

B. *The intensity of apoB-48 bands was quantified by densitometric scanning. Data are given as percentage of initial level (time 0). Each point represents the media ± standard deviation of 2 experiments. Statistical significance was evaluated by Student T-test.*

To confirm the lack of involvement of autophagic degradation, the experiment was conducted in the presence or in absence of NH_4Cl. ApoB-48 mutant expressing cells were incubated for 0, 1, 2 and 4 hours with or without NH_4Cl, in presence of cycloheximide. At each time point the cells were lysed (*see methods*) and the recombinant apoB-48 protein was analyzed by SDS-PAGE and Western blot. As a specific marker of autophagy we used LC3; in particular the LC3-II and LC3-I forms ratio was analyzed, as internal control, to assess that the inhibition occurred.

The intracellular content of mutant apoB-48 did not show significant differences in the presence or in the absence of the inhibitor, as shown in Figure 21.

The ratio between LC3-II and LC3-I showed a progressive increase in the presence of NH_4Cl indicating that the ammonium chloride has acted as lysosomal inhibitor (Figure 22)

This result confirms that autophagy is not involved in apoB-48-T26_27del intracellular degradation.

FIGURE 21

A

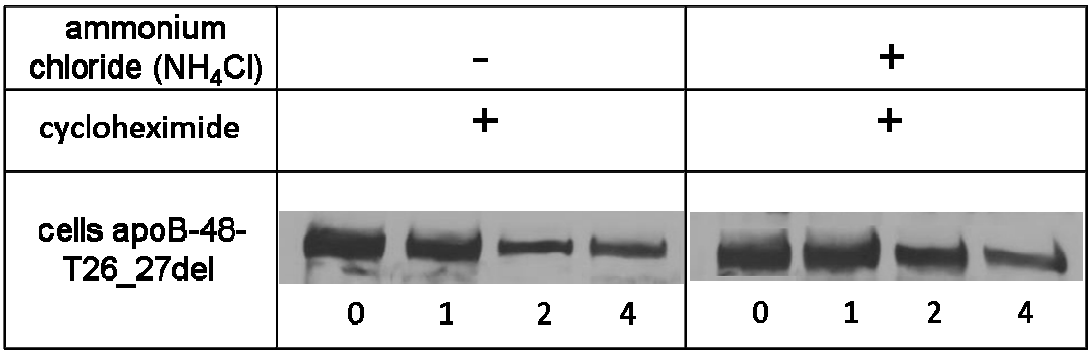

B

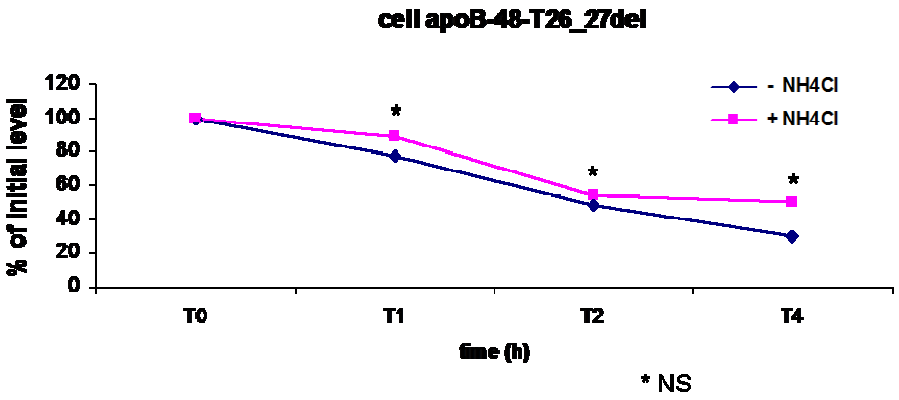

Figure 21. Effect of NH_4Cl on the autophagosome/lysosome system.

A. *Western blot analysis of human apoB-48 in cells expressing apoB-48-T26_27del. Cells were incubated in DMEM containing 20% FBS, 0,4 mM acid oleic and cycloheximide, with or without ammonium chloride (NH_4Cl) for 0, 1, 2 and 4 hours. At the indicated time points the cells were lysed and human apoB-48 was analyzed by SDS-PAGE and western blotting.*

B. *The intensity of apoB-48 bands was quantified by densitometric scanning. Data are given as percentage of initial level (time 0).*

FIGURE 22

A

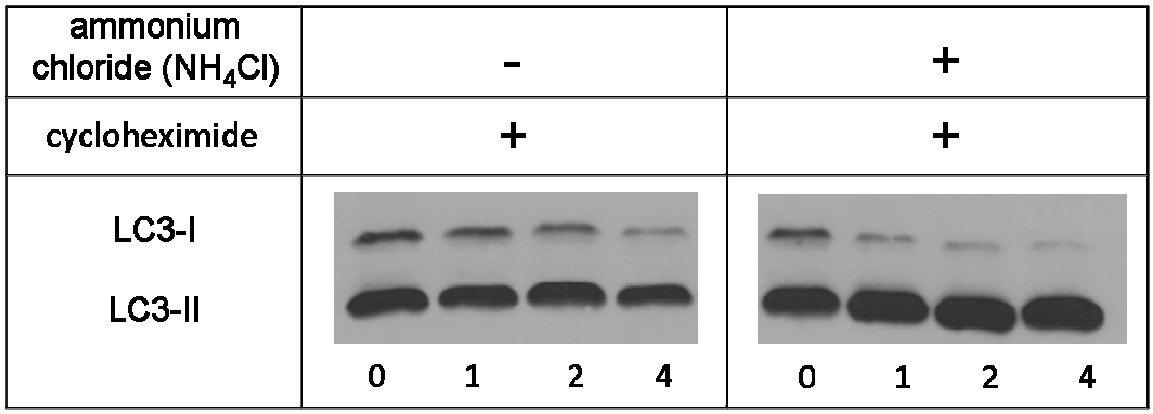

B

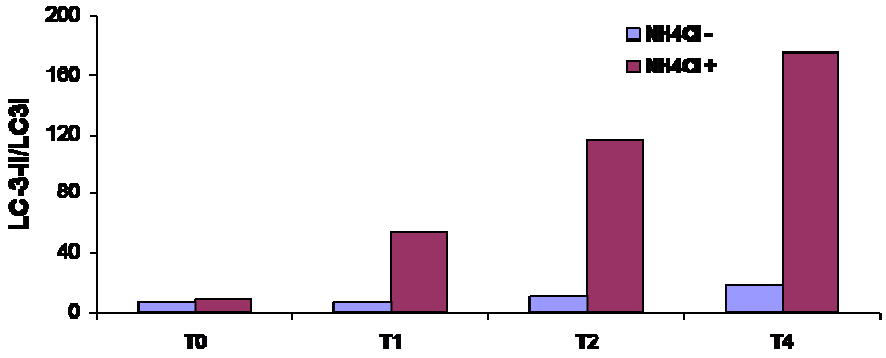

Figure 22. Effect of NH_4Cl on LC3-II/LC3-I ratio.

A. *Western blot analysis of LC3-I and LC3-II forms in cells expressing apoB-48-T26_27del. Cells were incubated in DMEM containing 20% FBS, 0,4 mM acid oleic and cycloheximide, with or without ammonium chloride (NH_4Cl) for 0, 1, 2 and 4 hours. At the indicated time points the cells were lysed and human apoB-48 was analyzed by SDS-PAGE and western blotting.*

B. *The intensity of LC3 bands was quantified by densitometric scanning. The histogram shows the ratio between LC3-II and LC3-I, used as internal control.*

PARTE II

4.3 *ANGPTL3* GENE MUTATIONS IN SUBJECTS WITH "ORPHAN" FHBL

Three years ago a exome sequencing had revealed the role of human ANGPTL3 gene in lipid metabolism. *Musunuru et al.* identified ANGPTL3 gene mutations in four individuals originally diagnosed as affected by FHBL and in whom mutations in the other candidate genes (*APOB* and *PCSK9)* had been excluded (64). These individuals had a peculiar plasma lipid profile, characterized by low total cholesterol, LDL and apoB (similar to that found in classic FHBL) as well as a reduction of plasma HDL. This condition has been named Familial Combined Hypolipidemia.

This observation prompted us to sequence ANGPTL3 gene in our series of FHBL subjects in whom no causative mutations in the other known candidate genes had been found ("orphan" FHBL) (87).

We identified a subject (D.V) with a lipid phenotype consistent with the diagnosis of Familial Combined Hypolipidemia. The proband (Figure 23) is 65-year-old white female who, at the age of 52 years, was referred to the Lipid Clinic for very low plasma lipid levels (Figure 23). The separation of plasma lipoproteins by density gradient ultracentrifugation showed an almost complete absence of the VLDL peak and a substantial reduction of the LDL and HDL. (87) The proband had no family history of cardiovascular disease and no clinical manifestations of cardiovascular disease. Abdominal ultrasound examination did not reveal the presence of fatty liver.

The sequence analysis of ANGPTL3 gene revealed that she was homozygous for a single nucleotide substitution (c.1198+1G>T) in intron 6 of *ANGPTL3*

gene affecting the donor splice site. The proband's offspring were heterozigote carriers of this mutation as shown in Figure 23.

FIGURE 23

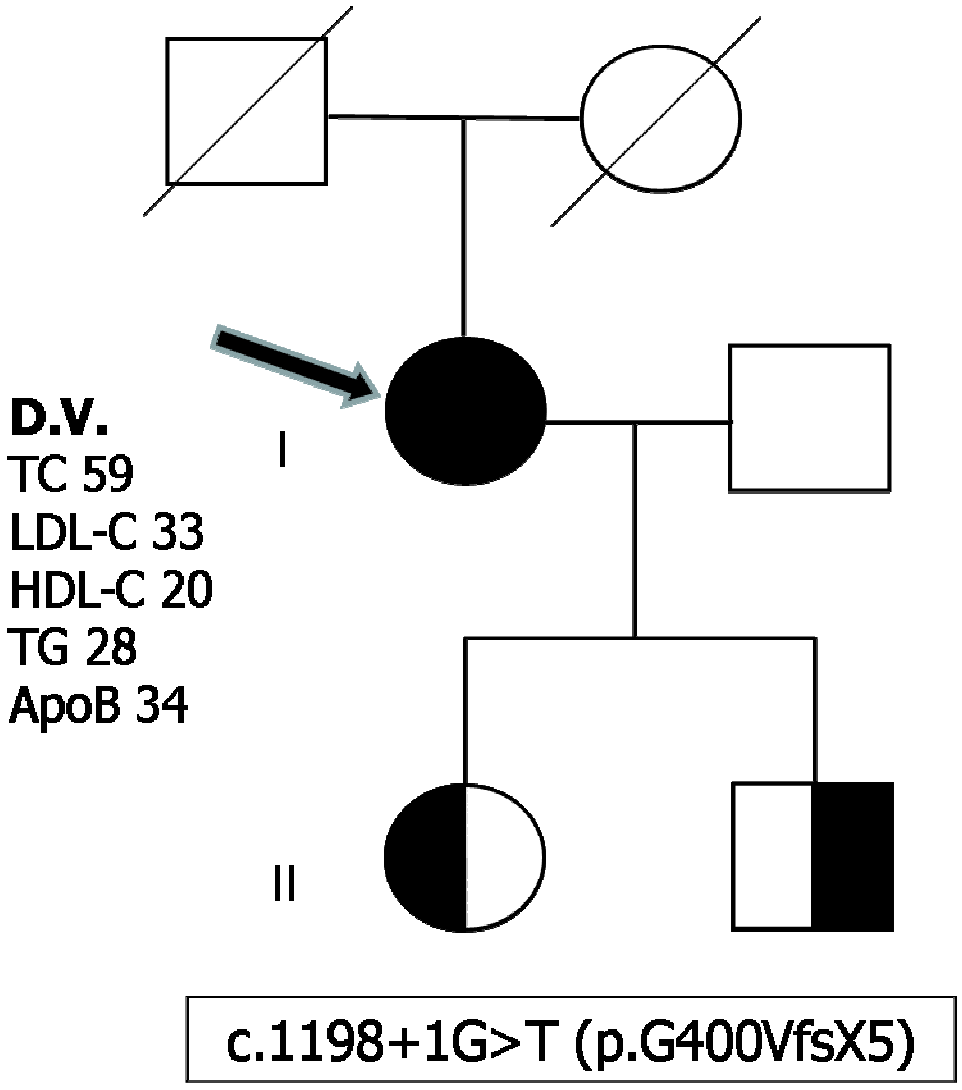

Figure 23. Pedigrees of D.V. kindred carrying the mutation c.1198 +1G>T in the ANGPTL3 gene. *The proband is indicated by an arrow. The homozygote and the simple heterozygotes are indicated by completely or half-filled symbols, respectively.*

4.3.1 IN VITRO STUDY OF SPLICE-SITE MUTATION

Computational splice site analysis predicted that the function of the canonical donor splice site was abolished. To verify the effect of this prediction we constructed a wild type and mutant *ANGPLT3* minigenes by the amplification of the appropriate *ANGPLT3* gene region from proband's genomic DNA. The minigenes were cloned into the expression vector and transfected in COS-1 cells.

The in vitro analysis of the transcripts showed that the transcript of the mutant minigene consisted of a fragment of 580 bp with respect to 409 bp of the wild type minigene (Figure 24 lane 5 and 6 respectively).

The splicing defect due to the c.1198 +1G>T mutation in intron 6 of *ANGPTL3* gene is illustrated in Figure 25.

The sequence of the mutant transcript showed that exon 6 was followed by the 5' half of intron 6 (171 bp) which in turn was followed by exon 7. The partial retention of intron 6, which was due to the activation of a cryptic donor site in intron 6, causes a shift in the reading frame leading to a premature termination codon at position 404 (p.G400VfsX5).

This abnormal mRNA is predicted to encode a truncated protein of 403 amino acids instead of 460 of the normal Angplt3 protein.

FIGURE 24

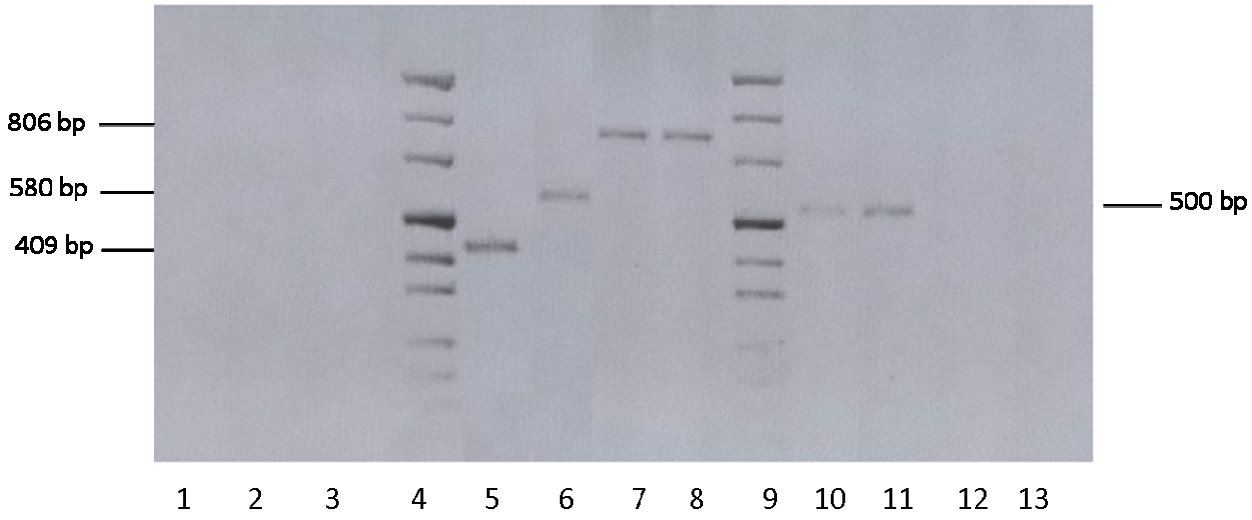

Figure 24. Analysis of the transcription products of ANGPLT3 minigene harbouring the c.1198 +1g>t mutation.

RNA isolated from COS-1 cells transfected with wild-type and mutant ANGPTL3 minigenes was reverse transcribed and the exon 6–exon 7 region of ANGPLTL3 cDNA was amplified by PCR (RT-PCR). The figure shows the agarose gel electrophoresis of the RT-PCR products. Untransfected cells (lanes 1–3); DNA size markers (lanes 4 and 9); ANGPTL3 cDNA in cells transfected with the wild-type (lane 5) and mutant (lane 6) minigene; genomic DNA of wild type and mutant minigenes (lanes 7 and 8); neomycin resistance gene in cells transfected with wildtype (lane 10) and mutant (lane 11) minigenes; "mock" RT-PCR in cells transfected with wild-type (lane 12) and mutant (lane 13) minigenes, respectively.

FIGURE 25

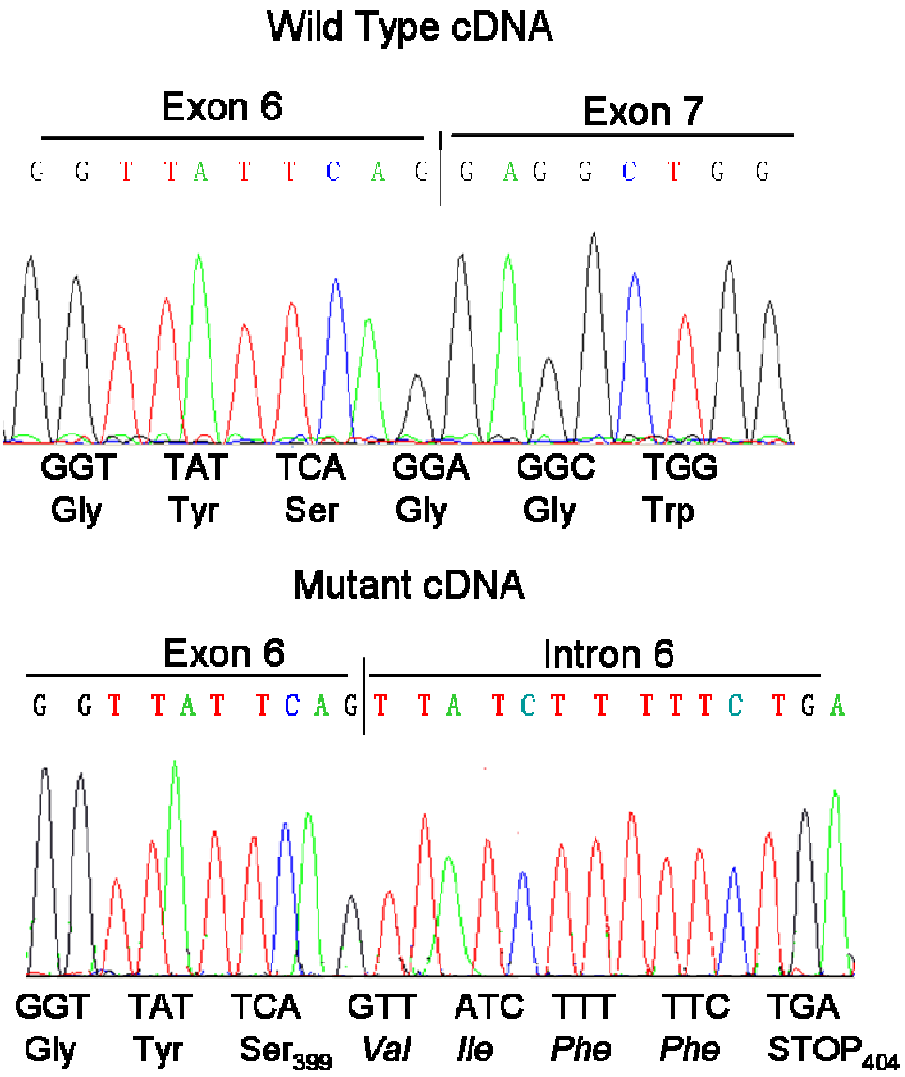

Figure 25. Nucleotide sequence of the transcription products.

Sequence analysis of the transcription products of the wild-type ANGPTL3 minigene (upper panel) and the mutant ANGPTL3 minigene harbouring the c.1198 +1 g>t mutation in intron 6 (lower panel).

The upper panel shows the sequence of the exon 6/exon 7 junction in the cDNA generated by wild-type ANGPTL3 minigene transfected in COS1 cells.

In the transcript generated by the mutant ANGPTL3 minigene (lower panel) exon 6 is followed by the 5' end of intron 6. The predicted translation product of this transcript is a truncated protein of 403 amino acids.

5. CONCLUSIONS

PART I

Only three apoB amino acid substitutions have been reported so far to be the cause of FHBL: R463W, L343V, and A31P (55, 56, 61). These mutations induce a severe defect on apoB-containing lipoproteins associated with a major apoB retention within endoplasmic reticulum (R463V and L343V) or in the Golgi (A31P). These mutations involve the N-terminal beta-alpha1domain of apoB which contains sequence elements shown to be important for the proper folding of apoB (4, 57) and for lipid recruitment during lipoprotein assembly and effective secretion (59).

In this study we analyzed the in vitro functional effect of two novel amino acid variants (T26_27del, Y102C) of apoB identified during a population screening of 100 blood donors recruited for low plasma TC (below the 2^{th} percentile).

The first variant (T26_27del) is a two amino acid deletion (Threonine and Tyrosine at position 26 and 27 respectively of mature protein); the second variant (Y102C) replaces a thyrosine at position 102 with a cysteine, a residue potentially involved in the formation of a new sulfide bridge. Both variants are located within the $\beta\alpha 1$ domain of apoB, specifically within the β-barrel. This domain may be critical for apoB-48 secretion; the two disulfide bonds (Cys51-Cys70 and Cys 218-Cys234) (61,88,89) and the correct folding of this region are essential for appropriate apoB containing lipoprotein secretion. Despite the similar localization in the protein of the two variants we found that the variant Y102C had no effect on apoB-48 secretion; maybe the substitution of tyrosine with a cysteine, both polar amino acids, does not affect the proper protein folds and consequently the apoB-48 secretion. On the contrary the variant

T26_27del causes a severe reduction of apoB-48 secretion and the lack of formation of apoB containing lipoproteins.

The effect of variant T26_27del is similar to that reported for A31P, which is located in the protein very closed to the T26_27del. In contrast to apoB-48-A31P that is retained in the Golgi, apoB-48-T26_27del appears to be retained mostly in the ER.

Our results show that the intracellular content of apoB-48-T26_27del decreased very rapidly even though it was not secreted, suggesting that a relevant proportion of mutant apoB-48 is degraded intracellularly .

The main pathways of intracellular apoB degradation involved are: endoplasmic reticulum association degradation (ERAD) and autophagy/PERPP.

The ERAD pathway is not only an ER quality control process but is also used to regulate metabolic processes by the ubiquitin-proteasome system (UPS). ERAD occurs when misfolded apoB is present in the cell or lipid supply/availability is reduced (20,21,90). To evaluate the involvement of this pathway, the cells were treated with an inhibitor of proteasomal degradation, the MG132.

We demonstrated that the majority of apoB-48-T26_27del is degraded by the ubiquitin-proteasome system. It is likely that the deletion of two amino acids (Threonine and Tyrosine) in the amino terminal region of apoB, lead to conformational changes in apoB protein causing gross misfolding. Consequently, its lipid-biding ability is reduced and the protein becomes more sensitive to proteasomal degradation.

To assess the involvement of autophagy in the apoB-48-T26_27del degradation, the cells were treated with two different lysosomal inhibitor, 3-methyl adenine (3-MA) and ammonium chloride (NH_4Cl). Our results indicate

that autophagy does not play a role in apoB-48-T26_27del degradation. The degradation of apoB-48-T26_27del occurs with a different mechanism with respect to that reported for apoB-48-A31P that escaping the ER quality control mechanism, accumulated in Golgi and was degraded through the autophagosome pathway.

We can not able to determine if the gross misfolding of apoB-48-T26_27del induce a oxidative stress and if the PERPP may be also involved in degradation of apoB mutant. In conclusion these studies on the functional effect of T26_27del variant support the hypothesis that this variant is the cause of FHBL.

PART II

In the present study we assess the functional effect of a splice site mutation identified in a subject with plasma lipid profile consistent with the diagnosis of Familial Combined Hypolipidemia (87).

The proband's lipid profile was characterized by a reduction of TC, LDL-C and apoB (hypobetalipoproteinemia) comparable to that observed in subjects with heterozygous FHBL caused by *APOB* mutations (45, 46, 87) associated with a marked reduction of HDL-C. This peculiar lipid profile, which resembles that found recently in carriers of ANGPTL3 LOF mutations (64) prompted us to resequence the *ANGPTL3* gene in the present study (87). The proband, negative for mutations in the other know candidate genes for hypobeta or hypoalphalipoproteinemia, was found to be homozygous for a single nucleotide substitution in the donor splice site of intron 6 (c. 1198 +1 G/T). This mutation had been reported previously by *Romeo et al* in heterozygous individuals of African descent and was assumed to be

deleterious. We performed in vitro studies by using the minigene strategy to assess that this mutation generates an abnormal mRNA predicted to encode a truncated protein. (87)

This result demonstrates that the LOF mutation identified in *ANGPTL3* gene in homozygous state is the cause of the combined hypolipidemia present in our proband. The plasma lipid profile of our proband was fairly similar to that of the individuals described by *Musunuru et al* (64) who were compound heterozygotes for LOF mutations in *ANGPTL3*.

Familial combined hypolipidemia does not seem to be associated with overt clinical manifestations. (65) Recent studies have indicated that ANGPTL3 is activated by ANGPTL8, a novel member of the angipoietin-like protein family. (65) In some populations, a common missense variant of ANGPTL8 was found to be associate with reduced plasma levels of some lipoprotein classes. (65)

The recent finding that complete ANGPTL3 deficiency is the cause of combined familial hypolipidemia raises various questions concerning the biochemical mechanism underlying this lipid disorder, and the role of ANGPTL3 as a possible target for hypolipidemic therapy (65).

It would be interesting to know whether the role of ANGPTL3 is confined to the inhibition of LPL and EL, or also involves the assembly and secretion of apoB-containing lipoproteins in the liver. It is possible that ANGPTL3 acts as a chaperone molecule that protects apoB from intracellular degradation before its incorporation into lipoprotein particles (65).

The observation that, a partial or complete deficiency of ANGPTL3 protein is cause of a variable decrease of plasma TG, LDL-C and HDL-C, suggests that ANGPTL3 might be a novel therapeutic target for lowering plasma cholesterol. ANGPTL3 inhibition through molecules or specific antibodies

might be protective against the accumulation of atherogenic lipoproteins by increasing the catabolism of apoB-containing lipoproteins.

6. REFERENCES

1. Hooper AJ, van Bockxmeer FM, Burnett JR. Monogenic hypocholesterolaemic lipid disorders and apolipoproteinB metabolism. Crit Rev Clin Lab Sci 2005; 42: 515-545.

2. Whitfield AJ, Barrett PH, van Bockxmeer FM, Burnett JR. Lipid disorders and mutations in the *APOB* gene. Clin Chem 2004; 50: 1725–1732.

3. Segrest JP, Jones MK, De Loof H, Dashti NJ. Structure of apolipoprotein B-100 in low density lipoproteins. Lipid Res. 2001 ; 42 :1346-1367.

4. Mann CJ, Anderson TA, Read J, et al. The structure of vitellogenin provides a molecular model for the assembly and secretion of atherogenic lipoproteins. J Mol Biol 1999; 285: 391– 408.

5. Segrest JP, Jones MK, Dashti NJ. N-terminal domain of apolipoprotein B has structural homology to lipovitellin and microsomal triglyceride transfer protein: a "lipid pocket" model for self-assembly of apoB-containing lipoprotein particles. J Lipid Res 1999; 40: 1401–1416.

6. Anderson TA, Levitt DG, Banaszak LJ. The structural basis of lipid interactions in lipovitellin, a soluble lipoprotein. Structure. 1998; 6: 895-909.

7. Hussain MM, Bakillah A, Nayak N, Shelness GS. J. Amino Acids 430-570 in Apolipoprotein B are critical for its binding to microsomal triglyceride transfer protein. J. Biol. Chem. 1998; 273: 25612-25615.

8. Bradbury P, Mann C. J, Kochl S, Anderson TA, Chester SA, Hancock JM, Ritchie PJ, Amey J, Harrison GB, Levitt DG, Brnaszak LJ, Scott J, Schoulders CC. J. Biol. Chem. 1999; 274: 3159-3164.

9. Fisher EA, Ginsberg HN. Complexity in the secretory pathway: the assembly and secretion of apolipoprotein B-containing lipoproteins. J Biol Chem 2002; 277: 17377-17380.

10. Brodsky JL, Fisher EA. The many intersecting pathway underlying apolipoprotein B secretion and degradation. Trends Endocrinol Metab 2008; 19: 254-259.

11. Hussain MM, Shi J, Dreizen P. Microsomal triglyceride transfer protein and its role in ApoB-lipoprotein assembly. J Lipid Res 2003; 44: 22-32.

12. Bakillah A., Jamil H., Hussain M.M. Lysine and arginine residues in the N-terminal 18% of polipoprotein B are critical for its binding to microsomal triglyceride transfer protein. Biochemistry 1998; 37: 3727-3734.

13. Gibbons GF, Wiggins D, Brown A-M, Hebbachi A-M. Synthesis and function of hepatic very-low-density lipoprotein. Biochem Soc Trans 2004; 32: 59-64.

14. Hussain MM, Fatma S, Pan X, Iqbal J. Intestinal lipoprotein assembly. Curr Opin Lipidol 2005; 16: 281-285.

15. Swift LL, Valyi-Nagy K, Rowland C, Harris C. Assembly of very low density lipoproteins in mouse liver: evidence of heterogeneity of particle density in the Golgi apparatus. J Lipid Res 2001; 42: 218–224.

16. Gusarova V, Brodsky JL, Fischer EA. Apolipoprotein B100 exit from the endoplasmic reticulum (ER) is COPII-dependent, and its lipidation to very low density lipoprotein occurs post-ER. J Biol Chem 2003; 278: 48051-48058.

17. Wang A-B, Liu D-P, Liang C-C. Regulation of human apolipoproteinB gene expression at multiple levels. Exp Cell Res 2003; 290: 1–12.

18. Avramoglu RK, Adeli K. Hepatic regulation of apolipoprotein B. Rev. Endocr Metab Disord 2004; 5: 293-301.

19. Pontrelli L, Sidiropoulos KG, Adeli K: Translational control of apolipoprotein B mRNA: regulation via cis elements in the 5′ and 3′ untranslated regions. Biochemistry 2004; 43: 6734-6744.

20. Ginsberg HN, Fisher EA. The ever-expanding role of degradation in the regulation of apolipoprotein B metabolism. J lipid Res. 2009; 50 Suppl:S162-6.

21. Jiang XC, Li Z, Liu R, Yang XP, Pan M, Lagrost L, Fischer EA, Williams KJ. Phospholipid Transfer Protein Deficiency Impairs Apolipoprotein-B Secretion from Hepatocytes by Stimulating a Proteolytic Pathway through a Relative Deficiency of Vitamin E and an Increase in Intracellular Oxidants. J Biol Chem 2005; 280: 18336-40.

22. Williams K J, Fless GM, Petrie KA, Snyder ML, Brocia RW., Swenson TL. Mechanism by which lipoprotein lipase alters cellular metabolism of lipoprotein (a), low density lipoprotein, and nascent lipoproteins. Roles for low density lipoprotein receptors and heparin sulphate proteoglycans. J. Biol. Chem.1992; 267, 13284–13292.

23. Shruthi S, Vembar and Jeffrey L. Brodsky. One step at a time: endoplasmic reticulum-associated degradation. Nat Rev Mol Cell Biol 2008; 9: 944–957.

24. Araki K, Nagata K. Protein folding and quality control in the ER. Cold Spring Harb Perspect Biol. 2012; 4: a015438

25. Hegde RS, Ploegh HL. Quality and quantity control at the endoplasmic reticulum. Curr Opin Cell Biol. 2010; 22: 437-46.

26. Deveraux Q, Ustrell V, Pickart C, Rechsteiner M. A 26 S protease subunit that binds ubiquitin conjugates. J Biol Chem. 1994; 269: 7059-61.

27. Raasi S, Wolf DH. Ubiquitin receptors and ERAD: a network of pathways to the proteasome. Semin Cell Dev Biol. 2007; 18: 780-91.

28. Husnjak K, Elsasser S, Zhang N, Chen X, Randles L, Shi Y, Hofmann K, Walters KJ, Finley D, Dikic I. Proteasome subunit Rpn 13 is a novel ubiquitin receptor. Nature. 2008; 453: 481-8.

29. Benoist F, Grand-Perret T. Co-translational degradation of apolipoprotein B100 by the proteasome is prevented by microsomal triglyceride transfer protein. Synchronized translation studies on HepG2 cells treated with an inhibitor of microsomal triglyceride transfer protein. J. Biol. Chem. 1997; 272: 20435–20442.

30. Dixon JL, et al. Oleate stimulates secretion of apolipoprotein B-containing lipoproteins from HepG2 cells by inhibiting early intracellular degradation of apolipoprotein B. J. Biol. Chem. 1991; 266: 5080–5086.

31. Zhou M, et al. Regulated Co-translational ubiquitination of apolipoprotein B100. A new paradigm for proteasomal degradation of a secretory protein. J. Biol. Chem. 1998; 273: 24649–24653.

32. Brodsky JL. The protective and destructive roles played by molecular chaperones during ERAD (ER associated degradation). Biochem. J. 2007; 404: 353–363.

33. Hrizo SL, et al. The Hsp110 molecular charperone stabilizes apolipoprotein B from endoplasmic reticulum associated degradation. J. Biol. Chem. 2007; 282: 32665–32675.

34. Qiu W, et al. Glucosamine-induced endoplasmic reticulum stress promotes ApoB100 degradation: evidence for Grp78-mediated targeting to proteasomal degradation. Arterioscler. Thromb. Vasc. Biol. 2005; 25: 571–577.

35. Siddiqi SA. VLDL exits from the endoplasmic reticulum in a specialized vesicle, the VLDL transport vesicle, in rat primary hepatocytes. Biochem. J. 2008; 413: 333–342.

36. Fromme JC, Schekman R. COPII-coated vesicles: flexible enough for large cargo? Curr. Opin. Cell Biol. 2005; 17: 345–352.

37. Mitchell DM, et al. Apoprotein B100 has a prolonged interaction with the translocon during which its lipidation and translocation change from dependence on the microsomal triglyceride transfer protein to independence. Proc. Natl. Acad. Sci. U. S. A. 1998; 95: 14733–14738.

38. Iwata A, et al. Increased susceptibility of cytoplasmic over nuclear polyglutamine aggregates to autophagic degradation. Proc. Natl. Acad. Sci. U. S. A. 2005; 102: 13135–13140.

39. Levine B, Kroemer G. Autophagy in the pathogenesis of disease. Cell 2008; 132: 27-42.

40. Ravikumar B, Sarkar S, Davies JE, et al. Regulation of mammalian autophagy in physiology and pathophysiology. Physiol Rev 2010; 90: 1383-435.

41. Choi AM, Ryter SW, Levine B. Autophagy in human health and disease. N Engl J Med. 2013; 14; 368: 651-62.

42. Singh R, Kaushik S, Wang Y et al. Autophagy regulates lipid metabolism. Nature 2009; 458: 1131-5.

43. Lin NY, Beyer C, et al. Autophagy regulates TNFα-mediated joint destruction in experimental arthritis. Ann Rheum Dis. 2012; [Epub ahead of print].

44. Schonfeld G. Familial hypobetalipoproteinemia: a review. J Lipid Res 2003; 44: 878-883.

45. Tarugi P, Averna M, Di Leo E, et al. Molecular diagnosis of hyobetalipoproteinemia: an ENID review. Atherosclerosis 2007; 195:e19-e27.

46. Schonfeld G, Lin X, Yue P. Familial hypobetalipoproteinemia: genetics and metabolism. Cell Mol Life Sci 2005; 62: 1372-1378.

47. Aguilar-Salinas CA, Barrett PH, Parhofer KG, et al. Apoprotein B-100 production is decreased in subjects heterozygous for truncations of apoprotein B. Arterioscler Thromb Vasc Biol 1995; 15: 71–80.

48. Elias N, Patterson BW, Schonfeld G. Decreased production rates of VLDL triglycerides and ApoB-100 in subjects heterozygous for familial hypobetalipoproteinemia. Arterioscler Thromb Vasc Biol 1999; 19: 2714–21.

49. Parhofer KG, Barrett PH, Bier DM, et al. Lipoprotein containing the truncated apo B-89 are cleared from human plasma more rapidly than apo B-100-containing lipoproteins in vivo. J Clin Invest 1992; 89: 1931–7.

50. Parhofer KG, Barrett PH, Aguilar-Salinas CA, et al. Positive linear correlation between the length of truncated apolipoproein B and its secretion rates: in vivo studies in human apo B-89, apo B-75, apo B-54.8, and apo B-31 heterozygotes. J Lipid Res 1996; 37: 844–52.

51. Krul ES, Parhofer KG, Barrett PH, et al. ApoB-75, a truncation of apolipoprotein B associated with familial hypobetalipoproteinemia: genetic and kinetic studies. J Lipid Res 1992; 33: 1037–50.

52. Zhu XF, Noto D, Seip R, et al. Organ loci of catabolism of short truncations of apoB. Arterioscler Thromb Vasc Biol 1997; 17: 1032–8.

53. Chen Z, Saffitz JE, Latour MA, et al. Truncated apo B-70.5-containing lipoproteins bind to megalin but not the LDL receptor. J Clin Invest 1999; 103: 1419–30.

54. Yao ZM, Blackhart BD, Linton MF, Taylor SM, Young SG, McCarthy BJ. Expression of carboxyl-terminally truncated forms of human apolipoprotein B in rat hepatoma cells. Evidence that the length of apolipoprotein B has a major effect on the buoyant density of the secreted lipoproteins. J Biol Chem 1991; 266: 3300-8.

55. Burnett JR, Shan J, Miskie BA et al. A novel nontruncating APOB gene mutation, R463W, causes familial hypobetalipoproteinemia. J Biol Chem 2003; 278: 13442–13452.

56. Burnett JR, Zhong S, Jiang ZG et al. Missense mutations in APOB within the $\beta\alpha 1$ domain of human ApoB-100 result in impaired secretion of ApoB and ApoB-containing lipoproteins in familial hypobetalipoproteinemia. J Biol Chem 2007; 282: 24270–24283.

57. Jiang ZG, Gantz D, Bullitt E, McKnight CJ. Defining lipid-interacting domains in the N-terminal region of apolipoprotein B. Biochemistry 2006; 45: 11799 –11808

58. Gretch DG, Sturley SL, Wang L, et al. The amino terminus of apolipoprotein B is necessary but not sufficient for microsomal triglyceride transfer protein responsiveness. J Biol Chem 1996; 271: 8682– 8691.

59. McLeod RS, Wang Y, Wang S, Rusiñol A, Links P, Yao Z. Apolipoprotein B sequence requirements for hepatic very low density lipoproteins assembly. Evidence that hydrophobic sequences within apolipoprotein B48 mediate lipid recruitment. J Biol Chem 1996; 271: 18445–18455.

60. Fouchier SW, Sankatsing RR, Peter J et al. High frequency of APOB gene mutations causing familial hypobetalipoproteinaemia in patients of Dutch and Spanish descent. J Med Genet 2005; 42: e23.

61. Zhong S, Magnolo AL, Sundaram M, et al. Non synonymous mutations within APOB in human familial hypobetalipoproteinemia: evidence for feedback inhibition of lipogenesis and postendoplasmic reticulum degradation of apolipoprotein B. J Biol Chem 2010; 285: 6453-6464.

62. Di Leo E, Magnolo L, Bertolotti M, et al. Variable phenotypic expression of homozygous familial hypobetalipoproteinaemia due to novel APOB gene mutations. Clin Genet 2008; 74: 267-273.

63. Najah M, Di Leo E, Awatef J, et al. Identification of patients with abetalipoproteinemia and homozygous familial hypobetalipoproteinemia in Tunisia. Clin Chim Acta 2009; 401: 51-56

64. Musunuru K., Pirruccello JP, Do R, Peloso GM, Guiducci C., Sougnez C, Garimella KV, Fischer S, Abreu J, Barry AJ, Fennell T, Banks E, Ambrogio L, Cibulskis K, Kernytsky A, Gonzalez E, Rudzicz N, Engert JC, DePristo MA, Daly MJ, Choen JC, Hobbs HH, Altshuler D, Schonfeld G, Gabriel SB, Yue P, Kathiresan S. Exome sequencing, ANGPTL3 mutations, and familial combined hypolipidemia. N Engl J Med. 2010; 363: 2220-2227.

65. Calandra S, Tarugi P, Averna M, Bertolini S. Familial combined hypolipidemia due to mutations in the *ANGPTL3* gene. Clin Lipidol. 2013; 8: 81–95.

66. Martín-Campos JM, Roig R, Mayoral C et al. Identification of a novel mutation in the ANGPTL3 gene in two families diagnosed of familial hypobetalipoproteinemia without APOB mutation. Clin. Chim. Acta 2012; 413: 552–555.

67. Minicocci I, Montali A, Robciuc MR et al. Mutations in the ANGPTL3 gene and familial combined hypolipidemia: a clinical and biochemical characterization. J. Clin Endocrinol. Metab.2012; 97: e1266–e1275.

68. Noto D, Cefalù AB, Valenti V et al. Prevalence of ANGPTL3 and APOB gene mutations in subjects with combined hypolipidemia. Arterioscler. Thromb. Vasc. Biol. 2012; 32: 805–809.

69. Shimizugawa T, Ono M, Shimamura M, Yoshida K, Ando Y, Koishi R, Ueda K, Inaba T, Minekura H, Kohama T, Furukawa H. ANGPTL3 decreases very low density lipoprotein triglyceride clearance by inhibition of lipoprotein lipase. J Biol Chem. 2002; 277: 33742-33748.

70. Hato T, Tabata M, Oike Y. The role of angiopoietin-like proteins in angiogenesis and metabolism. Trends Cardiovasc. Med. 2008; 18: 6–14.

71. Miida T, Hirayama S. Impacts of angiopoietin-like proteins on lipoprotein metabolism and cardiovascular events. Curr. Opin. Lipidol.2010; 21: 70–75.

72. Ono M, Shimizugawa T, Shimamura M, Yoshida K, Noji-Sakikawa C, Ando Y, Koishi R, Furukawa H. Protein region important for regulation of lipid metabolism in angiopoietin-like 3 (ANGPTL3): ANGPTL3 is cleaved and activated in vivo. J Biol Chem. 2003; 278: 41804-41809.

73. Camenisch G, Pisabarro MT, Sherman D, Kowalski J, Nagel M, Hass P, Gurney A, Bodary SC, Liang XH, Clark KR, Beresini M H, Ferrara N, Gerber HP. ANGPTL3 stimulates endothelial cell adhesion and migration via integrin alpha vbeta 3 and induces blood vessel formation in vivo. J. Biol. Chem. 2002; 277: 17281–17290.

74. Shimizugawa T, Ono M, Shimamura M, Yoshida K, Ando Y, Koishi R, Ueda K, Inaba T, Minekura H, Kohama T, Furukawa H. ANGPTL3 decreases very low density lipoprotein triglyceride clearance by inhibition of lipoprotein lipase. J Biol Chem. 2002; 277: 33742-33748.

75. Shimamura M, Matsuda M, Yasumo H, Okazaki M, Fujimoto K, Kono K, Shimizugawa T, Ando Y, Koishi R, Kohama T, Sakai N, Kotani K, Komuro R, Ishida T, Hirata K, Yamashita S, Furukawa H, Shimomura I. Angiopoietin-like protein3 regulates plasma HDL cholesterol through suppression of endothelial lipase. Arterioscler Thromb Vasc Biol. 2007; 27: 366-372.

76. Koishi R, Ando Y, Ono M et al. Angptl3 regulates lipid metabolism in mice. Nat. Genet 2002; 30: 151–157.

77. Köster A, Chao YB, Mosior M et al. Transgenic angiopoietin-like (angptl)4 overexpression and targeted disruption of angptl4 and angptl3: regulation of triglyceride metabolism. Endocrinology 2005; 146: 4943–4950.

78. Fujimoto K, Koishi R, Shimizugawa T, Ando Y. Angptl3-null mice show low plasma lipid concentrations by enhanced lipoprotein lipase activity. Exp. Anim. 2006; 55: 27–34.

79. Lee EC, Desai U, Gololobov G et al. Identification of a new functional domain in angiopoietin-like 3 (ANGPTL3) and angiopoietin-like 4 (ANGPTL4) involved in binding and inhibition of lipoprotein lipase (LPL). J. Biol. Chem.2009; 284: 13735–13745.

80. Liu J, Afroza H, Rader DJ, Jin W. Angiopoietin-like protein 3 inhibits lipoprotein lipase activity through enhancing its cleavage by proprotein convertases. J. Biol.Chem. 2010; 285: 27561–27570.

81. Adeyo O, Goulborne CN, Bensadoun A, Beigneux AP, Fong LG, Young SG. Glycosylphosphatidylinositol-anchored high density lipoprotein-binding protein 1 and the intravascular processing of triglyceride-rich lipoproteins. J. Intern. Med. 2012; 272: 528–540.

82. Nilsson SK, Anderson F, Ericsson M et al. Triacylglycerol-rich lipoproteins protect lipoprotein lipase from inactivation by ANGPTL3 and ANGPTL4. Biochim. Biophys. Acta. 2012; 1821: 1370–1378.

83. Sonnenburg WK, Yu D, Lee EC et al. GPIHBP1 stabilizes lipoprotein lipase and prevents its inhibition by angiopoietin-like 3 and angiopoietin-like 4. J. Lipid Res.2009; 50: 2421–2429.

84. Jaye M, Lynch KJ, Krawiec J, Marchadier D, Maugeais C, Doan K, South V, Amin D, Perrone M, Rader DJ. A novel endothelial-derived lipase that modulates HDL metabolism. Nat Genet. 1999; 2: 424–428.

85. Ishida T, Choi S, Kundu RK, Hirata K, Rubin EM, Cooper AD, Quertermous T. Endothelial lipase is a major determinant of HDL level. J Clin Invest. 2003; 111: 347–55.

86. Jin W, Wang X, Millar JS et al. Hepatic proprotein convertases modulate HDL metabolism. Cell Metab. 2007; 6: 129–136.

87. Pisciotta L, Favari E, Magnolo L, Simonelli S, Adorni MP, Sallo R, Fancello T, Zavaroni I, Ardigò D, Bernini F, Calabresi L, Franceschini G, Tarugi P, Calandra S, Bertolini S. Characterization of three kindreds with familial combined hypolipidemia caused by loss-of-function mutations of ANGPTL3. Circ Cardiovasc Genet. 2012; 5: 42-50

88. Huang XF, Shelness GS. Identification of cysteine pairs within the amino-terminal 5% of apolipoprotein B essential for hepatic lipoprotein assembly and secretion. J. Biol. Chem 1997; 272: 31872–31876

89. Tran K, Borèn J, Macri J, Wang Y, McLeod R, Avramoglu R K, Adeli K, Yao Z. Functional analysis of disulfide linkages clustered within the amino terminus of human apolipoprotein B. J. Biol. Chem. 1998; 273: 7244–7251

90. Sundaram M, Yao Z. Recent progress in understanding protein and lipid factors affecting hepatic VLDL assembly and secretion. Nutr Metab 2010; 7: 35-51.

91. Jessup W, Gelissen IC, Gaus K, Kritharides L. Roles of ATP binding cassette transporters A1 and G1, scavenger receptor BI and membrane lipid domains in cholesterol export from macrophages. Curr Opin Lipidol 2006; 17: 247-257.

92. Favari E, Zanotti I, Zimetti F, Ronda N, Bernini F, Rothblat GH. Probucol inhibits ABCA1-mediated cellular lipid efflux. Arterioscler Thromb Vasc Biol 2004; 24: 2345-2350.